UNIVERSITÀ' DEGLI STUDI DI TRIESTE

XXIV CICLO DEL DOTTORATO DI RICERCA IN
SCIENZE E TECNOLOGIE CHIMICHE E FARMACEUTICHE

Toxicological effects of palytoxin after cutaneous exposure

Settore scientifico-disciplinare BIO/15

DOTTORANDO
Dott. Marco Pelin

DIRETTORE
Prof. Enzo Alessio

RELATORE
Prof. Aurelia Tubaro

CORRELATORE
Dott. Chiara Florio

ANNO ACCADEMICO 2010/2011

ABSTRACT

Palytoxin (PLTX) is a marine toxin identified in *Palythoa* zoanthid corals and *Ostreopsis* dinoflagellates, representing an increasing hazard for human health. Human poisonings attributed to PLTX exposure are usually associated to ingestion of contaminated seafood and to marine aerosol exposure during *Ostreopsis* blooms. However, also dermatological problems have been recently associated to PLTX cutaneous exposure during *Ostreopsis* blooms as well as after handling of *Palythoa* corals. Despite the increasing human cases of dermotoxicity attributed to PLTX, very few data about its dermal toxicity are presently available. Hence, the aim of this study is to investigate the cutaneous effects of PLTX characterizing its mechanism of action. Thus, this toxicological *in vitro* study has been carried out on spontaneously immortalized human keratinocytes (HaCaT cells), as a first-round screening of dermotoxicity.

The entity of cytotoxicity induced by PLTX has been firstly investigated. A short time exposure (4 h) to PLTX reduces mitochondrial activity (MTT assay), cell mass (SRB assay) and plasma membrane integrity (LDH leakage) with different potencies (EC_{50} values of $6.1\pm1.3x10^{-11}$, $4.7\pm0.9x10^{-10}$ M and $1.8\pm0.1x10^{-8}$ M, respectively). All these effects are ouabain-sensitive corroborating the dependency of PLTX effects on the interaction with Na^+/K^+-ATPase. These results indicate that among the chain of intracellular events following the interaction of PLTX with the Na^+/K^+-ATPase the earliest is mitochondrial damage. This sustained cytotoxic effect can be explained by the high affinity of binding to HaCaT cells. Indeed, saturation experiment reveals a Kd affinity constant of $3.0\pm0.4x10^{-10}$ M after an exposure time as short as 10 minutes.

A possible mechanism of mitochondrial dysfunction can be reactive oxygen species (ROS) overproduction. Among all, only superoxide anion (O_2^-) seems to be produced by the toxin after only 1 h, whereas neither nitric oxide nor peroxynitrite formation are detected. Hence,

the mechanism of O_2^- production has been investigated. Real time PCR analysis together with western blot analysis suggest a possible involvement of NADPH oxidase (NOX) and inducible nitric oxide synthetase (iNOS) since an early increase of their gene and protein expression was observed after short (1 – 4 h) but not longer (24 h) exposure times. On the contrary, other enzymes involved in ROS production (i.e. COX-1, COX-2, XOD) seem to be not involved in PLTX effects. Moreover, using selective inhibitors of these enzymes, we found that only DPI, a nonspecific inhibitor of both NOX and NOS, is able to inhibit by 15%, 26% and 43% O_2^- production induced by 10^{-10}, 10^{-9} and 10^{-8} M PLTX, respectively. However, NMMA, inhibitor of NOS, significantly reduces only O_2^- produced by high (10^{-8} M) but no by low (10^{-9} and 10^{-10} M) PLTX concentrations, whereas the selective inhibitor of NOX apocynin is totally ineffective. Moreover, since their co-administration does not reproduce DPI effect, a prominent role of these enzymes in causing PLTX-induced oxidative stress seems unlikely. Another feasible source of O_2^- is mitochondria itself and its production is regulated by H^+ fluxes through mitochondrial membranes. Indeed, in presence of nigericin, an ionophore that reduces the H^+ imbalance, PLTX-induced O_2^- is significantly reduced by 23% (10^{-9} M PLTX) and 24% (10^{-8} M PLTX). Furthermore, the co-administration with rotenone, a complex I inhibitor, that *per se* is ineffective, results in a further inhibition of O_2^- production (-32% and -43% in the presence of 10^{-9} and 10^{-8} M PLTX, respectively). Moreover, O_2^- production turned out to be ouabain-sensitive and Na^+-dependent but Ca^{2+}-independent. Thus, on the basis of these results it has been hypothesized that PLTX binding to Na^+/K^+-ATPase induces intracellular overload of Na^+ followed by intracellular increase of H^+ with a consequent ΔpH increase across H^+-impermeable mitochondrial inner membrane and O_2^- overproduction by reverse electron transports through mitochondrial chain.

Under oxidative stress conditions, mitochondrial dysfunction can be mediated by mitochondrial permeability transition pore (MPTP), which opening, indeed, is induced by PLTX already after only 5 minutes exposure. MPTP opening, which turned out to be

cyclosporine A-independent, seems to be mainly induced by the sustained ionic imbalance, since in Na^+-free, Ca^{2+}-free medium and in presence of nigericin PLTX effect is strongly inhibited. The very rapid Na^+-dependent opening of MPTP suggests that this is the peculiar mechanism of PLTX cytotoxicity and cell death *primum movens*. Cell death induced by the toxin seems to occur with necrotic-like features. PLTX, indeed, induces a concentration- and time-dependent as well as irreversible uptake of PI after only 1 h exposure and confocal images revealed dramatic morphological alterations such as plasma membrane ruptures and leakage of cytolpasmic content after 4 h. By contrast, caspasis 3/7, 8 and 9 are not activated by PLTX up to 24 h, neither under recovery conditions. Moreover, apoptotic bodies formation is not observed, discarding apoptosis occurrence.

Finally, PLTX effects on some pro-inflammatory mediators such as cytokines (IL-1α, IL-6, IL-8 and TNF-α) and arachidonic acid metabolism products (PGE_2 and LTB_4) have been evaluated. The toxin (10^{-11} M) induces an early release of PGE_2 that is time-dependent after 2 h exposure. On the contrary, even if an early gene expression (1–4 h) is observed, the toxin induces a delayed release of IL-6 and IL-8 (24 h), whereas no effects have been observed evaluating IL-1α and TNF-α.

In conclusion, this study highlights the toxic *in vitro* properties of PLTX on human keratinocytes. The intracellular pathway of the sustained PLTX cytotoxicity leading to cell death has been characterized, as well as the inflammatory mediators involved in skin irritant properties of the toxin. These results can corroborate the use of non steroidal anti-inflammatory drugs in association with anti-inflammatory corticosteroids.

RIASSUNTO

La palitossina (PLTX) è una tossina marina identificata in coralli zoantidi appartenenti al genere *Palythoa* e dinoflagellati del genere *Ostreopsis*. Intossicazioni umane attribuite alla PLTX sono state solitamente associate all'ingestione di prodotti ittici contaminati, nonché da un'esposizione ad aerosol marino durante le fioriture di *Ostreopsis*. Tuttavia, anche problemi dermatologici sono stati recentemente associati alla PLTX in seguito ad esposizione cutanea durante fioriture di *Ostreopsis* o manipolando coralli *Palythoa*. Nonostante i crescenti casi di dermotossicità attribuiti alla PLTX, pochissimi dati sulla sua tossicità cutanea sono attualmente disponibili. Lo scopo di questo studio è stato, pertanto, indagare gli effetti cutanei della PLTX caratterizzando il suo meccanismo d'azione. E' stato quindi effettuato uno studio tossicologico *in vitro* su cheratinociti umani spontaneamente immortalizzati (cellule HaCaT), considerate metodo predittivo per uno screening preliminare di dermotossicità.

In primo luogo è stato caratterizzato il grado di citotossicità indotta dalla tossina. Un breve tempo d'esposizione (4 h) alla PLTX riduce l'attività mitocondriale (saggio MTT), la massa cellulare (saggio SRB) e l'integrità della membrana plasmatica (perdita LDH) con diversi valori di EC_{50} ($6.1 \pm 1.3 \times 10^{-11}$, $4.7 \pm 0.9 \times 10^{-10}$ M e $1.8 \pm 0.1 \times 10^{-8}$ M, rispettivamente). Tutti questi effetti sono sensibili alla ouabaina, corroborando la dipendenza degli effetti della PLTX sull'interazione con la Na^+/K^+-ATPasi. Questi risultati indicano che fra la catena di eventi intracellulari dopo l'interazione con l'ATPasi il più sensibile è un danno mitocondriale. Questo effetto può essere spiegato dall'alta affinità di legame della tossina con le cellule HaCaT. Infatti, esperimenti di saturazione rivelano una costante di affinità (Kd) pari a $3,0 \pm 0.4 \times 10^{-10}$ M dopo un tempo di esposizione molto breve (10 minuti).

Uno dei possibili meccanismi di disfunzione mitocondriale è una sovrapproduzione di specie reattive dell'ossigeno (ROS). Tra tutti, solo l'anione superossido (O_2^-) sembra essere prodotto dalla tossina dopo 1 h, mentre né ossido nitrico né formazione di perossinitrito sono stati

rilevati. Quindi, il meccanismo di produzione di O_2^- è stato studiato. Analisi real time-PCR ed analisi western blot suggeriscono un possibile coinvolgimento della NADPH ossidasi (NOX) e della forma inducibile dell'ossido nitrico sintetasi (iNOS) poiché un aumento precoce della loro espressione genica e stata osservata dopo brevi (1 - 4 h) ma non lunghi (24 h) tempi di esposizione. Al contrario, altri enzimi coinvolti nella produzione di ROS (COX-1, COX-2, XOD) sembrano non essere coinvolti nel meccanismo di produzione di O_2^- da parte della tossina. Inoltre, tramite l'utilizzo di inibitori selettivi di questi enzimi, è emerso che solo il DPI, un inibitore non specifico sia di NOX che di NOS, è in grado di inibire del 15%, 26% e 43% la produzione di O_2^- indotta da 10^{-10}, 10_{-9} e 10^{-8} M PLTX, rispettivamente. Tuttavia, l'NMMA, inibitore delle NOS, riduce in modo significativo solo O_2^- prodotto da alte (10^{-8} M), ma non basse (10^{-9} e 10^{-10} M) concentrazioni di PLTX, mentre l'inibitore selettivo delle NOX apocinina è totalmente inefficace. Inoltre, poiché la loro co-somministrazione non riproduce l'effetto inibitorio del DPI, un ruolo preminente di questi enzimi nel causare stress ossidativo sembra improbabile. Un'altra fonte possibile di O_2^- è il mitocondrio. La sua produzione è regolata dal flusso di H^+ attraverso le membrane mitocondriali. Infatti, in presenza di nigericina, uno ionoforo che riduce lo squilibrio protonico, i livelli di O_2^- indotti dalla PLTX vengono significativamente ridotti del 23% (10^{-9} M PLTX) e 24% (10^{-8} M PLTX). Inoltre, la co-somministrazione con il rotenone, un inibitore del complesso I della catena mitocondriale di trasporto degli elettroni, che è di per sé inefficace, induce un'ulteriore inibizione di produzione di O_2^- (-32% e -43% in presenza di 10^{-9} e 10^{-8} M PLTX, rispettivamente). Inoltre, la produzione di O_2^- risulta essere ouabaina-sensibile e Na^+-dipendente, ma Ca^{2+}-indipendente. Pertanto, sulla base di questi risultati è stato ipotizzato che il legame della PLTX con la Na^+/K^+-ATPasi induce un aumento intracellulare di Na^+ seguito da aumento intracellulare di H^+ con un conseguente aumento di ΔpH attraverso la membrana mitocondriale interna con una sovrapproduzione di O_2^- indotta dal trasporto inverso degli elettroni attraverso la catena mitocondriale.

In condizioni di stress ossidativo, la disfunzione mitocondriale può essere mediata dall'apertura dei pori di transizione mitocondriali (MPTP). La loro apertura, infatti, viene indotta dalla PLTX già dopo soli 5 minuti di esposizione. Tale apertura, che si è rivelata ciclosporinaA-indipendente, sembra principalmente indotta dallo squilibrio ionico indotto dalla tossina, poiché in terreni privo di Na^+ e privo di Ca^{2+} e in terreno contenente nigericina, l'attività della tossina è fortemente inibita. La rapidissima apertura di MPTP suggerisce che questo è il peculiare meccanismo di citotossicità della tossina e il *primum movens* della cellule morte. La morte cellulare sembra verificarsi con un danno necrotico. La PLTX, infatti, induce un uptake di PI (marker di necrosi) in maniera concentrazione e tempo-dipendente. Tale uptake è inoltre irreversibile, dopo solo 1 h di esposizione e immagini ottenute al microscopio confocale rivelano drammatiche alterazioni morfologiche, quali rotture della membrana plasmatica e la perdita di contenuto citoplasmatico dopo 4 h. Al contrario, le caspasi 3/7, 8 e 9 non sono attivate dalla PLTX fino a 24 h, né sotto condizioni di recovery. Inoltre, la formazione di corpi apoptotici non è stata rilevata, scartando l'ipotesi di una morte di tipo apoptotico.

Infine, gli effetti della PLTX su alcuni mediatori proinfiammatori quali citochine (IL-1α, IL-6, IL-8 e TNF-α) e metaboliti dell'acido arachidonico (PGE_2 e LTB_4) sono stati valutati. La tossina (10^{-11} M) induce una rapida produzione di PGE_2 che è tempo-dipendente dopo 2 ore di esposizione. Al contrario, la tossina induce un rilascio ritardato di IL-6 e IL-8 (24 h), anche se alterazioni dell'espressione genica si sono osservate dopo breve tempo di contatto con la tossina (1-4 h). mentre non sono stati osservati effetti valutando IL-1α e TNF -α.

In conclusione, questo studio mette in evidenza le proprietà tossiche *in vitro* della PLTX su cheratinociti umani. L'elevata citotossicità indotta dalla tossina conduce ad una morte cellulare di tipo necrotico mediata dai mitocondri. Infine, i mediatori infiammatori coinvolti nella proprietà irritanti della pelle della tossina sono stati caratterizzati, ponendo delle basi

molecolari per spiegare l'utilizzo di farmaci anti-infiammatori non steroidei in associazione con corticosteroidi.

INDEX ***Page***

INDEX ***Page***

4. Results

1. Introduction

1.1 Palytoxin

The history of palytoxin (PLTX) began many decades ago, when a group of researchers decided to test the veracity of the hawaiian legend *limu-make-o-Hana*, which literally means "The toxic seaweed of Hana". This legend tells of a man carrying a shark mouth on his back using it to kill fishermen entering in its fishing area. The fishermen, however, killed him and, after burning his body, they scattered his ashes. In the bay, called Hana, where the ashes were scattered, grew a toxic algae. The legend tells that the warriors used to go to this beach to dip the tips of their spears to make them fatal. Over the centuries the legend has become a taboo: anyone went to the bay would have been fall in disgrace. At the beginning of 60's, Prof. Helfrich discovered the exact location of the bay as well as the algae of the legend that was actually a coral belonging to the genus *Palythoa*, especially the species *P. toxica* (Moore et al., 1982). For this reason the molecule that was discovered ten years later by Prof. Scheuer was called palytoxin.

1.1.1 Origins

Zoanthid corals (*Palythoa* spp. and *Zoanthus* spp.)

PLTX has been isolated for the first time in the early 70's in Hawaii by Moore and Scheuer from zoanthid corals of the genus *Palythoa*, especially the species *P. toxica* (fig. 1A, Moore and Scheuer, 1971). In the following years PLTX and analogues were identified also in other species of corals in different parts of the world, such as *P. tuberculosa* (Uemura et al., 1981) and *P. margaritae* (Oku et al., 2004) along the Japanese coast, *P. caribaerorum* (Beress et al., 1983) and *P. mammilosa* along Puerto Rican and Jamaican coasts, and other species, present in tropical and subtropical areas of the planet. The toxicity of these coelenterates varies from species to species; the most toxic is *P. toxica*, which seems to produce PLTX throughout the year (Moore et al., 1982). In other species, by contrast, such as *P. tuberculosa* (Hashimoto et al., 1969) and *P. mammilosa* (Attaway and Ciereszko, 1974) the presence of the toxin was noted only periodically, especially during the spawning of zoanthids in the period between June and August.

Furthermore, the toxin has also been found in zoanthids belonging to the genus *Zoanthus* (fig. 1B), such as *Z. solanderi* and *Z. sociatus*, that live in colonies close to those of *Palythoa* and compete with them for space on the reef (Gleibs et al., 1995).

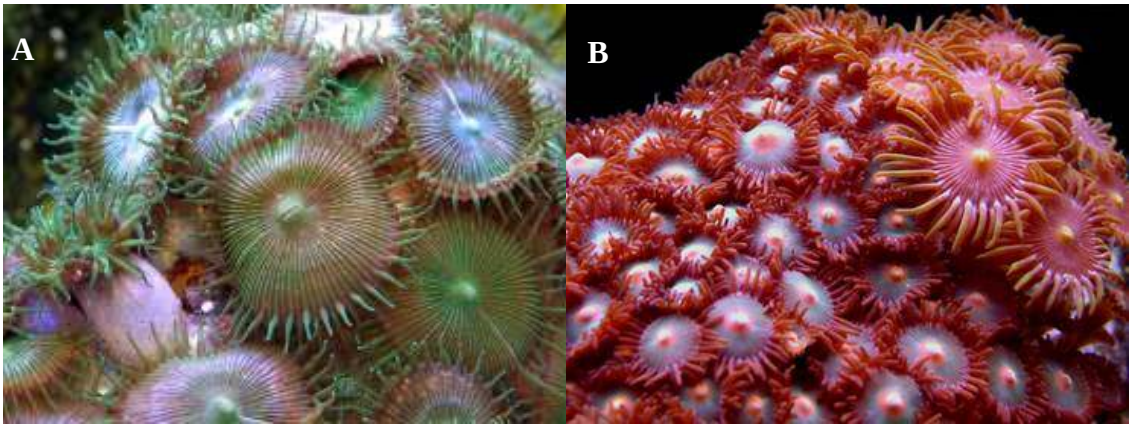

Fig. 1. *Images of Palythoa toxica* ***(A)*** *and Zoanthus spp.* ***(B)***.

Dinoflagellates (*Ostreopsis* spp.)

At the beginning of the 90's, compounds structurally related to PLTX have been identified in the benthic microalgae *Ostreopsis*, an epiphytic dinoflagellate that lives in tropical and temperate areas of the planet. *Ostreopsis* is widespread, indeed, in the Pacific, Atlantic and Indian oceans (Rhodes, 2011), but over the last few years, these microalgae have found the ideal conditions for their proliferation in temperate zones, such as the Mediterranean sea (Katikou, 2008). Different species of dinoflagellates belong to the genus *Ostreopsis*; almost all of them turned out toxic as producers of PLTX analogues:

- *O. ovata*. The smallest species of the genus, although no less toxic than the others (fig. 2). Producer of PLTX and of a new group of toxins called ovatoxins (ova), structural analogues of PLTX. The recently characterized ova-a is among all (ova-b, ova-c, ova-d, ova-e) the most studied. In recent years, this species has been observed in the Mediterranean sea with massive algal blooms, during which many people showed respiratory distress and dermatitis after marine aerosol exposure (Sansoni et al., 2003; Gallitelli et al., 2005; Durando et al., 2007).
- *O. siamensis*. It produces ostreocin-D (Ost-D), that was never detected in Mediterranean Sea, so far, despite the occurrence of *O. siamensis* blooms.
- *O. mascarensis*. The most widespread worldwide, although its presence has not been recorded till now in the Mediterranean sea. It produces mascarenotoxins a and b (MTX-a and MTX-b), the most involved in human intoxications recorded along Indian coasts (Hansen et al., 2001).

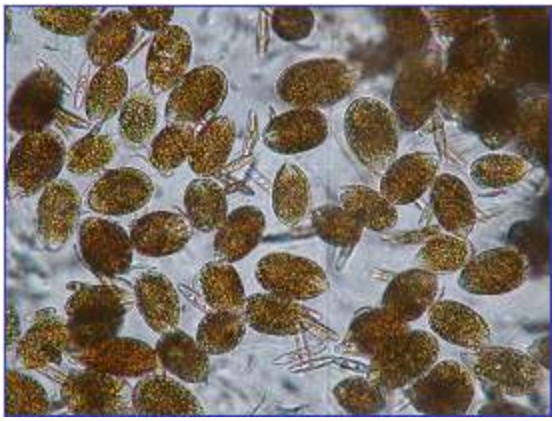

Fig. 2. *Images of Ostreopsis ovata.*

Bacteria

In early 2000, it was hypothesized that PLTX may have a bacterial origin (Frolova et al., 2000). In particular, attention has been focused on bacteria of the genus *Aeromonas* and *Vibrio*. In the following years, additional assumptions were made about the symbiosis of bacteria (belonging to the phyla *Firmicutes*, *Proteobacteria* and *Actinobacteria*) with coelenterates of the genus *Palythoa* and *Zoanthus*. However, to identify the bacteria a method showing the hemolytic activity of these microorganisms has been used, without a direct analytical verification of the presence of the toxin (Seeman et al., 2009). Recently, it has been discovered that PLTX and its analogue 42-OH-PLTX are also produced by the cyanobacteria of the genus *Trichodesmium*, very common in tropical and subtropical areas. These bacteria are eaten by other marine organisms that accumulate them without showing signs of toxicity (Kerbrat et al., 2011).

1.1.2 Chemical structure and chemical properties

PLTX was isolated in 1971 from soft corals of the genus *Palythoa*. During those years, it was thought that its molecular weight was about 3300 Da and that its chemical formula was $C_{145}H_{264}N_4O_{78}$, even assuming the lacking of repeated parts, or protein and glucidic parts. A decade later, its chemical structure was elucidated by two independent groups, one led by Prof. Hirata at Nagoya (Uemura et al., 1981), the other by Prof. Moore in Honolulu (Moore and Bartolini, 1981). Hence, the exact chemical formula of PLTX turned to be $C_{129}H_{223}N_3O_{54}$, with an exact molecular weight of 2680.13 Da.

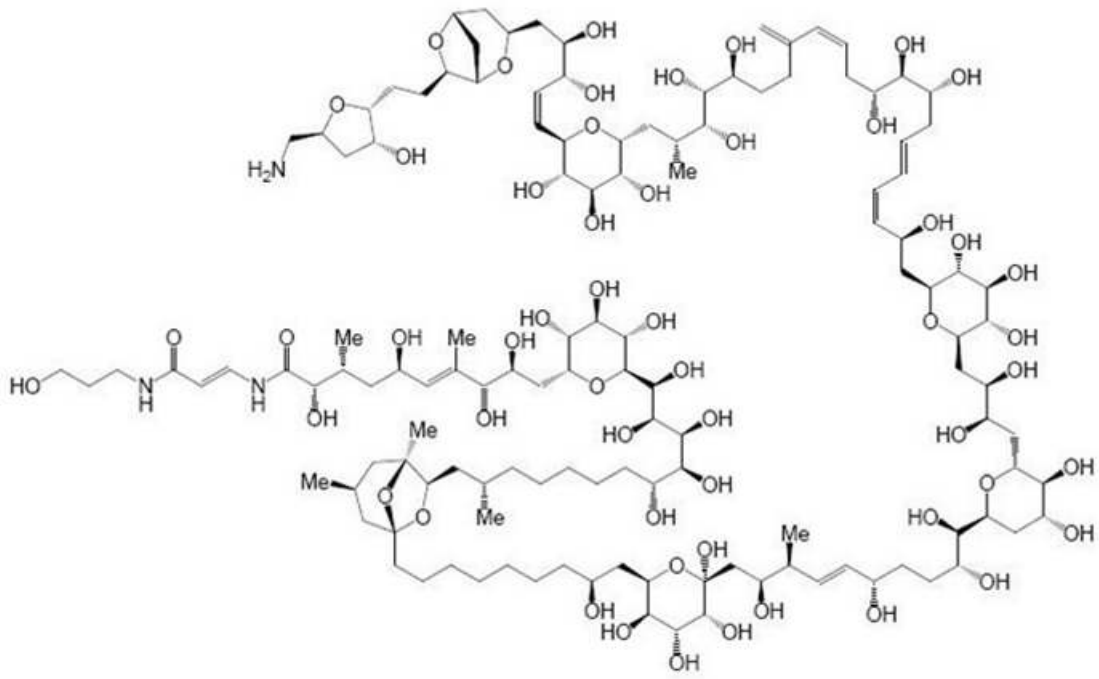

Fig. 3. *Chemical structure of PLTX.*

PLTX is considered one of the most complicate and large molecules found in nature. Its structure contains 129 aliphatic carbon atoms, 40 secondary hydroxy groups, two diene motifs, a conjugate acrylamide-enamide system, three unsaturations, two hydrophobic hydrocarbon chains, cyclic ethers systems and bicyclic acetals are found along its backbone

(fig. 3). The structure contains 64 chiral centres and 2 amino groups (Uemura et al., 1985), whereas the third nitrogen atom is on C115 in the form of primary amino group (Moore and Bartolini, 1981). Despite the complexity of this structure, in 1989 the entire molecule was synthesize in its carbossilic acid form (Kishi, 1989; Armstrong et al., 1989) and converted, some years later, into the natural PLTX, found in *P. tuberculosa* (Suh and Kishi, 1994).

PLTX is a white amorphous and hygroscopic solid. It is insoluble in non-polar solvents such as chloroform, ether and acetone, slightly soluble in methanol and ethanol, while it is soluble in piridin, dimethylsulfoxide and water. The repartition coefficient between 1-butanol and water is 0.21 at 25 ° C, on the basis of the comparison between the absorbance at 230 nm between the two phases. In aqueous solution it generates foam after stirring, probably caused by its amphipathic nature. Moreover, it is heat resistant and a melting point has not been already defined (Katikou, 2008).

The conformation of the toxin in aqueous solution has been investigated using the X-ray crystallography (SAXS, Small-angle X-ray Scattering) and the nuclear magnetic resonance (NMR). In this study, the structure of PLTX has been compared to that of N-acetyl-PLTX, which presents an acetyl on the primary amino group in C115. In particular, in aqueous solution N-acetyl-PLTX shows a monomeric form, assuming the shape of a horseshoe, which measures 30.6x23.4x13.0 Å. PLTX, instead, assumes a dimeric form in aqueous solution, acquiring the form of ∞ which measures 52.3x22.0x15.1 Å. Presently, the parts of PLTX involved in the dimer formation have not been identified, although it is thought that the hydrophobic region (C21-C40) and the region around the conjugated double bonds (C60-C84) are probably implicated. Moreover, also the terminal amino group is probably involved in the interaction of two molecules of PLTX since N-acetyl-PLTX not only is unable to dimerize, but also its biological activity is about 100 times lower than the reference compound (Inuzuka et al., 2008).

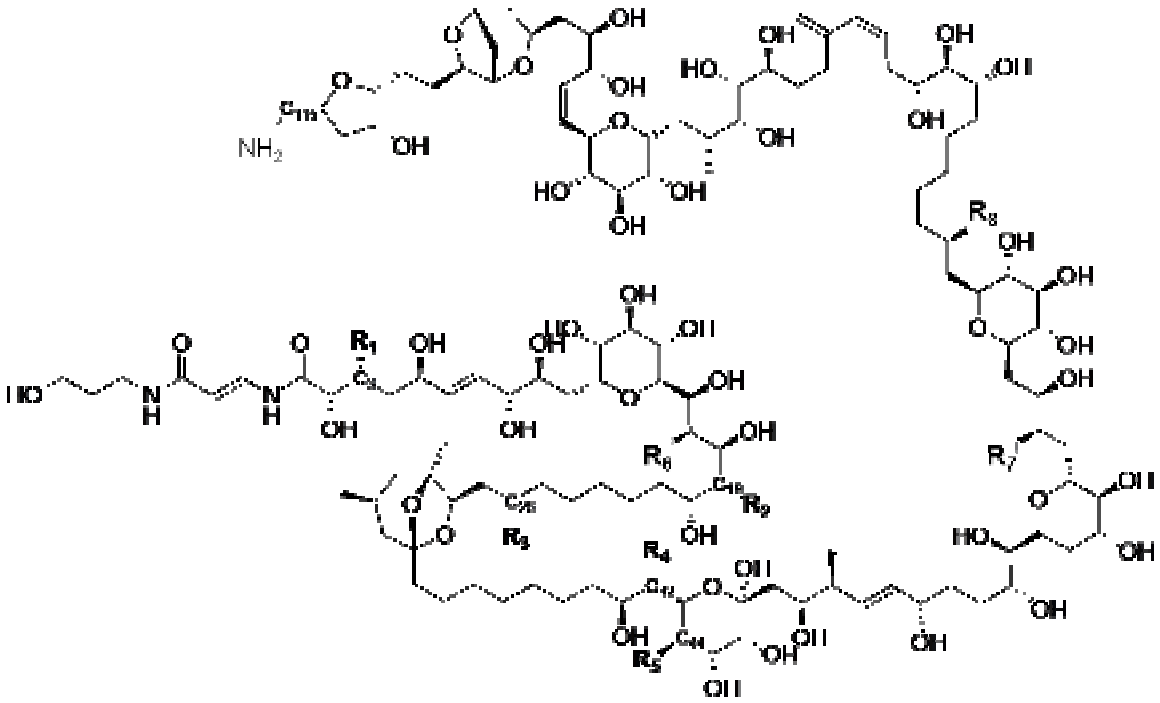

	n	R1	R2	R3	R4	R5	R6	R7	R8
Palytoxin	1	Me	OH	Me	H	OH	OH	OH	OH
Omopalytoxin	2	Me	OH	Me	H	OH	OH	OH	OH
Bisomopalytoxin	3	Me	OH	Me	H	OH	OH	OH	OH
Neopalytoxin	1	-	OH	Me	H	OH	OH	OH	OH
Deoxypalytoxin	1	Me	OH	Me	H	OH	OH	OH	H
42-hydroxypalytoxin	1	Me	OH	Me	OH	OH	OH	OH	OH
Ostreocin-D	1	H	H	H	OH	H	OH	OH	OH
Ovatoxin-a	1	Me	OH	Me	OH	H	H	H	OH

Fig. 4. *Differences on the molecular structures between PLTX analogues.*

Depending on the producing organism, there are several structural analogues of PLTX (fig. 4). For this reason nowadays we are dealing with a group of toxins called *Palytoxin-like compounds*. Some examples are the omopalitoxin, the bisomopalitoxin, the neopalitoxin and the deossipalitoxin, all identified in *P. tuberculosa* in the area of Okinawa. Their main differences are located essentially on the emiacetalic ring in C55 (Uemura et al., 1985). Recently, a new analogue of PLTX, the 42-hydroxy-PLTX (42-OH-PLTX), has been identified as the main compound of the species *P. toxica*. High resolution liquid chromatography associated with mass spectrometry analysis (HR LC-MS) have elucidated the

chemical formula of 42-OH-PLTX ($C_{129}H_{223}N_3O_{55}$) that presents an oxygen atom more than PLTX. The exact location of the additional oxygen atom has been identified by NMR analysis, and results to form an hydroxyl group in position C42 (Ciminiello et al., 2009). In addition, toxicological studies carried out on mice demonstrated that the acute toxicity after oral exposure of 42-OH-PLTX is comparable to that of PLTX (Tubaro et al., 2011).

Another PLTX analog is ostreocin-D (Ost-D). Its chemical formula is $C_{127}H_{219}N_3O_{53}$ with a molecular weight of 2636.47 Da. In its structure, two hydrogen atoms replace two hydroxyls of PLTX in C19 and C44. Moreover, in C42 the presence of an additional hydroxyl group, absent in PLTX, is detected (Katikou, 2008). The toxicity of Ost-D appears to be lower than that of PLTX (Ito and Yasumoto, 2009).

Recent studies have demonstrated the existence of another group of PLTX analogues: the group of ovatoxins. Among all, the first to be identified is ovatoxin-a (ova-a). Its chemical formula ($C_{129}H_{224}N_3O_{52}$ with a molecular weight is 2647.5 Da) as well as its chemical structure have been recently characterized (Ciminiello et al., 2012). Ovatoxins seems to be the major toxins produced by *Ostreopsis ovata*, at least in the Mediterranean sea. However, no toxicological studies have been performed so far, and the only carried out is a preliminary mouse lethality assessment after i.p injection suggesting that ova-a lethality lies below 7.0 μg/Kg (Ciminiello et al., 2012).

1.1.3 Human intoxications

Human hazard associated to PLTX resides in its accumulation in marine organisms, both through filtration and ingestion, and potentially entering, therefore, in human food chain. For example, some crustaceans (*Platypodiella spectabilis*), invertebrates (*Polychaete* spp., *Hermodice* spp., *Eunice* spp.) and starfish (*Acanthaster* spp.) living nearby the zoanthids colonies, accumulate PLTX (Gleibs et al., 1995). PLTX has also been identified in fish (*Chaetodon capistratus* and *Chaetodon sedentarius*) that feed *Palythoa*-colonizing invertebrates. The toxin has been found in the skin, muscles, intestines, gills, liver and eggs of these fish. Most of these marine organisms tolerates very well the toxin, showing no signs of toxicity, even at concentrations causing disturbances in humans (Gleibs and Mebs, 1999).

Moreover, also *Ostreopsis* spp. can be filtered or ingested by higher marine organisms: PLTX and analogues have been identified in crustaceans, mussels and echinoderms in the Mediterranean sea (Aligizaki et al., 2011). However, in these areas, marine organisms such as sea urchins and sea stars have shown signs of toxicity such as loss of spines and arms, respectively (Sansoni et al., 2003) although no human intoxications associated to their ingestion have been described in these areas, so far (Aligizaki et al., 2011).

Cases of poisoning following ingestion of contaminated seafood have been recorded mainly in tropical and subtropical areas, some of them turned out to be fatal. However, most of these intoxications have been ascribed to PLTX on the basis of screening tests that were performed on seafood samples collected or purchased after or before the poisoning episode, or on the basis of clinical observations, signs and symptoms. Indeed, only few cases have been documented in literature through a direct PLTX detection in the seafood leftovers that caused the poisoning (Tubaro et al., 2011). A fatal case after ingestion of a crab (*Demania reynaudii*) occurred in the Philippines, where a 49-years-man reported a metallic taste after consuming

the crab and, shortly after, developed a general malaise that initially involved the gastrointestinal apparatus (Alcala et al., 1988). The patient experienced nausea, tiredness, diarrhoea, and vomiting followed by dizziness, numbness of the extremities, muscle cramps and restlessness. After hospitalization he experienced alternating periods of normal heart rate and severe bradicardia (30 beats/min), rapid and shallow breathing, and cyanosis around the mouth and hands. Finally, the patient died 15 h after the crab ingestion. In this case, the causative toxin was suggested to be PLTX mainly on the basis of the chromatographic properties as well as by mouse bioassay (Alcala et al.,1988). In the same period, Noguchi et al. (1987) described a case of a man (54 years old) and a woman (79 years old) poisoned after parrotfish (*Scarus ovifrons*) consumption. The symptoms, developed within 17 and 49 h, respectively, were mainly dyspnoea, myalgia and convulsions. Myoglobinuria and high serum levels of CPK (creatine phosphokinase), AST (alanine aminotransferase) and LDH (lactate dehydrogenase) were recorded. The man recovered within one week, whereas the woman died for respiratory failure associated with muscular damage, 4 days later. Mouse bioassay revealed the presence of a "parrotfish toxin", with pharmacological and chemical properties generally consistent with a PLTX-like compound. A case of fatal poisoning due to contaminated tropical sardines (*Herklotsichthys quadrimaculatus*) involved a woman in Madagascar (Onuma et al.,1999). The patient referred an unusual metallic taste of the fish and within 2 h developed general malaise, uncontrollable vomiting and diarrhoea. The patient died after one day, whereas her son, who ate a similar fish, did not develop any symptoms. The causative toxin was identified as PLTX and/or analogues on the basis of its delayed haemolytic activity inhibited by an anti-PLTX antibody and confirmed by chromatographic analysis as well as by mass spectrometry data. More recently, eleven people out of 33 were intoxicated after a serranid fish (*Epinephelus* sp.) ingestion. The patients (ages between 27 and 57) suffered muscle pain, followed by discharge of black urine and low back and shoulder pain. The hematological analysis revealed significantly increased serum levels of CPK, up to

nearly 24,000 IU/l. All the patients recovered after more than one month. Uncooked fish muscle flesh from the leftovers was analysed for the presence of PLTX by mouse bioassay and hemolysis assay (Taniyama et al., 2002).

In the temperate area, such as the Mediterranean sea, human hazards due to PLTX intoxications are mainly associated to *Ostreopsis* blooms. Since the beginning of the 1970s, this benthic dinoflagellates appeared in temperate climates and gradually their blooms became a recurring phenomenon in the Mediterranean sea (Katikou, 2008; Rhodes, 2011). In particular, since the end of the last decade, massive blooms of *Ostreopsis* spp. occurred along the Italian, French and Spanish coastlines, sometimes resulting in respiratory and febrile syndrome outbreaks in humans exposed to sea-spray aerosol, containing fragments of algal cells and/or PLTX, and directly to seawater during recreational activities (Brescianini et al., 2006; Gallitelli et al., 2005; Kermarec et al., 2008; Mangialajo et al., 2008; Monti et al., 2007; Rhodes, 2011; Tichadou et al., 2010; Tognetto et al., 1995; Totti et al., 2007; Zingone et al., 2006). The first cases of *Ostreopsis* blooms along Italian coast associated to human illnesses were recorded in 1998, 2000 and 2001 along the Tuscany coast (Sansoni et al., 2003) and along Bari coast in 2001 (Di Turi et al., 2003). In 2003 and 2004, in the same area, concomitantly with two *Ostreopsis* blooms, 28 persons exposed to marine aerosol developed respiratory syndromes associated with fever, conjunctivitis and dermatitis (Tubaro et al., 2011). The most prominent episodes of human poisoning related to *Ostreopsis ovata* blooms occurred in the summers 2005 and 2006 along the coast of Genoa and La Spezia. In that period, seawater analysis showed the presence of high densities of *O. ovata* and, for the very first time, of a putative PLTX and its analogue ovatoxin-a (Brescianini et al., 2006; Ciminiello et al., 2006, 2008). In July 2005, a total of 209 patients required hospitalization for cough, dyspnoea, sore throat, rhinorrhoea, fever ≥38°C, headache, lacrimation,

nausea/vomiting and dermatitis with a mean onset of symptoms equal to 4 h 33 min after the beginning of exposure. During the summer 2006, another 19 subjects presented the above-described symptoms concomitantly with a new *Ostreopsis ovata* algal bloom close to Genoa and La Spezia (Durando et al., 2007). In recent years, blooms of *O. ovata* and *O. siamensis* were recorded in the Mediterranean coasts of Spain and France (Battocchi et al., 2010; Vila et al., 2001). In Spain (August 2004), an outbreak of respiratory syndrome involved 200 people exposed to *Ostreopsis* bloom in Catalonia. Within 3 h after seawater aerosol exposure, patients referred rhinorrhoea (74%), rhinitis (66%), throat irritation (63%), cough (60%), expectoration (52%), eye irritation (41%) and headache (40%), but no hospitalization was required (Kermarec et al., 2008). In France, the first cases of human illness in concomitance to *Ostreopsis* blooms (25,000–900,000 cells/l seawater) were documented in August 2006, along Bouches-du-Rhône, where four divers were involved. The symptoms referred included lips and tongue irritation (100%), headache (100%), throat irritation (25%), fever (25%) and diarrhoea (25%) (Kermarec et al., 2008; Tichadou et al., 2010).

1.1.4 Mechanism of action

The main biological target of PLTX is the Na^+/K^+-ATPase on the plasmatic membrane of a large variety of cellular types (Habermann, 1989). Na^+/K^+-ATPase is a transmembrane pump belonging to the family of *P-type ATPase* essential for maintaining cellular homeostasis. Its task is to transport outside the cell three Na^+ ions for two K^+ ions with a cyclic process that exploits the hydrolysis of ATP and that takes the name of Albert-Post cycle (fig. 5).

It is largely known that PLTX binding to the eterodimer α-β of the Na^+/K^+-ATPase changes it from a pump to an unspecific cationic channel inducing a consistent cationic disequilibrium at the cellular level (Artigas and Gadsby, 2004; Hilgemann, 2003). This binding, allowed in the E_2P conformational states of the pump, due to the major PLTX affinity for the ATPase (Artigas and Gadsby, 2004, Harmel and Apell, 2006, Rodrigues et al., 2008), makes the cysteins substituted for several residues in the fifth and sixth putative transmembrane helices (Guennoun and Horisberger, 2000; 2002). The consequence is a rearrangement of the α-helices in the protein's membrane domain, which allows the opening of the cytoplasmatic gate of the pump. Moreover, in the E_2P conformational states the extracellular gate is physiologically open. Hence, as shown in figure 5 the contemporary opening of the two gates induces the formation of the channel that is opened as long as the pump is phosphorilated (the dephosphorilation of the pump allows its conformational change into the state E_1). Furthermore, PLTX binding reduces the rate of pump dephosphorilation, therefore, protracting the opening of the channel (Artigas and Gadsby, 2004, Harmel and Apell, 2006, Rodrigues et al., 2008). Once dephosphorilated, the pump can come back in its ordinary cycle. However, there is a controversy whether the dephosphorilation causes also the detach of PLTX.

In view of this peculiar mechanism of action, lots of studies report the ability of the cardio-active glycoside ouabain to inhibit some PLTX effects *in vitro* (Habermann and Chhatwall,

1982; Schilling et al., 2006; Vale-Gonzalez et al., 2007, Pelin et al., 2012). Notwithstanding, some speculations try to investigate if Na^+/K^+-ATPase is really the only specific target of PLTX. Indeed, it seems that it could interfere also with the functionalities of other *P-type ATPases* such as SERCA (Sarcoplasmic Reticulum Ca^{2+} pump) (Coca et al., 2008, Kockskamper et al., 2004) and the non-gastric H^+/K^+ -ATPase pump (Scheiner-Bobis et al., 2002, Qiu et al., 2006).

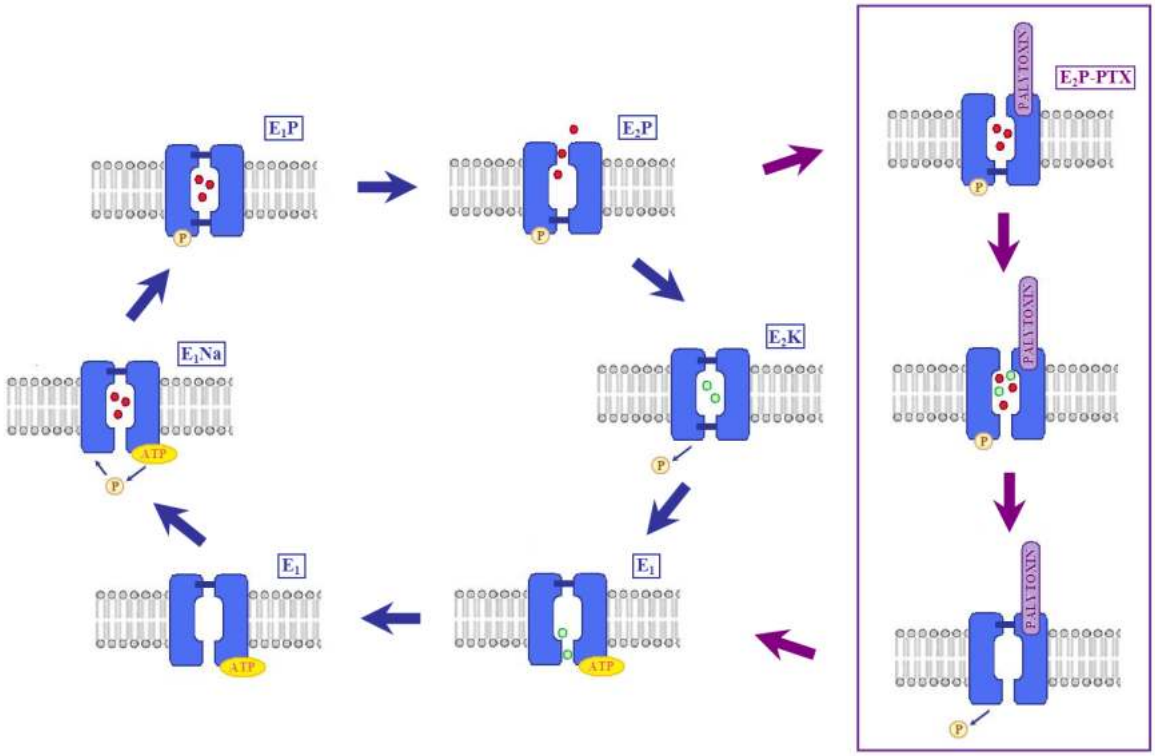

Fig. 5. *Albert-Post model for Na^+,K^+ ATPase pump. The pump alternates cyclically in two principal conformational states E_1 and E_2. In the state E_2P the pump is phosphorilated; this conformation allows the binding of the palytoxin that induces changes in the α-helices resulting in the opening of the intracellular gate. The binding impairs also the dephosphorilation of the pump, so that the opening of the so constituted unspecific cationic channel is prolonged. At the end, when dephosphorilated, the pump returns into its physiological cycle.*

1.1.5 Toxic effects *in vitro* and *in vivo*

The effects of PLTX are strictly linked to its mechanism of action. Indeed, the transformation of the Na^+/K^+-ATPase in an unspecific channel results in a modification of the cellular ion homeostasis. The first event consists in an increased intracellular concentration of Na^+ that causes a depolarization of cellular membrane, increased by the massive efflux of K^+ and by Ca^{2+} influx (Wu, 2009). Ca^{2+} influx seems to be mediated by the reverse functioning of the Na^+/Ca^{2+} exchanger (NCE) caused by the enhanced level of Na^+ and by voltage-dependent L-type Ca^{2+}-channels. The increased concentrations of Ca^{2+} may trigger Ca^{2+}-dependent cytotoxic effects. Among all, actin cytoskeletal disorganization (Ares et al., 2005), loss of plasma membrane integrity (Sheridan et al., 2005) and cell death (Schilling et al., 2006) seem to be the most common effects. Moreover, the intracellular increase of Na^+ seems to induce an acidification of the cytoplasm, probably due to the reverse functioning of the Na^+/H^+ exchanger (NHE) (Rossini and Bigiani, 2011). Furthermore, the increased level of Na^+ itself is believed to directly cause cell toxicity (Dubois and Cohen, 1977; Muramatsu et al., 1984; Sheridan et al., 2005). These events have different consequences on cell viability, with different effects depending on the cell model.

Considering excitable cells, for instance, PLTX induces dramatic electrophysiological alterations that culminate in disruption of the cardiac excitation-contraction coupling, thus impairing heart functions (Kockskämper et al., 2004). Other relevant effects on excitable cells are neurotransmitter release and an uncontrolled muscle contraction, at least considering neuronal and muscular cells respectively (Rossini and Bigiani, 2011). Neurotransmitter and hormone release seem to be Ca^{2+}-dependent events, at least considering norepinephrine release from rat pheochromocytoma cells (Tatsumi et al., 1984), acetylcholine release from rat cerebrocortical synaptosomes (Satoh and Nakazato, 1991) and catecholamine release from cultured bovine adrenal chromaffin cells (Nakanishi et al., 1991). In cerebellar granule cells,

PLTX-induced membrane depolarization activates voltage dependent Na^+-channel and Ca^{2+}-channel, as well as NCE. The subsequent Ca^{2+} influx induces activation of excitatory amino acid (EAA) receptors through glutamate release (Vale et al., 2006). Furthermore, uncontrolled muscle contraction induced by the toxin could have not only a Ca^{2+}-dependent mechanism, but can be caused also by an uncontrolled neurotransmitter release. Indeed, in axons and Schwann cells the most dramatic feature after PLTX exposure is the depletion of synaptic vesicles from putative release sites in the axons (Amir et al., 1997).

On non-excitable cells, cytotoxic effects are as well dependent on ionic imbalance induced by PLTX. Associated with the disruption of ionic balance is the osmotic effect that PLTX exerts in many cellular systems, as underscored by cell swelling and haemolysis of erythrocytes (Rossini and Bigiani, 2011). Also in these cell models, Na^+ overload can trigger Ca^{2+} overload, inducing Ca^{2+}-dependent cytotoxic effects such as actin depolymerisation in rabbit intestinal cells (Ares et al., 2005) as well as in human intestinal cells (Valverde et al., 2008b). Finally, it has been demonstrated that intracellular calcium overload may trigger directly cell death cascades in bovine aortic endothelial cells (Schilling et al., 2006).

Studies conducted on different cell models, such as rat liver cells, murine and rat macrophages, porcine and bovine endothelial cells, mouse fibroblasts and rat keratinocytes, have revealed that PLTX acts as a tumour promoter. In these models PLTX stimulates the metabolism of arachidonic acid and prostaglandin production, common effects to many tumour promoters (Wattenberg, 2007). The mechanism leading to tumour promotion could also be explained by activation of the three major MAP kinases (MAPK), ERK, JNK and p38, thereby regulating gene transcription of several pro-tumour factors. In addition, studies performed on murine Swiss 3T3 fibroblasts have demonstrated the ability of the toxin to modulate the activity of the receptors for epidermal growth factor (EGF) (Wattenberg, 2007).

The effects of PLTX observed *in vitro*, together with its mechanism of action, can explain the effects of the toxin observed *in vivo*. After oral administration (gavage) in mice, PLTX shows a high toxicity with a 50% lethal dose (LD_{50}) of 767 μg/kg with symptoms such as difficulty of breathing, cyanosis and paralysis. Hemato-clinical analysis revealed high levels of CPK and LDH at a dose of 600 μg/kg, as well as AST at upper doses. Histological analysis revealed acute inflammation in non-glandular portion of the stomach of the mice survived for 24 hours after treatment (Sosa et al., 2009). However, the toxin appears to be highly more toxic after parenteral routes. The LD_{50} calculated after intravenous administration is, indeed, of 0.74 μg/kg (Mahnir et al., 1992). After intratracheal administration in mice, PLTX causes hemorrhage and alveolar destruction and death at a concentration of 2 μg/kg (Ito and Yasumoto, 2009).

Cardiovascular toxicity of PLTX was evaluated in anesthetized dogs. However, PLTX used in this study was only partially purified, owning a MW of 3300 Da. Intravenous administration of 0.06 μg/kg PLTX induces a transient increase in blood pressure followed by a rapid hypotension and death within 5 minutes. In this model, moreover, PLTX causes constriction of the coronary as well as femoral and kidney arteries inducing blood flow interruption at the concentration of 0.04 μg/kg (Ito et al., 1982).

1.2 Palytoxin and the skin: toxic effects after cutaneous exposure

1.2.1 Human reports after palytoxin cutaneous contact

The risk for human health associated to PLTX exposure is not limited by the quite well-documented number of case reports dealing with contaminated seafood (Cap. 1.1.3). An alternative exposure route, even if highly underestimated, is the cutaneous contact with PLTX (fig. 6).

Today, zoanthids are commonly sold in the home aquarium trade and there is a great deal of conflicting information available to assess the risks of PLTX exposure from store-bought aquarium zoanthids. Indeed, well documented examples of PLTX poisonings from direct contact with zoanthids are limited. One of the first reports occurred during the first collections of *P. toxica* in Hawaii in the early 1960's (Moore et al., 1982). While collecting zoanthid colonies in shallow rock pools, with bare hands and feet resulting in small cuts and abrasions, a researcher experienced dizziness, nausea, headache, increasing malaise, and discomfort to the hands and feet. The first well documented case of PLTX–induced toxicity due to handling a zoanthid coral (*Parazoanthus* ssp.) has been recently reported. The patient, who cut his fingers while cleaning his seawater aquarium, experienced dermal distress with swelling, paresthesia and numbness around the site of injury as well as systemic symptoms. Analysis on the coral revealed the presence of PLTXs (Hoffmann et al., 2008). Signs of dermotoxicity (edema, erythema, urticarial rush and pruritus) that persisted for several days, associated to metallic taste and perioral paresthesia have been described in a patient handling a zoanthid coral with intact skin. The developed symptoms suggested the authors to attribute the observed effects to PLTX, even without confirming analytical data. Moreover, on the basis of the systematic symptoms observed, a possible dermal absorption of the toxin has been hypothesized (Nordt et al., 2009). Another case of PLTX dermal toxicity involved a man in Georgia who contacted with his left hand a "red and pink zoanthid". The symptoms resulted

in chest pain, light-headedness, weakness and numbness on the left arm, requiring hospitalization (Deeds and Schwartz, 2010). Upon admission, the patient showed elevated CPK levels suggestive of mild rhabdomyolysis, and his heart rate and blood pressure were elevated (116 bpm and 184/96 mmHg, respectively).

Fig. 6. *Amatorial images taken by aquarium hobbyist of presumed PLTX-induced dermatitis after cutaneous contact with zoanthid corals (source: www.wetwebmediaforum.com; www.algaebase.org).*

In the temperate area of Mediterranean sea, instead, the risk is associated to *Ostreopsis* blooms. As previously described (Cap. 1.1.3), the epidemiological data describe toxic effects via aerosol exposure to seawater during *O. ovata* blooms; the symptoms developed were rhinorrhoea, cough, respiratory distress, fever, conjunctivitis and also skin irritation (Durando et al., 2007; Gallitelli et al., 2005; Kermarec et al., 2008; Tichadou et al., 2010). Moreover, in summer 2005, a 5 % incidence of dermatitis was also recorded after exposure to marine aerosol during *Ostreopsis ovata* blooms in Genoa (Northern Italy) (Durando et al., 2007). However, this incidence is probably underestimated because of the non-required hospitalization due to the low hazard of this symptom with respect to the other. Erythematous dermatitis were also observed in patients exposed to marine aerosol during *Ostreopsis* blooms along Puglia coasts (Gallitelli et al., 2005). Recently, in the same area, dermatological problems arose in fishermen after the contact with the brown mucilaginous water dripping from the fishing nets containing up to 1.12×10^8 cells/L of *Ostreopsis ovata* (Ungaro, personal

communication). Although chemical analyses were not carried out, it could be hypothesized that PLTX and/or PLTX–like compounds were responsible for the observed cutaneous effects. Furthermore, observations carried out by the "French Mediterranean Coast *Ostreopsis* Surveillance Network" performed along the French Mediterranean and Monaco coasts from 2006 to 2009 concluded that symptoms observed after direct exposure to *O. ovata* were variable, but skin irritation was the most common sign and might be the only one in presence of low *Ostreopsis* concentrations in seawater (Tichadou et al., 2010).

1.2.2 The skin

Skin is a highly vulnerable and visible organ that interfaces with the environment. Therefore, the anatomical structure of the skin is important to bring its functionalities of environmental barrier, penetrations, absorption and immunological defense from chemicals, particles or other insults. Skin is the largest organ system of the body and is anatomically divided into two principal layers: the epidermis (composed of a stratified epithelium) and the underlying dermis (fig. 7, Monteiro-Riviere, 2010).

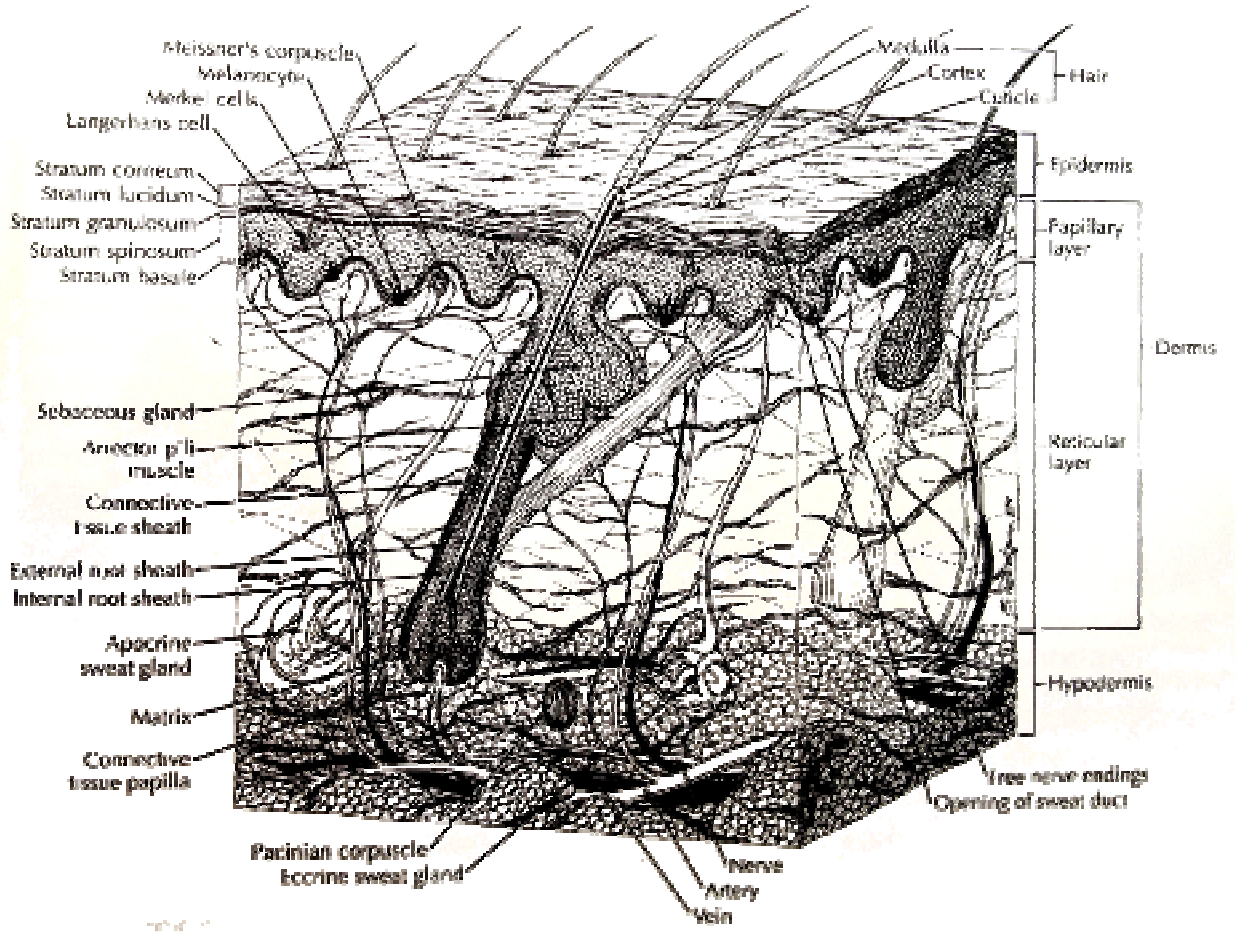

Fig. 7. *Scheme of a generic skin illustrating the cell layers and general overview of the skin structures (source: Monteiro-Riviere, 2010).*

Epidermis

The epidermis is a keratinized stratified squamous epithelium derived from ectoderm and forms the outermost layer of the skin. The epidermis consists of two primary cell types: the keratinocytes and the non-keratinocytes. The latter consist mainly in melanocytes (pigment formation), Merkel cells (sensory perception) and Langerhans cells (immunological function). The firsts, instead, are the major cell type of the epidermis and consist of filamentous proteins and keratins. These cells undergo a spontaneous proliferation, differentiation and keratinization in order to form the different layer of the epidermis (Monteiro-Riviere et al., 1990). These layers are organized in:

- *stratum basale*, constituted by a single layer of columnar or cuboidal cells that are anchored to the basement membrane by hemidesmosomes and laterally to each other and to the upper layer (*stratum spinosum*) by desmosomes. Cell turnover in normal human skin is maintained by constant mitosis and takes approximately 30 days.
- *stratum spinosum*, consists of several layers of polyhedral-shaped cells characterized by the high number of tonofilaments and connected by tight junctions.
- *stratum granulosum*, constituted by three to five layers of flattened cells containing irregularly shaped keratohyalin granules. These granules contain structural proteins involved in keratinization and barrier function.
- *stratum lucidum*, present only in specific area of the body where the skin is thick and lacks of hair.
- *stratum corneum*, the outermost layer of the epidermis, directly in contact with the environment. It consists of several layers of completely keratinized dead cells, constantly replaced.

Keratinization is the process by which in the *stratum basale* keratinocytes differentiate migrating upward till the *stratum corneum*. The signal inducing this spontaneous differentiation seems to come by the α5β1 integrin that holds keratinocyes to the basement membrane. The process involves an increased volume of the cytoplasm and synthesis of differentiation products such as tonofilaments, keratohyalin granules and lamellar granules. As the cellular contents increase, the nuclei as well as other cellular organelles such as mitochondria and ribosome disintegrate and the lamellar granules discharge their contents into the intercellular space, hence, coating the cells. The final product of the keratinization process is *stratum corneum* formation, that consists of protein-rich cells containing fibrous keratin and keratohyalin surrounded by a thicker plasma membrane coated by a lipid matrix derived from the granules membranes (Elias, 1983).

Dermis

The dermis is of mesodermal origin, owning the function of supporting the epidermis through a network of irregular connective tissues extending to the hypodermis or subcutaneous tissue (fig. 7). The matrix of this connective tissue is composed by collagen and both elastic and reticular fibres, firmly connected in an amorphous mucopolysaccharides substance providing the physical support for nerves and vascular networks. The main cell types present in the dermis are fibroblast, mast cells and macrophage. Furthermore, along nerves, blood and lymphatic vessels plasma cells, chromatophores, fat cells and leukocytes are often found. A major component of the dermis is the extensive network of capillaries in order to maintain body temperature. Indeed, blood flow through skin can vary by a factor of 100-fold depending on the environment conditions, making the skin one of the most highly perfused organ of the body (Monteiro-Riviere, 2010).

1.2.3 Skin inflammation

The skin has important biological functions, by which the most evident is the constitution of an effective physical barrier to the environment that is, consequently, exposed to harmful external hazards. Considering the large variety of these stimuli it is difficult to completely summarize all the reactions involved in skin inflammation. Hence, in view of the chemical properties of PLTX, this chapter will be focused only on skin reactions involved in chemical insults. Among these reactions the most common are atopic dermatitis (AD) and irritant contact dermatitis (ICD). The latter is a non-immunological, local inflammatory skin reaction localised in epidermis and in outer dermis, occurring in response to irritant chemical exposure (Welss et al., 2004), whereas AD is an allergic-based inflammation disease characterized by an intense infiltration of lymphocytes, monocytes and eosinophils (Briganti and Picardo, 2003). In both cases, keratinocytes, as the predominant cell type in skin, play a basic role in the initiation, modulation and regulation of cutaneous inflammatory reactions due to chemical or physical insults. These regulations consist mainly in generation of cytokines via transcription factors activation and regulation of ROS balance (Cap. 1.2.4). There is increasing evidence that epidermal cytokines may have an important role in mediating inflammatory and immune responses in the skin, resulting in vasodilation and infiltration of immune system cells into the epidermis and the dermis. Thus, the resulting pathophysiological signs are erythema, skin induration and oedema, as summarized in figure 8. A part from keratinocytes, a number of cell types in the epidermis are capable of secreting cytokines, including Langerhans cells, melanocytic cells, and even Merkle cells. However, in the epidermis keratinocytes are the major source of cytokines that normally are not actively secreted by keratinocytes. However, a number of agents are capable of mediating keratinocyte cytokine production, including cytokines themselves (Ansel et al., 1990).

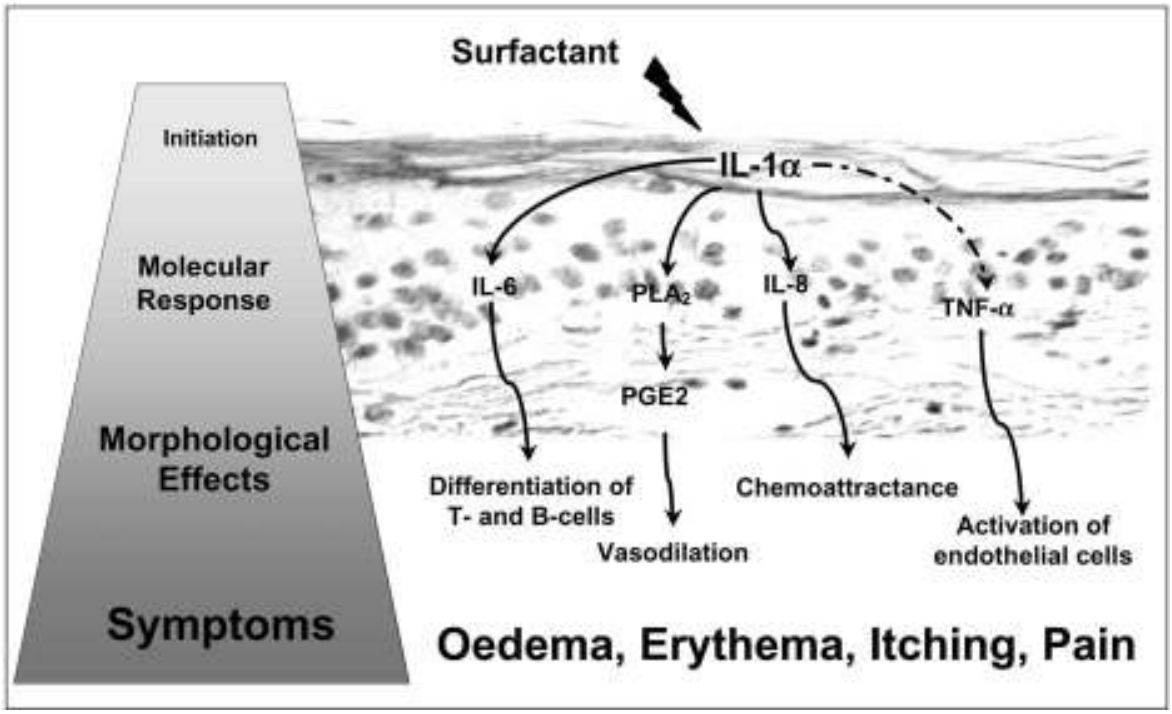

Fig. 8. *Proposed mechanism of the pathway of skin inflammation induced by irritant substances such as surfactants. The process initiates with the release of IL-1α, subsequently leading to the induction of secondary mediators (molecular responses), followed by morphological alterations and, finally, the onset of typical symptoms of contact dermatitis (source: (Welss et al., 2004).*

Skin cytokines can have pro- as well as anti-inflammatory behaviour, and dysfunction in their balances can induce inflammatory diseases (Feliciani et al., 1996). Cytokines provide a cell-to-cell communication system between adjacent cells (paracrine effect), between cells at distant sites (endocrine effect), and intercellular effects (autocrine effect). While cytokines have diverse functions, they have common characteristics. Cytokines can be divided into different groups basing on their functions, origin and chemical structures: interleukins (IL), tumour necrosis factors (TNF), chemokines, colony-stimulating factors (CSF), interferons (IFN) and growth factors (GF).

Cytokine	Produced by Keratinocytes	Functions
IL-1	Yes	Keratinocyte and endothelial cell proliferation; neutrophils, NK, T-cell, B-cell, and macrophage activation. Chemotactic for T- and B-cells. Induces PMN degranulation and adherence on endothelium. Cytostatic and/or cytotoxic for certain tumor cell lines. Increased collagen synthesis by fibroblasts and fibroblast proliferation, but also increased collagenase activity. Induces hepatic synthesis of certain acute-phase proteins, pyrogenic and cachectic effects. Increases synthesis of CSFs, IL-1, IL-2, IL-2R, IL-6, IL-8, IFN-7, TxA2, PGE2, LTB4. Increases ICAM-1, ELAM, VCAM-1 expression. Several overlapping effects with IL-6 and TNF-a
IL-2	No	T-cell growth factor, induces lymphokine-activated killer cells, activates cytotoxic T-cells
IL-3	(mouse)	Supports the growth and differentiation of pluripotent bone-marrow-derived stem cells, growth factor for mast cells
IL-4	No	B-cell growth and differentiation factor, growth factor for T-cells and mast cells. Eosinophil recruitment
IL-5	No	B-cell activation, growth and differentiation, eosinophil differentiation and chemoattraction
IL-6	Yes	Induces hepatic synthesis of acute-phase plasma protein, stimulates B-cells, weak antiviral properties. Several overlapping effects with IL-1 and TNF-a
IL-7	Yes	B- and T-cell proliferation, maturation of eosinophils and B- and T-cell precursors
IL-8	Yes	Chemotactic for neutrophils and T-lymphocytes
IL-9	No	T-cell growth factor in leukemic cell lines
IL-10	Yes	Inhibitory factor in contact sensitization and inhibits T-cell proliferation; IL-2 mediated; TH-2 cytokine with inhibitory effects on TH-1 cytokines
IL-11	Yes	To be elucidated
IL-12	Yes	Increases TH-1 response. Important in TH-1/TH-2 balance.
IL-13	No	Induces IL-1 ra and IL-6 mRNA production on monocytic cells
IL-15	?	T- and B-cell activation, IL-2 receptor-related
GM-CSF	Yes	Stimulates formation of granulocytes, macrophages, and, at higher concentrations, eosinophil colonies from pluripotent hematopoietic stem cells
G-CSF	Yes	Preferentially stimulates granulocyte colonies and, at higher concentrations, macrophage colonies
M-CSF	Yes	Stimulates macrophage colonies from pluripotent stem cells
TNF-a	Yes	Necrosis of some tumors *in vivo,* cytostatic for certain cell lines *in vitro,* many overlapping functions with IL-1; several overlapping effects with IL-6 and IL-1
TNF-p	No	Cytostatic and cytotoxic for some tumor cell lines *in vitro,* necrosis of some tumors *in vivo,* many overlapping functions with IL-1
IFN-7	No	**Cytotoxic for T-cell, NK, and monocytes, stimulates IL-1 and IL-2 synthesis, induces immunoglobulin production, upregulates ICAM-1 expression**

Tab. 1. *Function of immunoregulatory and pro-inflammatory cytokines present in human keratinocites (source: Feliciani et al., 1996, modified).*

Keratinocytes synthesize and secrete a variety of these cytokines (table 1, Feliciani et al., 1996), the most important of them are:

- *Interleukin 1 alpha (IL-1α)*. Is believed that IL-1α is the main switch in the initiation of skin inflammation. It is constitutively expressed in keratinocytes of all epidermal layers, accumulated in the cytoplasm or in a membrane-bound form. Therefore, IL-1α is only released from leaky cells following cell injury or membrane perturbation. Moreover, IL-1α induces the expression of itself as well as other pro-inflammatory cytokines like IL-6 and IL-8 by binding to the IL-1 receptor I, which is expressed on keratinocytes plasma membrane. At the molecular level IL-1 is a potent regulator of NF-*k*B pathway as well as activator of the activating protein 1 (AP-1), therefore controlling various genes expression associated with the regulation of epidermal homeostasis and inflammation (Welss et al., 2004).

- *Interleukin 6 (IL-6)*. The major mediator of the acute phase response of skin inflammation also acting as an endogenous pyrogen. It is produced by keratinocytes, monocytes, Langerhans cells, fibroblasts, T-cells, endothelial cells and melanocytes. IL-6 is a pleiotropic cytokine that augments immunoglobulin production by B-cells, enhances B-cell growth and differentiation, stimulates the proliferation of T-cells as well as of keratinocytes themselves. It is able to synergize with IL-1 in augmenting antigen presentation, thus enhancing inflammatory reactions (Feliciani et al., 1996).

- *Interleukin 8 (IL-8)*. It is a potent neutrophil chemoattractant and activating factor produced by a variety of cells, including monocytes, fibroblasts, endothelial cells, keratinocytes, melanocytes and Langerhans cells. Its production is augmented by the primary cytokine IL-1, IFN-γ and TNF-α. IL-8 is primarily a neutrophil chemoattractant with some T-cell chemoattractant activity by enhancement of cell adhesion molecule on neutrophils. Intradermal injected IL-8 induces neutrophil accumulation in dermis surrounding the dermal blood vessels.

- *Interleukin 10 (IL-10)*. IL-10 has immunosuppressive properties and may inhibit cytokine synthesis as well as T-cell proliferation. Cellular sources of IL-10 include macrophages, B cells and keratinocytes (Feliciani et al., 1996). IL-10 might represent an important co-factor in the recovery phase of skin inflammation, since it has been demonstrated that it is a natural suppressant of irritant responses, and it limits immunopathologic damage in the skin (Wells et al., 2004).
- *Tumor necrosis factor alpha (TNF-α)*. It is a pleiotropic pro-inflammatory cytokine that influences the development of inflammation by inducing the expression of cell adhesion molecules. TNF-α is stored in the epidermal mast cells, monocytes, macrophages, lymphocytes and produced by keratinocytes after stimulation (Wells et al., 2004). TNF-α induces fever, hypotension, leukopenia, local tissue necrosis, PGE_2 and collagenase synthesis, fibroblast proliferation, and collagen synthesis (Feliciani et al., 1996).
- *Interferon*. IFNs are intimately concerned in innate immunity and involved in helping to induce the acquired immune response. Among all, the most important is IFN-γ, the most potent activator of antigen presentation and major histocompatibility complex (MHC) class II expression. In general, all IFN (α, β, γ) are powerful upregulators of MHC class I.

Another important pathway driving cutaneous inflammation involves the eicosanoids, which are generated from arachidonic acid (AA) metabolism, after its release from the membrane-bound form by activation of phospholipase A_2 (PA_2). Indeed, eicosanoids, such as prostaglandins (PGs) and leukotrienes (LTs), are important mediators of the inflammation. The oxidative metabolism of AA is catalysed by two main enzymes: cyclooxigenase (COX) and lipoxygenase (LOX), producing PGs and LTs, respectively (fig. 9). The firsts are key

enzymes involved in a variety of physiological functions. At least two isoforms have been well characterized: COX-1 is the house-keeping isoform constitutively expressed in most tissues, whereas COX-2 is induced by pro-inflammatory agents. LOX are a family of non-heme iron dioxygenases that insert molecular oxygen into polyunsaturated fatty acids. There are several isoforms, among which the most common in human epidermis is e12S-LOX (Bickers and Athar, 2006).

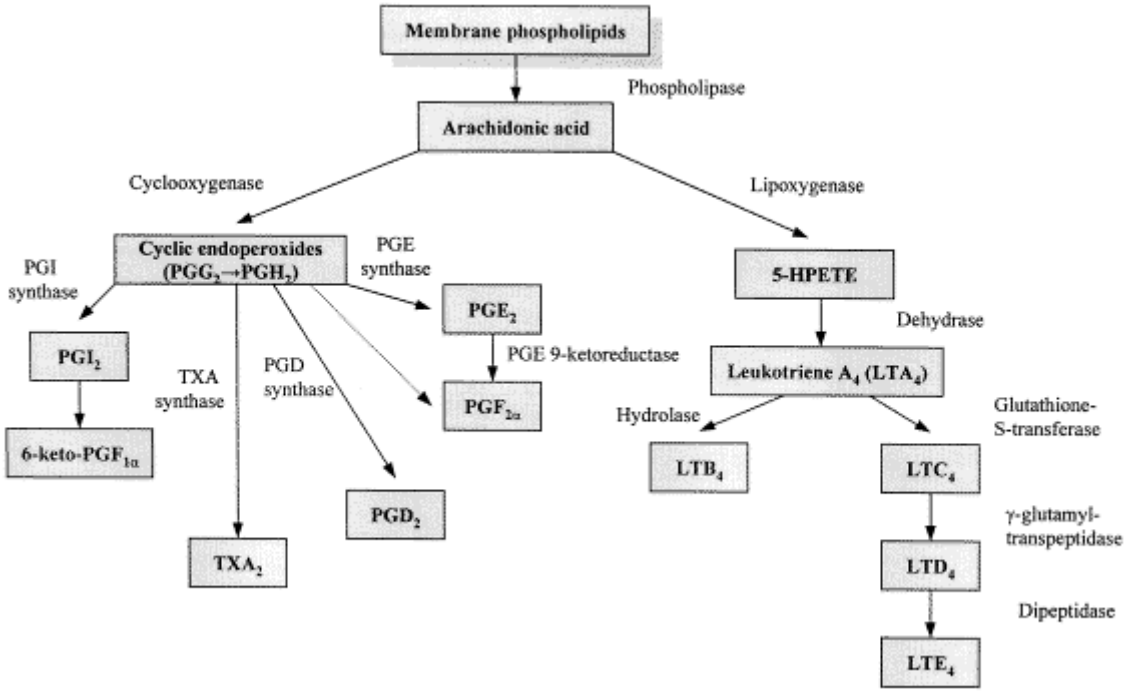

Fig. 9. *Scheme of arachidonic acid (AA) metabolism. After the release of the membrane-bound form of AA by Phospholipase A_2 (PA_2), prostaglandins (PGs) and leukotrienes (LTs) are synthesized by activation of cyclooxigenase (COX) and lipooxigenaase (LOX).*

Regarding skin inflammation, prostaglandin E_2 (PGE_2) is the best investigated prostaglandin. For instance, high level of PGE_2 has been found to be released after irritation with various irritants (Welss et al., 2004) as well as in sensitive and diseased (psoriasis and eczema) skin types (Reilly et al., 2000). Moreover, increased concentrations of arachidonic acid and prostaglandins have been found in human sustained skin inflammation induced by ultraviolet irradiation. Furthermore, also abnormal AA metabolism by the LOX pathways is associated

with lesion inflammatory skin disorder. For instance, leukotriene B4 (LTB_4) is one of the most potent chemokinetic agents for polymorphonuclear cells *in vitro* and *in vivo* (Black et al. 1985). Enhanced levels of LTB_4 and 5-lypoxigenase metabolites of AA have been also identified in inflamed skin due to atopic dermatitis and psoriasis (Ruzicka et al., 1986).

1.2.4 Oxidative stress in skin

Skin provides the major interface between the environment and the body, constantly exposed to chemical and physical environment pollutants. These compounds or their metabolites are inherent oxidants and/or directly or indirectly drive the production of a variety of reactive oxygen species (ROS). Hence, it is well accepted that ROS imbalance is largely involved in the pathogenesis and maintenance of skin inflammation diseases, such as atopic dermatitis, psoriasis and irritant contact dermatitis (Briganti and Picardo, 2003). Moreover, it has been recently observed the induction of oxidative stress following irritation (Welss et al., 2004). Some skin irritants, indeed, generate free radicals and ROS directly through metabolic activation, redox cycling or other mechanism, which function as second messengers (Turner et al., 1998; Bickers and Athar, 2006). However, non-physiologic level of ROS can cause cellular damage by oxidising nucleic acids, proteins and membrane lipids, resulting in altered gene expression and cytotoxicity. Superoxide anion (O_2^-) is one of the primary ROS, which formation is generally catalysed by a flavonic group (i.e. NADPH, NADH, FADH2) through the one-electron reduction of molecular oxygen. Further reduction of oxygen produces hydrogen peroxide (H_2O_2). This can arise from the dismutation of O_2^- that can occur spontaneously at low pH as well as catalysed by superoxide dismutase (SOD) (Hancock et al., 2001). Nitric oxide (NO) is another ROS, implicated in the pathogenesis of several inflammatory diseases and in the paracrine regulation of various biological functions. Its synthesis requires NO synthase (NOS), which converts L-arginine and oxygen into citrulline and NO. Moreover, NO can react with O_2^- to rapidly form peroxinitrite ($ONOO^-$), a highly reactive oxidising agent that elicits cytotoxicity and tissue damages (Chung et al., 1997). NO enhances and triggers several pro-inflammatory process by lipid peroxidation, inhibition of mitochondrial respiratory chain enzymes, inhibition of Na^+/K^+-ATPase, inactivation of Na^+-channel, protein and DNA modifications. Furthermore, it has been demonstrated that $ONOO^-$

is produced in response to a wide range of toxicologically relevant molecules, including environmental toxins (Szabo, 2003).

There is compelling evidence that oxidative stress is involved in the damage of cellular constituents (i.e. DNA), cell membrane lipids and proteins. Indeed, DNA damages induced by ROS includes DNA base damage, DNA single-strand and double-strand breaks, crosslinking between DNA and proteins inducing chromosomal aberrations that may be mutagenic. Furthermore, in keratinocytes exposed to irritant stimuli, several stress-sensitive protein kinases, involving ROS as mediators, are activated. ROS directly alter kinases, phosphatases and transcription factors. Indeed, it has been demonstrated that in human keratinocytes, ROS induce the activation of AP-1 and NF-*k*B, as well as to activate the MAPK pathway, by activating ERK and JNK. ERK pathway mainly mediates cellular response to growth factors, whereas JNK and p38 pathways are involved in cytokines production and physical stress responses (Bickers and Athar, 2006).

On the whole it is reasonable to conclude that high concentrations of ROS are cell and tissue damaging, whereas, by contrast, moderate amounts of ROS take part in cell regulation, acting as second messenger and signal transduction molecules. This suggests that cellular redox levels, especially in keratinocytes, plays a pivotal role in skin homeostasis and that skin diseases could result from an imbalance of the redox state (Briganti and Picardo, 2003).

2. Aim of the study

Palytoxin (PLTX), a marine toxin identified in *Palythoa* zoanthid corals and *Ostreopsis* dinoflagellates, represents an increasing hazard for human health. Human poisonings attributed to PLTX are usually associated to ingestion of contaminated seafood, and to marine aerosol exposure during *Ostreopsis* blooms. However, also dermatological problems have been recently associated to *Ostreopsis* blooms as well as to *Palythoa* corals handling. Well documented reports of poisonings from direct contact with PLTX are limited, but it seems to be well known among the zoanthid coral growers that these coelenterates can cause toxicity through their handling by bare hands. Moreover, the consciousness of the hazard associated to *Ostreopsis* blooms is also increasing among the fishermen.

However, despite the increasing human cases of dermotoxicity attributed to PLTX, scientific literature concerning PLTX dermotoxicity is scarce, and this arises the need for experimental data characterizing PLTX effects on the skin. Hence, the aim of this study is to investigate the harmful potential of PLTX after cutaneous exposure and to gain new insight about its mechanism of action. Thus, a toxicological *in vitro* study will be carried out on spontaneously immortalized human keratinocytes (HaCaT cells), as a first-round screening of dermotoxicity.

The first step of the study will be the characterization of PLTX cytotoxic effects, with particular attention to the putative intracellular pathway involved in cell death. It is known that the molecular target of the toxin is the Na^+/K^+-ATPase. By transformation of the latter in a cationic channel, PLTX induce a massive ionic imbalance. The identification of the chain of intracellular events that follow this primary effect would help to investigate the crucial steps in the signal transduction pathways that culminate in cell death. Hence, this study will focus on the sequence of intracellular alterations following PLTX exposure, investigating the role of mitochondria, of reactive oxygen species, of ionic imbalance itself as well as the nature of cell death induced by the toxin.

Finally, the possibility that PLTX can evoke an inflammatory response in the skin will be investigated with a preliminary evaluation of the ability of the toxin to induce the release of pro-inflammatory mediators from keratinocytes. The results of this study will be useful for addressing a proper pharmacological approach for the treatment of PLTX-induced dermatitis.

3. Materials and methods

3.1 Chemicals

Palytoxin, isolated from *P. tuberculosa*, was purchased from Wako Pure Chemical Industries Ltd. (Osaka, Japan; lot number WKL7151, purity > 90%), HaCaT cell line was purchased from Cell Line Service (DKFZ, Eppelheim, Germany) and all cell culture reagents were from Euroclone (Milan, Italy).

All the other reagents of analytical grade were purchased from Sigma-Aldrich (Milan, Italy) if not otherwise specified.

3.2 HaCaT cells culture

HaCaT cells were cultured in DMEM supplemented with 10% fetal bovine serum (FBS), $1.0x10^{-2}$ M L-Glutamine, $1.0x10^{-4}$ g/ml penicillin and $1.0x10^{-4}$ g/ml streptomycin at 37°C in a humidified 95% air/5% CO_2 atmosphere. Cell passage was performed 2 days post-confluence, once a week.

All the experiments were performed between passage 44 and 70.

3.3 Spectroscopic tests

3.3.1 MTT assay

Cells were seeded in 96-well plates at a density of $3x10^3$ cells/well and after 72 h in culture exposed to PLTX for 4 h. Cells were then washed and wells refilled with fresh culture medium containing 0.5 mg/ml 3-(4,5-Dimethylthiazol-2-yl)-2,5-diphenyltetrazolium bromide (MTT). After 4 h, the insoluble crystals were solubilized by 200 µl/well DMSO and the absorbance was measured by an Automated Microplate Reader EL 311s (Bio-Tek Instruments, Winooski, VT) at 540/630 nm. Data are reported as % of control and are the means ± SEM of at least 3 independent experiments performed in triplicate.

3.3.2 Sulforhodamine B assay

Cells ($3x10^3$/well), seeded in 96-well plates for 72 h, were exposed to PLTX for 4 h. For time course studies, cells were exposed 24 h after plating to $1.0x10^{-10}$ or $1.0x10^{-11}$ M PLTX for 1 up to 24 h. Cells were then fixed for 1 h with 50% trichloroacetic acid (TCA) and exposed to a 0.4% sulforhodamine B (SRB) solution for 30 minutes. The incorporated dye was solubilized in Tris Base Solution pH 7.4. The absorbance was measured by a Automated Microplate Reader EL 311s (Bio-Tek Instruments, Winooski, VT) at 570 nm. Data are reported as % of control and are the means ± SEM of at least 3 independent experiments performed in triplicate.

3.3.3 Lactate dehydrogenase release assay

Cells ($8x10^3$/well) were cultured in 96-well plates for 72 h. Culture medium was then removed and substituted with 200 µl/well of serum-free medium and cells exposed to PLTX for 4 h. Lactate dehydrogenase (LDH) release was measured following the "Tox-7 in vitro

toxicology kit" (Sigma-Aldrich, Milano) manufacturer's indications. Absorbance was measured by an Automated Microplate Reader EL 311s (Bio-Tek Instruments, Winooski, VT) at 490/690 nm. Data are reported as % of positive control and are the means ± SEM of 3 independent experiments performed in quadruplicate.

3.3.4 NBT assay

Cells were plated in 96-well plates at a concentration of $15x10^3$ cells/well. After 4 days in culture, medium was removed and wells refilled with 200 µl of 0.5 mg/ml Nitro Blue Tetrazolium chloride (NBT) in PBS containing $2.5x10^{-2}$ M HEPES. Cells were exposed to PLTX for 1 h and the diformazan solubilized with 140 µl/well DMSO and 120 µl/well 2M KOH. The absorbance was measured by an Automated Microplate Reader EL 311s (Bio-Tek Instruments; Winooski, VT) at 630 nm. Data are reported as % of negative control (cells not exposed to the toxin) and are the mean ± SEM of at least 4 independent experiments performed in quintuplicate.

3.3.5 Griess test

Cells ($10x10^3$ cells/well) were plated for 3 days in 96-well plate. Wells were refilled with PBS containing $5x10^{-2}$ M Hepes and exposed to PLTX for 1h. Griess assay was then performed on 85 µL of medium following manufacturer's instructions (Bioxytech® Nitric Oxide Assay, OxisResearch™, USA). Optical density was measured by an Automated Microplate Reader EL 311s (Bio-Tek Instruments, Winooski, VT) at 540 nm. Data are reported as % of negative control (cells not exposed to the toxin) and are the means ± SEM of 4 independent experiments performed in quintuplicate.

3.4 Fluorimetric tests

3.4.1 Propidium iodide uptake

Cells ($1x10^5$ /well) were seeded for 3 days in 96-well plates and cell membrane integrity was evaluated by measuring propidium iodide (PI) fluorescence inside the cells. Cells were exposed to PLTX for increasing time intervals up to 24 h. Culture medium was then removed and cells were rinsed with 200 µL of $3.0x10^{-6}$ M PI in PBS. As a positive control, 4 µL of Triton-X 0.1% in PBS were added. After 30 minutes fluorescence intensity was read by a Fluorocount microplate Fluorometer (Packard, Germany) with excitation length of 530 nm and emission length of 590 nm. All the samples were then permeabilized with 4 µL of Triton-X 0.1% for 30 minutes to obtain total cell content for each sample and fluorescence read. Data are reported as % of positive control after normalization on cell content and are the mean ± SEM of 4 independent experiments performed in quadruplicate.

3.4.2 DCFDA probe

Cells were plated in 96-well plates at a density of 10×10^3 cells/well and after 3 days in culture exposed for 1 h to PLTX (10^{-8} – 10^{-12} M). Cells were then refilled with PBS containing $1.0x10^{-4}$ M 2',7'-Dichlorofluorescin diacetate (DCFDA) and cells maintained for 30 minutes at 37°C in the dark. Cells were then washed with PBS and fluorescence read by a Fluorocount microplate Fluorometer (Packard, Germany) with excitation length of 485 nm and emission length of 570 nm. Data are reported as % of negative control (cells not exposed to the toxin) and are the mean ± SEM of 4 independent experiments performed in quintuplicate.

3.4.3 JC-1 probe

Cells ($3x10^4$ /well) were cultured in 96-well plate for 3 days and mitochondrial permeability transition pore (MPTP) opening was evaluated using JC-1 Mitochondrial staining kit (Sigma-Aldrich, Milano) following manufacturer's instruction. After PLTX exposure, 50 µL/well working solution of JC-1 (25 µL 200 µM JC-1 diluted with 4 ml of bi-distilled water, 1 ml of 5x staining buffer and 5 mL of culture medium) were added for 20 minutes at 37°C. Cells were then washed twice with ice-cold culture medium and fluorescence was immediately measured by a Fluorocount microplate Fluorometer (Packard, Germany). JC-1 aggregates red fluorescence (intact mitochondria) was detected with an excitation length of 530 nm and an emission length of 590 nm whilst the monomers green fluorescence (disrupted mitochondria) with a 485 nm and 570 nm filter combination. Results were expressed as a ratio between red and green fluorescence and were reported as a % relative to the positive control (0.1 µg/mL valynomicin) and are the mean ± SEM of 5 independent experiments performed in quadruplicate.

3.4.4 Caspasis activation

After 3 days in culture, cells ($1x10^5$ /well) were exposed to PLTX for increasing time intervals up to 24h. Caspasis 3/7, caspase 8 and caspase 9 activations were evaluated following manufacturer's instructions (Sensolyte® AFC Caspase Substrate Sampler Kit, Anaspec). Fluorescence was measured with a Fluorocount microplate Fluorometer (Packard, Germany). Data are reported as % of positive control (10 µM camptothecin) and are the mean ± SEM of 3 experiments performed in quadruplicate.

3.5 Immunocytochemical analysis

3.5.1 DAPI: apoptotic bodies formation

Cells ($2x10^5$ cells/well) were seeded in 24-well plates. After 2 days in culture, cells were exposed to $1.0x10^{-8}$ and $1.0x10^{-9}$ M PLTX for 4 and 8 h and fixed for 30 minutes in 4% PFA at RT. Cells were then washed twice in PBS, and DNA was stained with 1 µg/mL 4',6-diamidino-2-phenylindole (DAPI) for 5 minutes. Images were taken by a epifluorescent microscope (Eclipse E800, Nikon).

3.5.2 DiL: cell membranes integrity

Cells ($2x10^5$ cells/well) were seeded for 2 days in 24-well plates. After staining of plasma-membrane with 10^{-4} M 1,1′-dioctadecyl-3,3,3′,3′-tetramethylindocarbocyanine perchlorate (DiL), cells were exposed to $1.0x10^{-8}$ and $1.0x10^{-9}$ M PLTX for 4 and 8 h. Cells were then fixed for 30 min at RT in 4% PFA and washed twice with PBS. Cell membrane morphology was evaluated by confocal microscopy (Eclipse C1si, on an inverted microscope TE2000U, Nikon).

3.5.3 Palytoxin binding

Cells ($2x10^5$ cells/well) were seeded in 24-well plates. After 2 days in culture, cells were exposed to $1.0x10^{-10}$ and $1.0x10^{-9}$ M PLTX for 10 minutes. Cells were then washed with PBS, fixed for 30 minutes in 4% PFA and blocked for 30 minutes in TBB buffer (Tris-HCl 50 mM, NaCl 0.15 M, 2% BSA and 0.2% Tween 20, pH 7.5) containing 10% horse serum. PLTX binding was then detected by 1:500 monoclonal mAb against PLTX (gently gifted by Dr. Mark Poli, USARMIID) and by 1:200 anti-mouse secondary Ab AlexaFluor488 conjugated. Nuclei were detected by 1 µg/mL DAPI for 5 minutes in PBS. Images were taken by a epifluorescent microscope (Eclipse E800, Nikon).

For immuncolocalization analysis, after DAPI staining, cells were incubated with 10^{-4}M DiL for 10 minutes and images were taken by an epifluorescent microscope (Eclipse E800, Nikon).

3.5.4 May Grumwald-Giemsa

Cells ($2x10^5$/well) were seeded in a 6-well plate for 2 days. Cells were then exposed to PLTX for 4 h and fixed for 1 minute in MeOH. Cells were then stained for 5 minutes in May-Grunwald stain (0.25% in MeOH) and for 7 minutes in Giemsa stain solution (0.1% in PBS). Cells were then washed with distilled water and 40x optical images were taken by light transmission microscope (Orthoplan Leitz, Germany).

3.6 Real time PCR analysis

Cells were seeded for 48 h in 25 cm^2 flask at a density of $5x10^5$ cells/flask. Cells were then exposed for 1, 2, 4, 12 and 24 h to $1.0x10^{-11}$ M PLTX. For the recoveries experiments, cells were exposed for 1 h to $1.0x10^{-11}$ M PLTX, washed and then exposed for 1, 3, 11 and 23 h of recovery time in toxin-free medium. After treatment, cells were collected, washed with ice-cold PBS, total RNA extracted by High Pure RNA Isolation kit (Roche) following manufacturer's instructions and then retrotrascripted by PCR with SuperScriptII 200U (Invitrogen). To quantify the mRNA expression of specific genes, SYBR green real time qPCR assay was performed by LightCycler technology (Roche, Mannheim, Germany) in 20 µl PCR mixture volume consisting of 10 µl of 2X Quantitect SYBR Green PCR Master Mix containing HotStarTaq DNA polymerase (Qiagen, Hilden, Germany), 400 nM of each oligonucleotide primer and 100 ng of retrotranscribed total RNA extracted from each sample per reaction. The amplification was performed with initial activation of HotStar Taq DNA Polymerase at 95°C for 15 min and 40 cycles in three steps: 94°C for 10 s, 60°C for 15 s, 72°C for 30 s for all tested genes. Following cycling, to ensure specificity, melting curve analysis was carried out to verify the amplification of PCR products starting at 60°C and ramping to 95°C at 0.1°C/second. The relative quantifications were performed by specific standard external curves. The normalisation was performed by parallel amplification of beta actin. The specific oligo pairs to amplify genes encoding for ROS producer enzymes (COX-1, COX-2, iNOS, eNOS, nNOS and Nox-2) as well as for β-actin were already published (Dodd et al 2000, Houliston et al 2002, Pierzchalska et al 2007, Fink et al 2008, Gibellini et al 2008). The specific oligo pairs to amplify genes encoding pro-inflammatory cytokines (IL-6, IL-8, IL-1α and TNF-α) were chosen basing on literature data (Lee et al., 2009; Gibellini et al., 2008; Törmä et al., 2006; Wolf et al., 2002). The oligo primer sequences for XO were: forward 5'-GCATATCATTGGTGCTGTGG-3', reverse 5'-GGTCCCCTTTCTCGATCTTC-3'. All aligo pairs were from Invitrogen-Molecular Probes, Milano.

3.7 Western blot analysis

Cells ($1.5x10^6$) were seeded for 4 days in 75 cm^2 culture flask. Cells were then exposed to $1.0x10^{-11}$ M PLTX for 1, 2, 4, 12 and 24 h. Cells were then collected, washed with ice-cold PBS and total protein extracted by 200 µL Lysis Buffer (Tris HCl 10 mM, EDTA 100 mM, NaCl 100 mM and SDS 0.1%) containing 10% of protease inhibitor. Samples were then run on 10% acrilamide gels in a Trys-Glycine buffer using a PAGEr™ Minigel Chamer (Lonza) and then semi-dry blotted for 2h with 50 mA current on PVDF membrane. Membranes were blocked for 1h with 3% not-fat milk in PBS and incubated overnight at 4°C with primary antibodies: anti-actin 1:10000 (Millipore), anti-NOS 1:1000 (Millipore) and anti-NOX 1:500 (Millipore). Membranes were then washed twice with PBS and incubated for 1h at 37°C with secondary anti-rabbit HRP-conjugated 1:10000. Chemiluminescence was developed by using LiteAblot® TURBO (Euroclone) following manufacturer's instructions and fixed on Kodak Biomax light film.

Western blot analysis performed to evaluate BNIP3 expression was carried out exposing HaCaT cells ($1.5x10^6$ for 4 days) for 4 h to 10^{-13}, 10^{-11} and 10^{-9} M PLTX. Total protein content was extracted as described above and samples were run in 10% acrilamide gels and semi-dry blotted as illustrated above. Membranes were blocked for 1h with 5% not-fat milk in TTBS and incubated overnight at 4°C with primary antibodies: anti-actin 1:2000 (Millipore) and anti-BNIP3 1:1000 (GeneTex). Membranes were then washed four times with TTBS and incubated for 1h at 37°C with secondary anti-rabbit HRP-conjugated 1:5000. After four washes with TTBS, chemiluminescence was developed by using Western blotting luminol reagents (Santa Cruz Biotechnology) following manufacturer's instructions and fixed on Kodak Biomax light film.

3.8 Cell cycle analysis

After 2 days from seeding in 12-well plate, $5x10^5$ cells/well were exposed for 4 or 8 h to $1.0x10^{-8}$ and $1.0x10^{-9}$ M PLTX. Cells were then detached with a PBS solution containing 0.05% EDTA and 0.1% Trypsin and collected in cytofluorimetric tubes. Cells were washed in ice-cold PBS and fixed in 1 mL 70% EtOH. The samples were than stained overnight at 4°C with a PBS solution containing 10 µg/mL PI, 0.05 µg/mL FITC and 40 µg/mL RNAse and cell cycle analysis performed by a cytofluorimeter Cytomics FC 5000 (Coulter Instrumentation, CA, USA). Results are presented as percentage of cells in G0-G1, S and G2M phases, obtained by 5 replicates.

3.9 Binding experiments

Cells ($1x10^4$/well) were seeded in 96-well plates and maintained in culture for 3 days. After 10 minutes exposure to PLTX, cells were washed twice with PBS and fixed for 30 minutes with 4% PFA. Cells were then blocked for 30 minutes in TBB buffer containing 10% horse serum and the toxin detected by 2 µg/mL mouse mAb against PLTX for 1 h at 37°C. Cells were then washed three times with PBS containing 0.1% Tween 20 (PBS/Tw) followed by three washes with PBS. PLTX mAb was detected exposing the cells to a HRP conjugated secondary antibody against mouse (DakoCytomation, Milano) for 1 h at 37°C. After three washes with PBS/Tw and three washes with PBS the colorimetric reaction was started by adding 60 µL 3,3',5,5'-Tetramethylbenzidine (TMB) substrate and stopped by adding 30 µL H_2SO_4 1M. The absorbance was read at 450 nm by a Spectra® photometer (Tecan Italia; Milan, Italy).

3.10 ELISA tests

The amounts of pro-inflammatory cytokines (IL-6, IL-8, IL-1α and TNFα) and pro-inflammatory mediators (PGE_2 and LTB_4) released by the cells were evaluated by ELISA test using commercial kits (Bender MedSystems GmbH and Oxford Biomedical Research, respectively).

Cells were seeded in 25 cm^2 flask at a density of $5x10^5$ cells/flask and after 48 h in culture treated with PLTX following the same experimental conditions of the PCR analysis. Culture mediums of the same samples used for the real time PCR analysis were collected and maintained at -80°C. The ELISA tests were performed according to the manufacturer's instructions, on 50 µL of each samples and absorbances were read at 640 nm by an Automated Microplate Reader EL 311s (Bio-Tek Instruments, Winooski, VT). Results are presented as ng/mL of analyte released by the cells, calculated on the basis of the respective calibration curves and are the mean ± SEM of three independent experiments performed in duplicate.

3.11 Statistical analysis

Results are presented as mean ± SEM from at least three independent experiments. Data were analyzed by two-way ANOVA and Bonferroni post test (Prism GraphPad, Inc.; San Diego, CA) and significant differences were considered at $p < 0.05$. Paired data were analyzed by a two - tailed Student's *t*-test and significant differences were considered at $p < 0.05$.

EC_{50} values were calculated by nonlinear regression using a four parameters curve-fitting algorithm of the SigmaPlot software (Jandel Scientific; Erkrath, Germany). The time required to reduce by 50% cell vitality (T½) was calculated by nonlinear regression using a one phase exponential decay algorithm of the GraphPad Prism software version 4.03 (Prism GraphPad Inc.; San Diego, CA).

The amount of cytokines and pro-inflammatory mediators released by the cells were calculated by nonlinear regression of the respective standard curves using a five parameters curve-fitting algorithm of the SigmaPlot software (Jandel Scientific; Erkrath, Germany).

4. Results

4.1 Cytotoxicity of palytoxin on HaCaT cells

4.1.1 Concentration-dependency of palytoxin effects

Cytotoxicity of PLTX on HaCaT cells was initially investigated by three methods that evaluate different end points: the MTT reduction assay, that measures the dehydrogenases activity in mitochondria, the SRB assay, that indicates cell mass through the measurement of cellular protein content and, finally, the LDH release, a direct marker of cell death.

Figure 10 shows the concentration-effect curves obtained considering these three different end points after 4 h exposure to increasing PLTX concentrations ($1.0x10^{-16}$–$1.0x10^{-7}$ M). The toxin exerted a concentration-dependent reduction of mitochondrial activity starting from $1.0x10^{-12}$ M (-36±7%) that at $3.0x10^{-9}$ M was almost totally abolished (-92±1%). The concentration of PLTX that reduced mitochondrial activity by 50% (EC_{50}) was $6.1±1.3x10^{-11}$ M (fig. 10).

The PLTX concentration–dependent cytotoxic effect was confirmed by SRB assay carried out in cells treated with PLTX under the same experimental conditions. However, compared to the MTT assay, the potency by which PLTX induced the cytotoxic effect was slightly reduced, with an EC_{50} value of $4.7±0.9x10^{-10}$ M. Indeed, a reduction of cell mass was observed at $5.0x10^{-12}$ M PLTX (-19±1%) with a maximum effect at $1.0x10^{-8}$ M PLTX (-90±1%).

Finally, the amount of the cytoplasmic enzyme LDH released by damaged cells was evaluated. As shown in figure 10, after 4 h exposure to the toxin, a concentration–dependent leakage of LDH was found with an EC_{50} of $1.8±0.1x10^{-8}$ M. At $1.0x10^{-7}$ M PLTX, the release of LDH was equal to that of positive controls (lysed cells, 100% release).

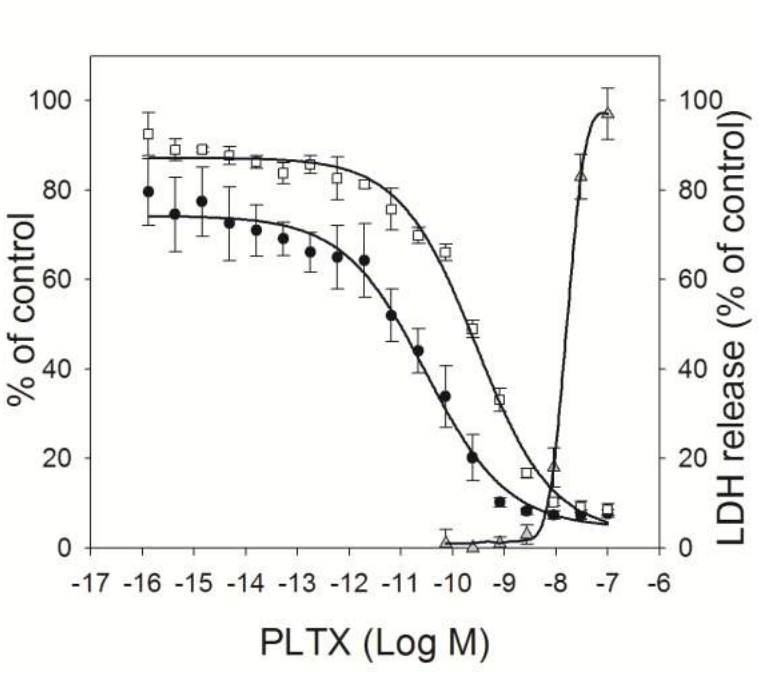

Fig. 10. *PLTX effect on mitochondrial activity (●, MTT assay), cell mass (□, SRB assay) and LDH release (▲). Cells were exposed to increasing concentrations of PLTX for 4 h before performing the assays. Data are reported as % of controls and are the means ± SEM of 4 independent experiments performed in triplicate.*

4.1.2 Time-dependency of palytoxin effects

The influence of time on PLTX effect was investigated exposing the cells to $1.0x10^{-10}$ M PLTX, a concentration that *per se* reduced cell mass by 30 % within 4 h. A significant reduction of protein content was found after an exposure time as short as 1 h (-20±3%, $p<0.001$). As shown in figure 11, prolonging the exposure up to 24 h, the cytotoxic effect increased with a T½ (the time required to reduce by 50% cell mass) of 5.1 h (95% confidence limits: 4.0-7.0 h).

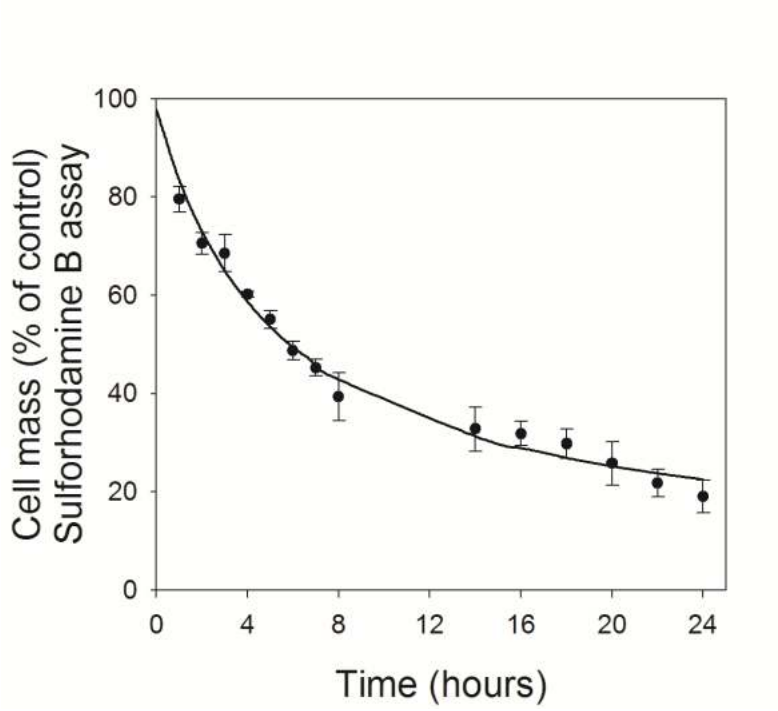

Fig. 11. *Time course of PLTX-induced cytotoxic effect (SRB assay). Cells were exposed to $1.0x10^{-10}$ M PLTX for 1 to 24 h before performing the SRB assay. Data are reported as % of control and are the means ± SEM of 3 independent experiments performed in quadruplicate.*

4.1.3 Irreversibility of palytoxin cytotoxic effect

In order to evaluate whether the damage induced by PLTX was reversible, HaCaT cells were exposed for increasing time intervals (1 up to 8 h) to $1.0x10^{-11}$ M PLTX, a concentration that *per se* reduced cell mass by nearly 20% after 4 h contact. Cell medium was then replaced by toxin-free medium and cells were maintained in culture for 24 h. As shown in figure 12, 1 h exposure to $1.0x10^{-11}$ M PLTX was sufficient to reduce by nearly 40% cell mass, that was further reduced to more than 80% after 8 h of contact. A half-time of 1.3 h (95% confidence limits: 0.9-2.2 h) was calculated.

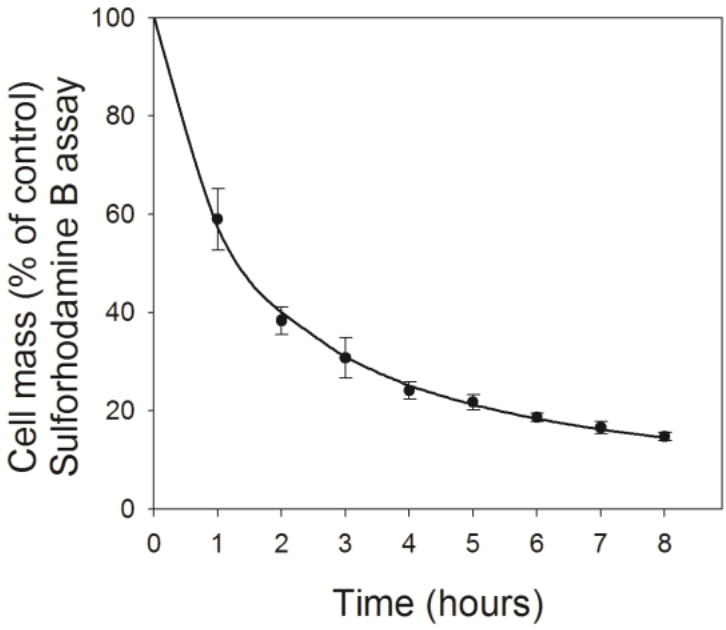

Fig. 12. *Reversibility of PLTX-induced cytotoxic effect (SRB assay). Cells were exposed to $1.0x10^{-11}$ M PLTX for 1 up to 8 h and then to toxin-free medium for 24 h before performing the SRB assay. Data are reported as % of control and are the means ± SEM of 3 independent experiments performed in quadruplicate.*

4.2 Effect of ouabain on palytoxin-induced cytotoxicity

The Na^+/K^+-ATPase is considered the main molecular target of PLTX and several experimental data demonstrated that ouabain, a well known blocker of the pump, counteracts some PLTX activities *in vitro* (Habermann and Chhatwall, 1982; Schilling et al., 2006; Vale-Gonzalez et al., 2007; Pelin et al., 2012). Cells were pre-exposed for 1 h to $1.0x10^{-5}$ M ouabain and then to the toxin for 4 h. Figure 13 shows the effects of ouabain on PLTX–mediated mitochondrial activity reduction (A), cell mass reduction (B) and LDH release (C).

Ouabain, that *per se* reduced mitochondrial activity by 37±3% with respect to controls, reverted PLTX toxic effect. Indeed, in presence of oubain, the toxic effect of $3.0x10^{-12}$, $3.0x10^{-11}$ and $3.0x10^{-10}$ M PLTX was reduced by 12±2% ($p < 0.01$), 20±4% ($p < 0.01$) and 40±6% ($p < 0.001$), respectively. Ouabain antagonistic effect was evident also on PLTX-induced cell mass reduction (fig. 13B). Compared to cells exposed to PLTX alone, ouabain (16±1% of cell mass reduction with respect to controls) almost totally prevented the cytotoxic effect of $3.0x10^{-11}$ M PLTX ($p < 0.001$) and reduced it by 55±3% ($p < 0.001$) at $3.0x10^{-9}$ M PLTX.

In figure 13C the effect of ouabain on PLTX-induced LDH release is shown. Ouabain, which induction of LDH release was almost null, completely abolished the LDH release induced by the toxin. The effect of $1.0x10^{-8}$ and $3.0x10^{-8}$ M PLTX was reduced by 86±6% ($p < 0.01$) and 97±1% ($p < 0.001$), respectively.

Fig. 13 (next page). *Effect of ouabain on PLTX-induced mitochondrial activity reduction (**A**, MTT assay), cell mass reduction (**B**, SRB assay) and LDH release (**C**). Cells were exposed to $1.0x10^{-5}$ M ouabain for 1 h and then to PLTX for 4 h before performing the assays. Histograms represent cells exposed to PLTX in the absence (■) or in the presence of ouabain (▨). Data are reported as % of control and are the means ± SEM of 4 independent experiments performed in quadruplicate. Statistical differences: **, $p < 0.01$; ***, $p < 0.001$ (Student t-test).*

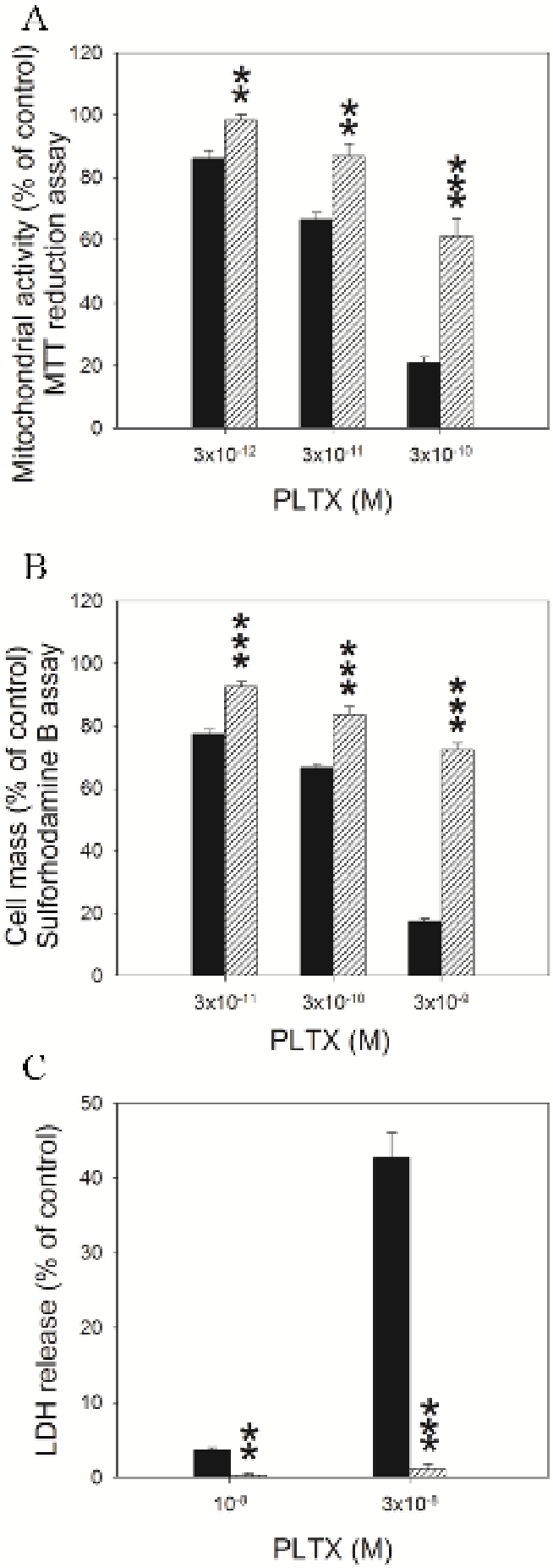
A
Mitochondrial activity (% of control)
MTT reduction assay
120
100
80
60
40
20
0
***
***
***
3x10-12
3x10-11
3x10-10
PLTX (M)
B
Cell mass (% of control)
Sulforhodamine B assay
120
100
80
60
40
20
0
***
***
***
3x10-11
3x10-10
3x10-9
PLTX (M)
C
LDH release (% of control)
50
40
30
20
10
0
**
***
10-9
3x10-8
PLTX (M)

4.3 Binding of palytoxin on HaCaT cells

To demonstrate the occurrence of PLTX binding on HaCaT cells, immunocytochemical analyses were firstly performed using monoclonal antibody against the toxin. Subsequently, PLTX binding was characterized by ELISA test performed on HaCaT cells in culture.

4.3.1 Immunocytochemical analysis

To demonstrate the binding of PLTX to intact cells, immunocytochemical analyses were performed as a qualitative assay. Cells were exposed for 10 minutes to $1.0x10^{-10}$ and $1.0x10^{-9}$ M PLTX and washed twice with PBS in order to remove the unbound toxin. PLTX binding was recognized by adding monoclonal antibody against PLTX and, subsequently, an anti mouse secondary antibody AlexaFluor488-conjugated (green fluorescence). Nuclei were then stained with DAPI (blue fluorescence) and images taken by an epifluorescence microscope. In figure 14 the images obtained exposing the cells to the toxin are compared to the untreated controls. The presence of $1.0x10^{-10}$ and $1.0x10^{-9}$ M PLTX was easily detected by the green signal that, by contrast, was absent in the untreated controls.

In order to evaluate the localization of the toxin on the cell, preliminary co-localization experiments were performed. Cells were exposed for 10 minutes to $1.0x10^{-10}$ PLTX and, after two washes with PBS, the toxin detected as described above (green fluorescence). Nuclei were then stained with 1 μg/mL DAPI (blue fluorescence) and plasma membrane stained with $1.0x10^{-5}$ M DiL (red fluorescence). In figure 15, the three fluorescence are shown alone and after merging. Cells exposed to the toxin displayed a marked green fluorescence (PLTX) that was almost completely overlapped to the red one (membrane) indicating the presence of a binding site for the toxin at the cell surface.

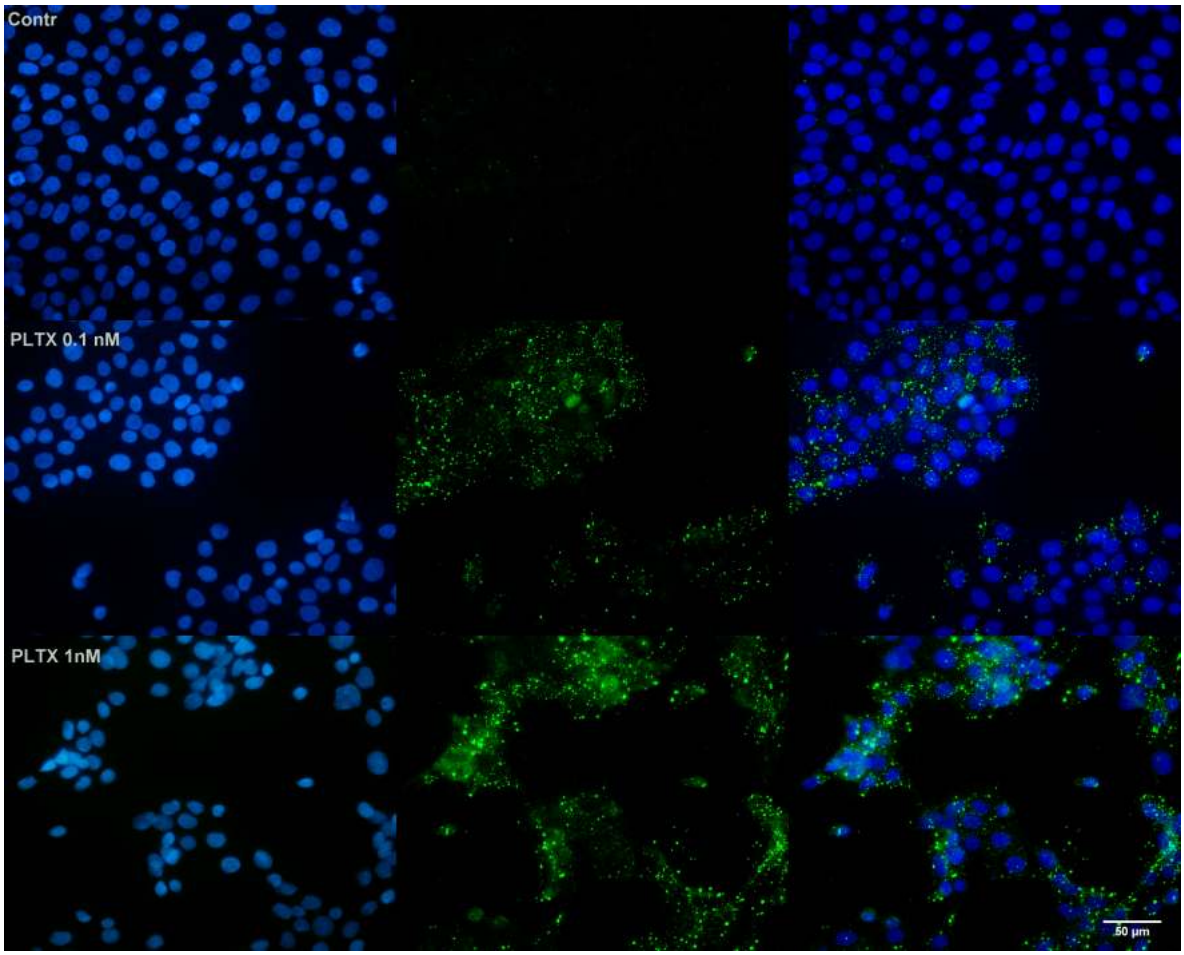

Fig. 14. *Immunocytochemical analysis of PLTX binding on HaCaT cells. Cells were exposed to $1.0x10^{-10}$ and $1.0x10^{-9}$ M PLTX for 10 minutes and PLTX bound detected by monoclonal Ab against PLTX and anti-mouse secondary Ab AlexaFluor488-conjugated (green fluorescence). Nuclei were stained with 1 µg/mL DAPI (blue fluorescence). Images were taken by a epifluorescent microscope (Eclipse E800, Nikon).*

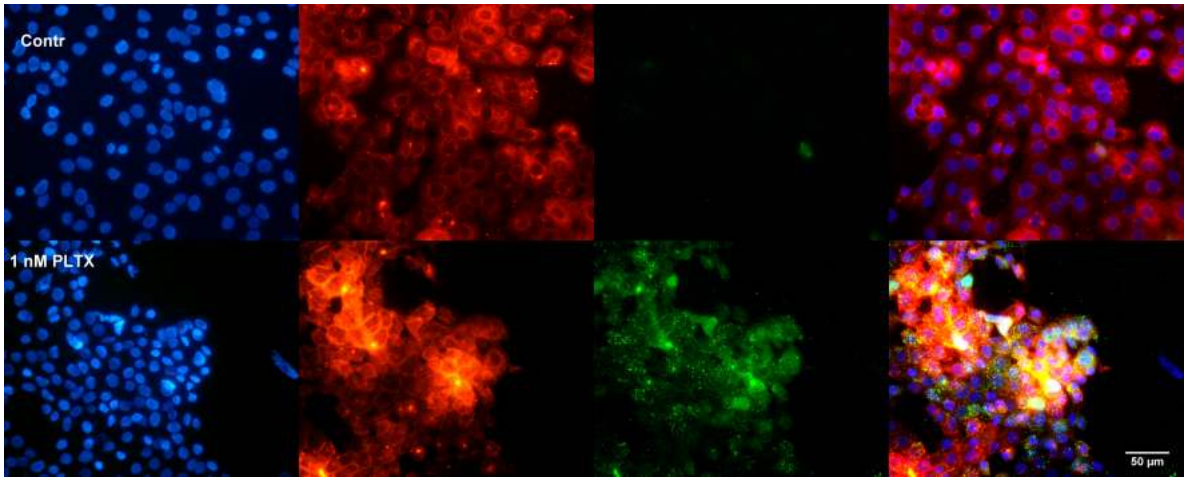

Fig. 15. *Co-localization analysis performed on HaCaT cells. Cells were exposed to $1.0x10^{-10}$ M PLTX for 10 minutes and PLTX bound detected by monoclonal Ab against PLTX and anti-mouse secondary Ab AlexaFluor488-conjugated (green fluorescence). Nuclei were stained with 1 µg/mL DAPI (blue fluorescence) and cell membrane with $1.0x10^{-5}$ M DiL (red fluorescence). Images were taken by epifluorescent microscope (EclipseE800, Nikon).*

4.3.2 Binding experiments

To characterize the binding of PLTX to HaCaT cells, saturation experiments were performed exposing intact cells to increasing toxin concentrations ($1.0x10^{-11}$-$1.0x10^{-8}$ M) for 10 minutes. Nonspecific binding was measured in the presence of $1.0x10^{-3}$ M ouabain. At the end of incubation, PLTX binding was measured by ELISA assay: cells were washed twice in PBS, fixed in 4% PFA and bound PLTX revealed by mAb anti PLTX and anti mouse Ab HRP-conjugated. Panel A of figure 16 shows the three curves depicting the total binding of PLTX (PLTX alone), the nonspecific binding obtained in presence of ouabain, and the specific binding of PLTX (obtained by subtracting the nonspecific binding from the total one). In panel B, PLTX specific binding is reported in a semi-logarithmic graph (fig. 16B). From this curve, Kd value was calculated by nonlinear regression analysis and was equal to $3.0\pm0.4x10^{-10}$ M.

Experiments were then carried out exposing the cells to the PLTX Kd concentration ($3.0x10^{-10}$ M) for increasing time intervals (fig. 17). Association curve of PLTX was obtained exposing the cells to PLTX up to 30 minutes. Under this condition, PLTX was found to quickly bind to HaCaT cells: indeed, an exposure time as low as 10-15 minutes was sufficient to reach the equilibrium. After 30 minutes exposure to $3.0x10^{-10}$ M PLTX, dissociation experiments were than carried out exposing the cells for increasing time intervals up to 30 minutes to the displacer ouabain ($1.0x10^{-3}$ M). Ouabain ability to displace PLTX from its binding sites turned out to occur very rapidly. Indeed, 5 minutes exposure was sufficient to induce a significant displacement of PLTX. However, ouabain was not able to totally displace PLTX, at least up to 30 minutes exposure.

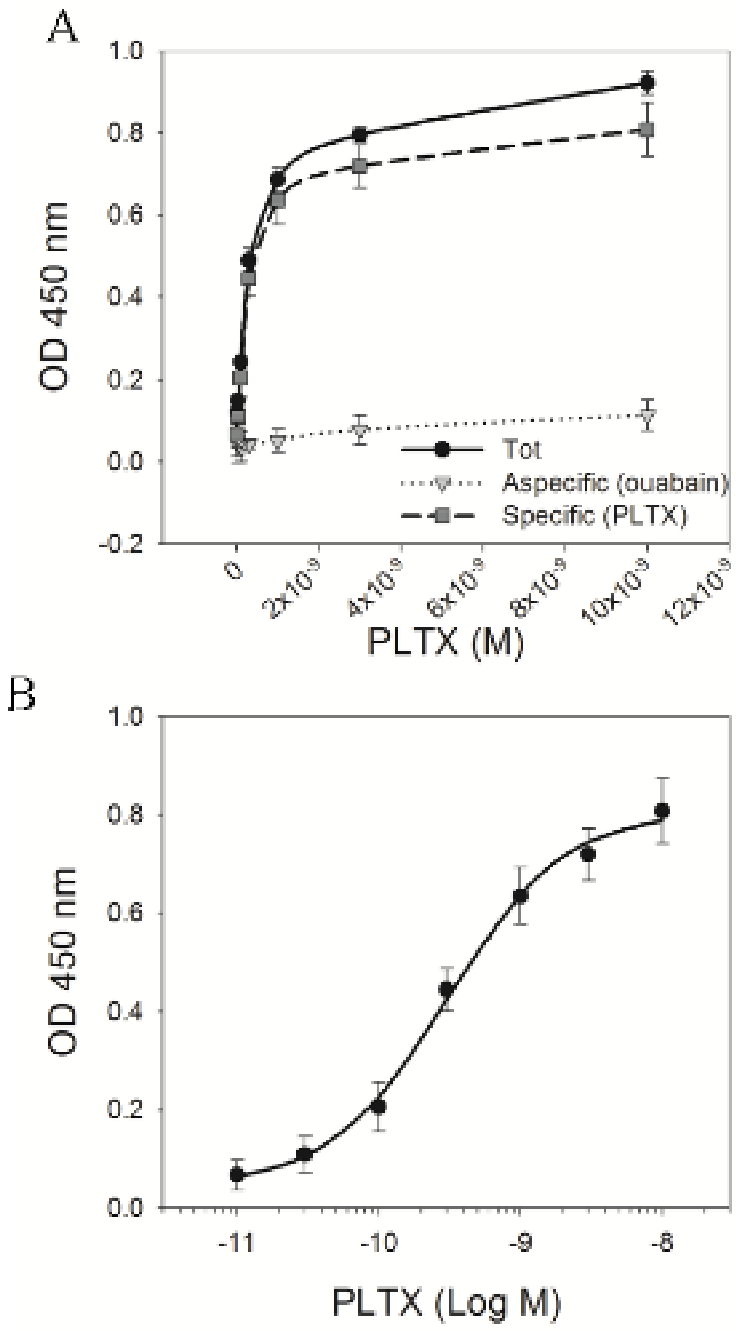

Fig. 16. *PLTX binding to intact HaCaT cells. Cells were exposed for 10 minutes to PLTX ($1.0x10^{-11}$-$1.0x10^{-8}$ M) and the amount of PLTX bound evaluated by ELISA assay.* ***(A)*** *Total binding of PLTX is represented by black dots (●), nonspecific binding, given by PLTX binding in presence of $1.0x10^{-3}$ M ouabain is represented by gray triangles (▽) and the specific binding of PLTX, obtained subtracting the nonspecific binding from the total one isrepresented by gray squares (■).* ***(B)*** *Specific binding of PLTX shown in logarithmic scale. Data are the means ± SEM of 3 experiments performed in triplicate.*

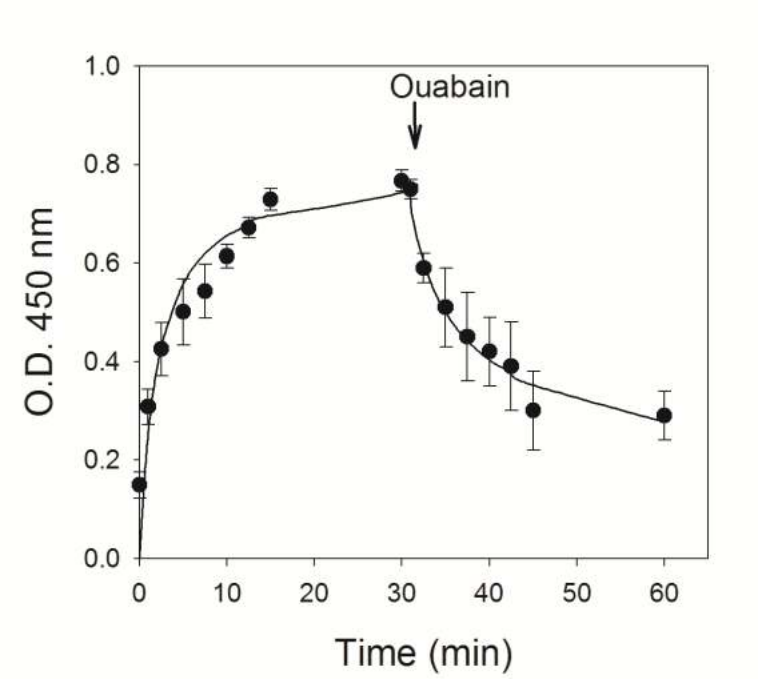

Fig. 17. *PLTX binding: association and dissociation experiments. Cells were exposed for increasing time intervals up to 30 minutes to $3.0x10^{-10}$ M PLTX (association) and subsequently exposed for increasing time intervals up to 30 minutes to $1.0x10^{-3}$ M ouabain. Data are reported as mean ± SEM of 3 experiments performed in quadruplicate.*

4.4 Palytoxin effects on oxidative stress

To evaluate the ability of PLTX to induce oxidative stress, cells were exposed to increasing PLTX concentrations (10^{-12} – 10^{-8} M) for 1 h and the intracellular levels of three different reactive oxygen species (ROS) was measured. The amount of superoxide anion, nitric oxide and peroxynitrite produced were evaluated by NBT assay, Griess assay and DCFDA fluorescence, respectively. As shown in figure 18, PLTX induced a concentration-dependent increase of superoxide anion, that reached 76±4% with respect to the untreated controls at $1.0x10^{-8}$ M PLTX. A significant increase (~15%, $p<0.001$) of superoxide was detectable even at picomolar PLTX concentrations. Under the same experimental conditions neither nitric oxide nor peroxynitrite formation was detected.

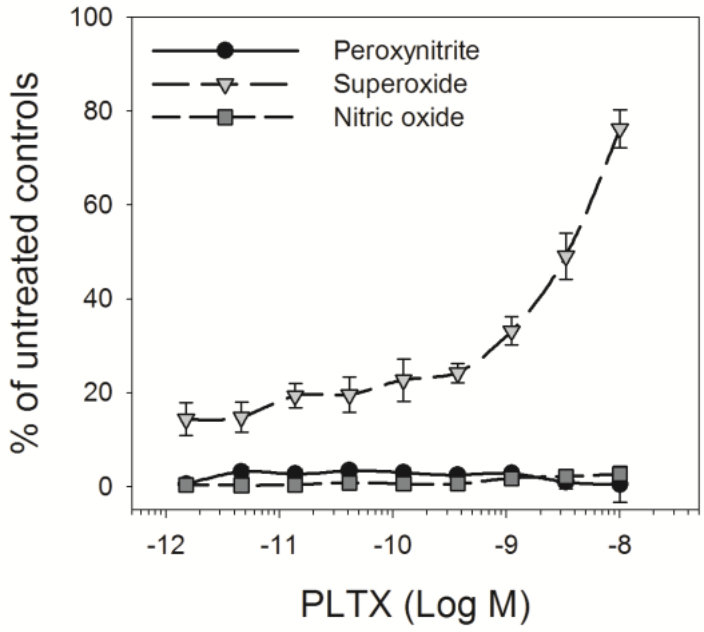

Fig. 18. *Reactive oxygen species (ROS) induced by PLTX. Cells were exposed for 1 h to increasing concentrations of the toxin and superoxide anion (▽), nitric oxide (■) and peroxynitrite (●) were evaluated by NBT assay, Griess assay and DCFDA fluorescence, respectively. Data are reported as % of production with respect to untreated controls and are the means ± SEM of 4 independent experiments performed in quintuplicate.*

4.5 Mechanism of superoxide anion production

To evaluate the mechanism of superoxide induction by PLTX, the role of different enzymes involved in superoxide production have been investigated by genetic, protein and functional approaches.

4.5.1 Effects of PLTX on superoxide anion producer enzymes gene and protein expressions

PLTX effects on gene expressions of ROS-producing enzymes were investigated by real time PCR. Figure 19A shows gene expression profiles of COX-1, COX-2, NOX, iNOS, eNOS, nNOS and XO of cells exposed to $1.0x10^{-11}$ M PLTX for 1, 2, 4, 12 and 24 hours. Under these conditions, no changes in COX-1 and COX-2 gene expressions were observed. On the contrary, a significant, early increase of NOX expression (4.7 folds with respect to untreated controls, $p<0.05$) was found after 2 h of continuative exposure to the toxin followed by a reduction to the control levels after longer exposure periods (4, 12 and 24 h). A similar pattern was observed evaluating XO gene expression, with an increase of ~4 folds only after short exposure time (1-2 h). An early increase of iNOS gene expression was observed between 1-4 h exposure (5.6 folds, $p<0.05$ after 2 h), whereas nNOS and eNOS gene expression were modified only after 12 h exposure to the toxin, with a ~4 folds increase for both enzymes.

These results were confirmed by western blot analysis: one hour exposure increased protein expression of NOX, followed by a progressive reduction after 24 h. Similarly, an increase of iNOS protein expression was observed that peaked at 2 h (fig. 19B).

Similar changes in gene expressions were found exposing the cells for 1 h to $1.0x10^{-11}$ M PLTX, and then to a recovery periods of 1, 3, 11 and 23 hours in toxin-free medium (fig. 19C). Indeed, 1 h exposure to the toxin followed by 1 h recovery time induced a 4.9 folds

increase, with respect to controls, in NOX gene expression, as well as in iNOS gene expression (5.8 folds). A 4 fold increase in the expression of the genes encoding for nNOS and eNOS isoforms was observed prolonging the recovery time to 11 hours. No changes were observed for the other ROS-producing enzymes.

Fig. 19 (next page). *Effects of PLTX on superoxide-producer enzymes gene and protein expressions.* ***(A)*** *Effects of continuous exposure to PLTX on NOX, iNOS, eNOS, nNOS, COX-1, COX-2 and XO gene expressions. Cells were exposed for increasing time intervals (1 up to 24h) to $1.0x10^{-11}$ M PLTX and gene expressions evaluated by real time PCR* ***(B)*** *Effects of continuous exposure to PLTX on NOX and iNOS protein expression. Cells were exposed for increasing time intervals (1 up to 24h) to $1.0x10^{-11}$ M PLTX and protein expressions evaluated by western blot analysis. β-actin was chosen as a control protein.* ***(C)*** *Effect of recovery conditions on ROS-producer enzymes gene expressions. Cells were exposed for 1 h to $1.0x10^{-11}$ M PLTX followed by recovery time intervals of 1 up to 23 h in toxin-free medium and gene expressions evaluated by real time PCR. Statistical differences: *, $p < 0.05$ (Student t-test).*

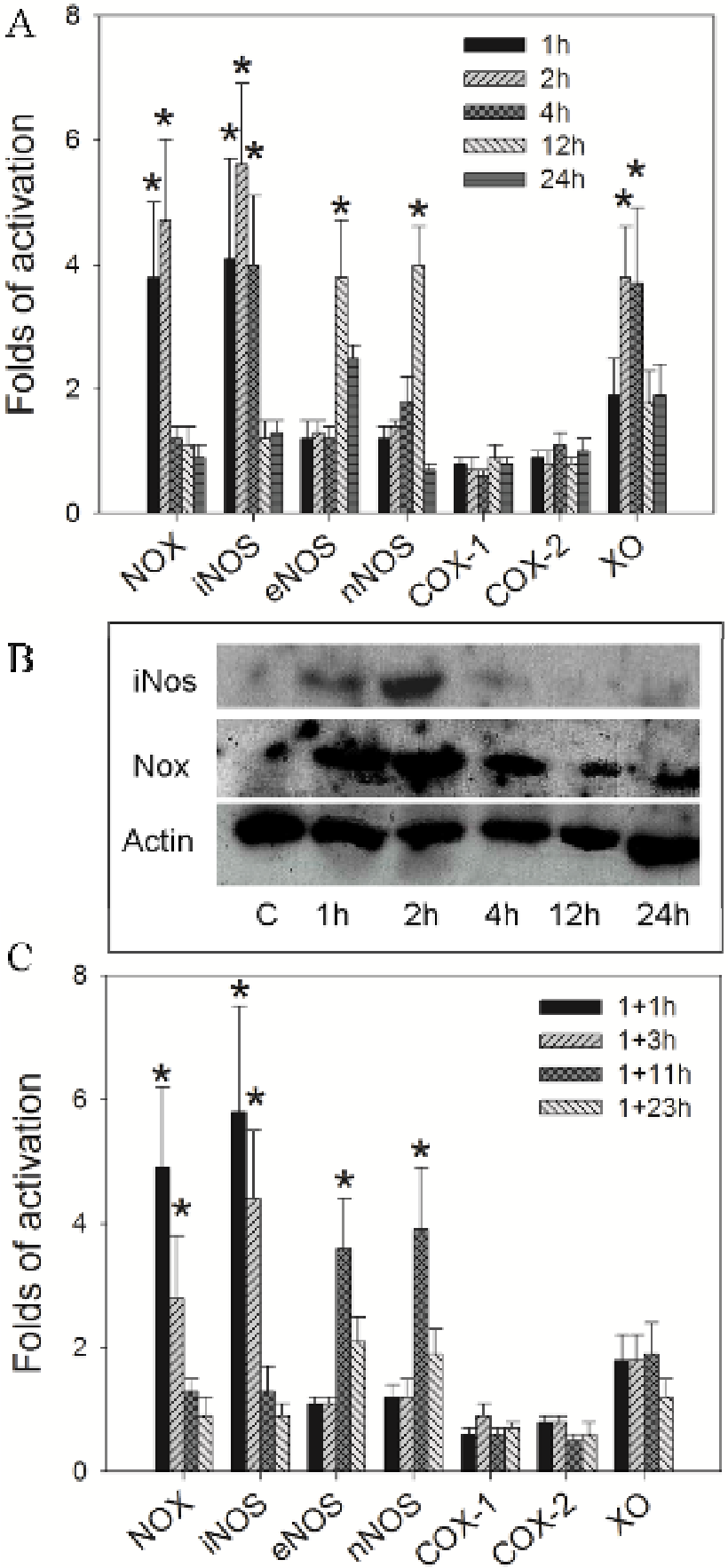
A
Folds of activation
0
2
4
6
8
1h
2h
4h
12h
24h
NOX
iNOS
eNOS
nNOS
COX-1
COX-2
XO
B
iNos
Nox
Actin
C
1h
2h
4h
12h
24h
C
Folds of activation
0
2
4
6
8
1+1h
1+3h
1+11h
1+23h
NOX
iNOS
eNOS
nNOS
COX-1
COX-2
XO

4.5.2 Effects of PLTX on the functional activation of superoxide anion producer enzymes

In order to identify the enzymes involved in PLTX- dependent superoxide anion production, PLTX effects were evaluated in presence of well known inhibitors of the considered enzymes: DPI ($5.0x10^{-6}$ M), a nonselective inhibitor of NOX and NOS, apocynin ($1.0x10^{-5}$ M), a specific inhibitor of NOX, NMMA ($1.0x10^{-4}$ M), a specific inhibitor of NOS, indomethacin ($1.0x10^{-4}$ M), inhibitor of COX, and allopurinol ($1.0x10^{-4}$ M), an inhibitor of XO. Cells were pre-exposed for 1 h to the inhibitors and then to three toxin concentrations (10^{-10}, 10^{-9} and 10^{-8} M). Figure 20A shows the percentage of superoxide production with respect to the controls (cells not exposed to the toxin) in presence or absence of the inhibitors after 1 h exposure to the toxin. In comparison to PLTX alone, only DPI was able to reduce by 15% ($p<0.05$), 26% ($p<0.001$) and 43% ($p<0.01$) the amount of superoxide induced by 10^{-10}, 10^{-9} and 10^{-8} M PLTX, respectively. Furthermore, at the highest concentration of PLTX ($1.0x10^{-8}$ M) also NMMA reduced PLTX effect, decreasing superoxide anion levels by 42% ($p<0.01$). By contrast, the presence of the other inhibitors did not affect PLTX-induced superoxide production.

Figure 20B shows the % of mitochondrial activity recorded in presence of the inhibitors compared to those obtained by PLTX alone after 4 h exposure. Also in this case, the NOX/NOS nonspecific inhibitor DPI was able to significantly counteract PLTX-induced cytotoxicity. Indeed, at 10^{-10} and 10^{-8} M PLTX, mitochondrial activity was increased by 10% ($p<0.05$) and 11% ($p<0.01$), respectively.

In accordance to the lack of effect of the other inhibitors in preventing PLTX-induced ROS production, no changes of mitochondrial activity were found, with respect to PLTX alone.

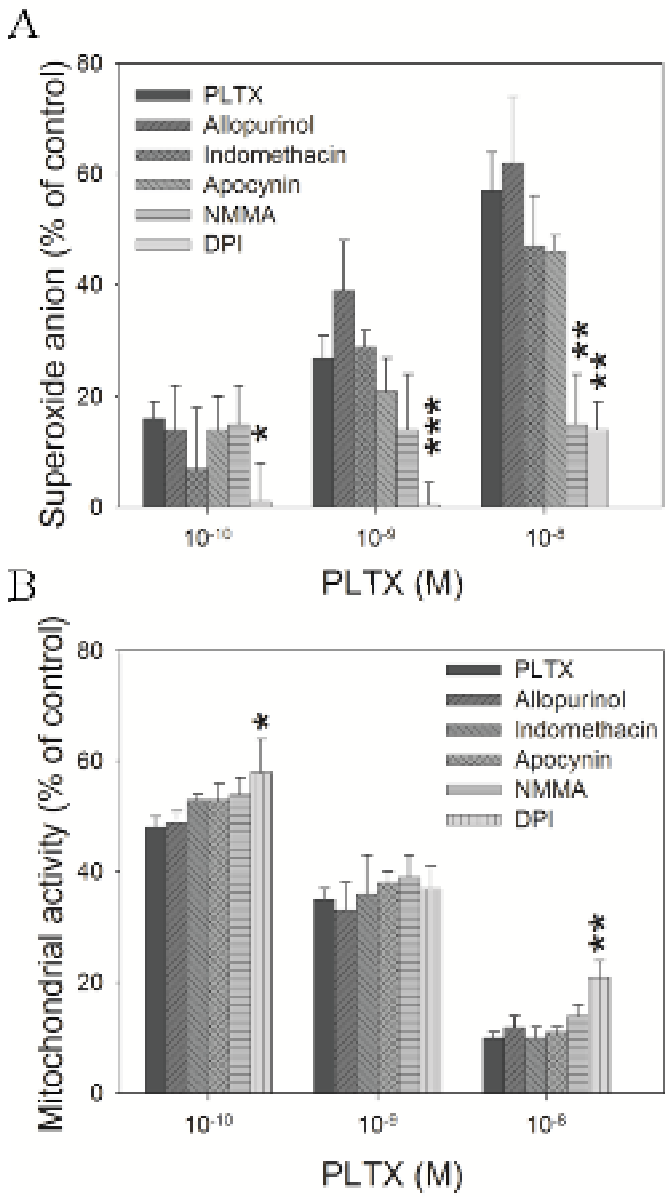

Fig. 20. *Effects of selective inhibitors of superoxide-producer enzymes on PLTX activity. Cells were exposed for 1 h to1.0x10^{-4} M allopurinol, 1.0x10^{-4} M indomethacin, 1.0x10^{-5} M apocynin, 1.0x10^{-4} M NMMA and 5.0x10^{-6} M DPI, and then to PLTX (10^{-10}-10^{-8} M).* ***(A)*** *The amount of superoxide was measured by NBT assay after 1 h exposure* ***(B)*** *Mitochondrial activity was measured by MTT assay after 4 h exposure. Data are presented as % with respect to negative controls (cells not exposed to PLTX) and are the mean ± SEM of 4 independent experiments performed in quintuplicate.*

Since only DPI, a nonspecific inhibitor of both NOX and NOS, exerted inhibitory effects on PLTX-induced ROS production and cytotoxicity, whereas NMMA, selective inhibitor of NOS, was only partially active, we investigated if the dual inhibition of both enzymes was necessary in order to counteract PLTX activity. To this aim, NBT and MTT assays were

performed exposing the cells to NMMA and apocynin in association. As shown in panel A of figure 21, however, in the presence of apocynin, NMMA ability to reduce PLTX-induced superoxide production was totally abolished. In the same manner, co-administration of apocynin and NMMA was not able to at least partially restore the mitochondrial dysfunction induced by the toxin (fig. 21B).

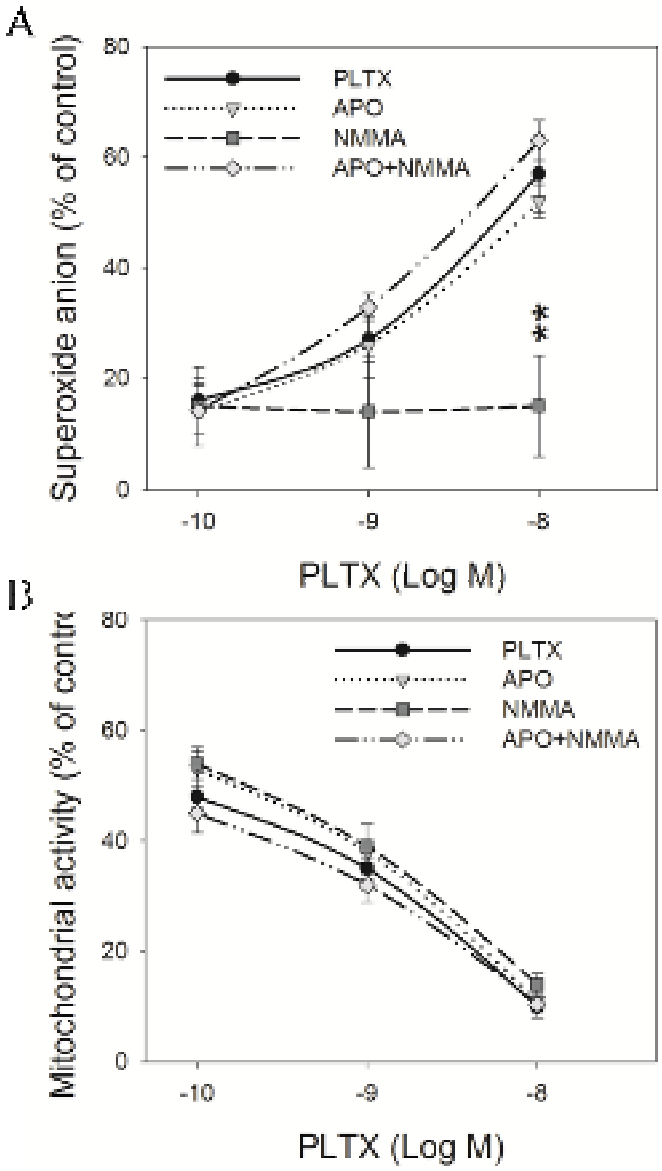

Fig. 21. *Effects of apocynin, NMMA and their co-administration on PLTX-mediated superoxide production and mitochondrial dysfunction. Cells were exposed for 1 h to 1.0x10^{-5} M apocynin, 1.0x10^{-4} M NMMA and their association and then to 10^{-10}, 10^{-9} and 10^{-8} M PLTX for 1 h to evaluate superoxide by NBT assay* ***(A)*** *or for 4 h to evaluate mitochondrial activity by MTT assay* ***(B)****. Data are presented as % of superoxide production or mitochondrial activity with respect to controls (cells not exposed to PLTX) and are the mean ± SEM of 4 independent experiments performed in quintuplicate.*

4.6 Mitochondria as a source of superoxide anion: role of mitochondrial electron transport chain

Another feasible source of superoxide anion is the mitochondria, by reverse electron transport through the mitochondrial electron transport chain. Thus, we investigated the role of NADH-ubiquinone oxidoreductase (complex I) exposing the cells to the complex I inhibitor rotenone ($5.0x10^{-6}$ M), whereas the role of protonic influx was studied exposing the cells to nigericin ($5.0x10^{-6}$ M), an ionophore that exchanges H^+ for K^+. In presence of nigericin, PLTX-induced superoxide production was significantly reduced by 23% (10^{-9} M PLTX, $p<0.05$) and 24% (10^{-8} M PLTX, $p<0.05$). Furthermore, the co-administration with rotenone, that *per se* was ineffective, resulted in a further inhibition of PLTX-induced superoxide production (-32% and -43% in the presence of 10^{-9} and 10^{-8} M PLTX, respectively, $p<0.01$) (fig. 22A). On the other hand, nigericin was ineffective in reducing PLTX mitochondrial toxicity (fig. 22B) but, when administered in association with rotenone, that *per se* counteracted the effects of 10^{-9} and 10^{-10} M PLTX, exerted a mixed effect, inhibiting rotenone activity at a low PLTX concentration (10^{-10} M) and enhancing it at a higher PLTX concentration (10^{-8} M).

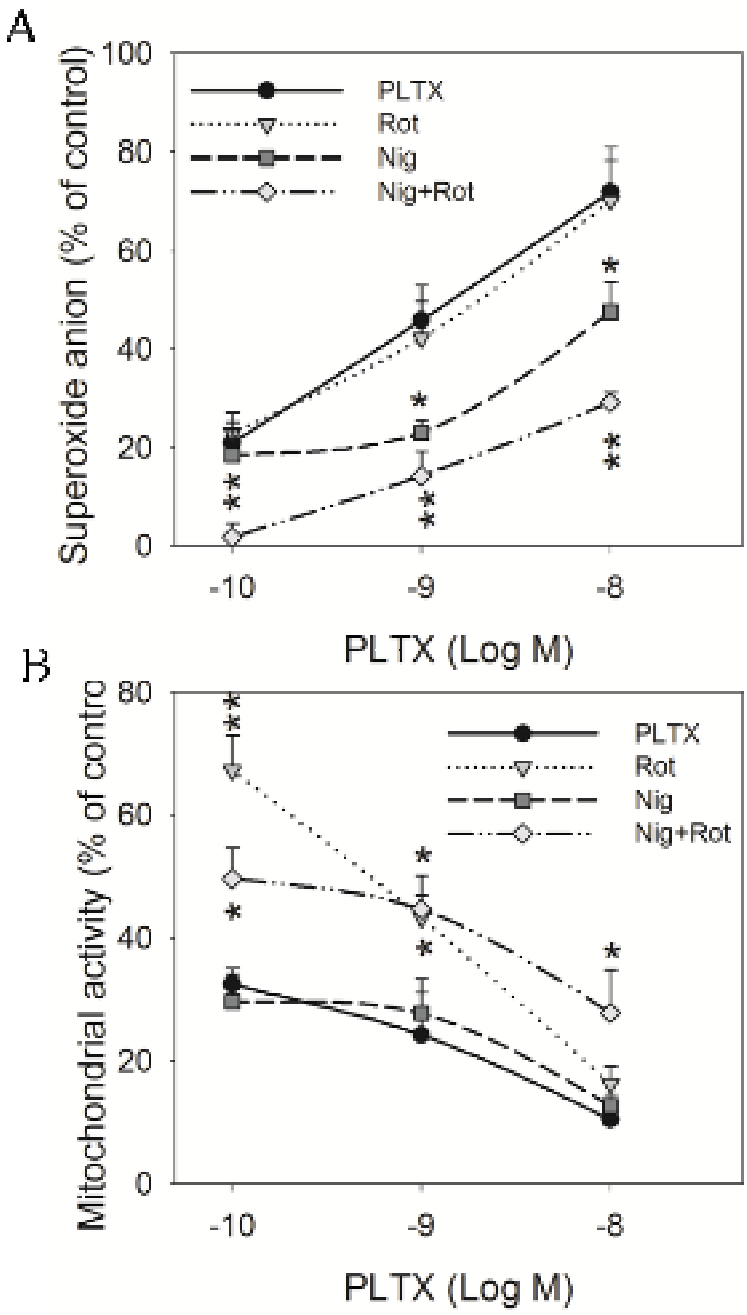

Fig. 22. *Involvement of mitochondrial transport chain in PLTX-induced superoxide production and mitochondrial dysfunction. Cells were exposed for 1 h to 5.0x10^{-6} M rotenone, 5.0x10^{-6} M nigericin and their association and then to 10^{-10}, 10^{-9} and 10^{-8} M PLTX. The amount of superoxide was measured after 1 h by NBT assay* ***(A)*** *and mitochondrial activity after 4 h by MTT assay* ***(B)****. Data are presented as % of superoxide production or mitochondrial activity with respect to controls (cells not exposed to PLTX) and are the mean ± SEM of 4 independent experiments performed in quintuplicate.*

4.7 Role of ionic imbalance on palytoxin-induced oxidative stress

4.7.1 Palytoxin-induced oxidative stress is ouabain-sensitive

To investigate the relationship between PLTX-induced production of superoxide anion and Na^+/K^+-ATPase activity, NBT reduction assay was performed exposing the cells to $1.0x10^{-5}$ M ouabain for 1 h and then for 1 h to the toxin ($1.5x10^{-12}$-$1.0x10^{-8}$ M). As shown in figure 23, ouabain, that *per se* induced a 12±9% increase of superoxide anion production with respect to controls (untreated cells), almost abolished PLTX–dependent ROS accumulation at all PLTX concentrations.

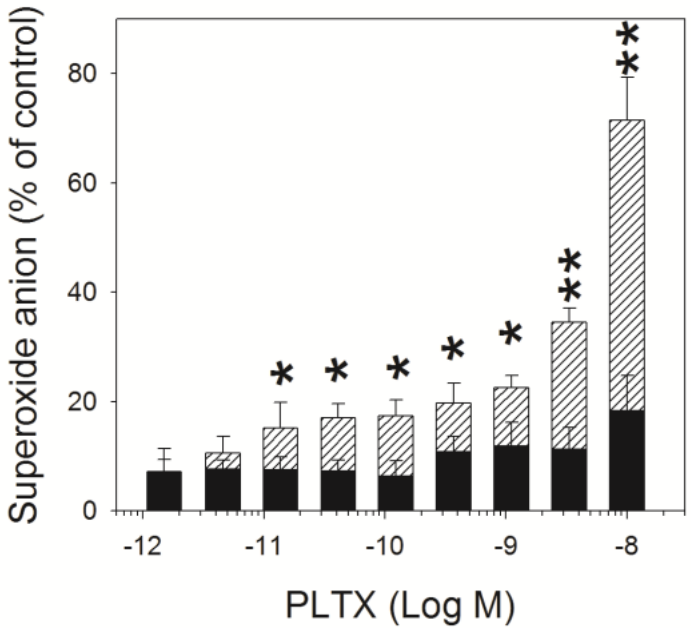

Fig. 23. *Effect of ouabain on PLTX-induced superoxide anion production. Cells were exposed to $1.0x10^{-5}$ M ouabain for 1 h and then to PLTX for 1 h before performing the NBT assay. Histograms represent cells exposed to PLTX in the absence (▨) or presence of ouabain (■). Data are reported as % of control and are the means ± SEM of 4 independent experiments performed in quadruplicate. Statistical differences: *, $p < 0.05$; **, $p < 0.01$ (Student t-test).*

4.7.2 Palytoxin-induced oxidative stress and cytotoxicity depend on ionic imbalance

It has been demonstrated that the transformation of the Na^+/K^+-ATPase into a cationic channel due to its interaction with PLTX induces an intracellular increase of Na^+ and, consequently, of Ca^{2+}. To evaluate the involvement of these two cations in the early cell damage induced by PLTX, NBT and MTT assays were performed in presence or absence of extracellular Na^+ or Ca^{2+}. Figure 24A shows superoxide production induced by 1 h exposure to PLTX in presence of both Na^+ and Ca^{2+} (D-PBS with Ca^{2+}/Mg^{2+}), in Ca^{2+}-free medium (D-PBS without Ca^{2+}/Mg^{2+} plus $1.0x10^{-3}$ M EGTA) and in Na^+-free medium (Locke's solution, composed by N-methyl-$_D$-Glucamine 0,14 M, KCl $4.4x10^{-3}$ M, $CaCl_2$ $2.5x10^{-3}$ M, $MgSO_4$ $1.2x10^{-3}$ M, KH_2PO_4 $1.2x10^{-3}$ M, EDTA $1.0x10^{-5}$ M, Hepes $1.0x10^{-2}$ M and D-Glucose $2.5x10^{-2}$ M, pH 7.4). The withdrawal of Na^+ completely abolished the superoxide production induced by all PLTX concentrations tested ($4.0x10^{-11}$–$1.0x10^{-8}$ M). On the contrary, within the same concentrations interval, PLTX induction of superoxide anion was not affected by the removal of Ca^{2+} from the medium, since in this condition superoxide anion levels were comparable to those found in the cells exposed to Na^+/Ca^{2+}-containing medium.

In figure 24B, mitochondrial dysfunction induced during 4 h exposure to PLTX in medium with Na^+ and Ca^{2+}, in Ca^{2+}-free medium and in Na^+-free medium, is presented. Compared to the activity of PLTX in D-PBS, the effect of the toxin after 4 h exposure in a Ca^{2+}-free medium was significantly reduced at all the PLTX concentrations considered. Moreover, in Na^+-free medium, PLTX cytotoxic effect was almost totally abolished for toxin concentrations ranging from $3.0x10^{-10}$ to $3.0x10^{-8}$ M. Under this condition, only at $1.0x10^{-7}$ M PLTX, a reduction of mitochondrial activity of 34±6% with respect to untreated cells was observed.

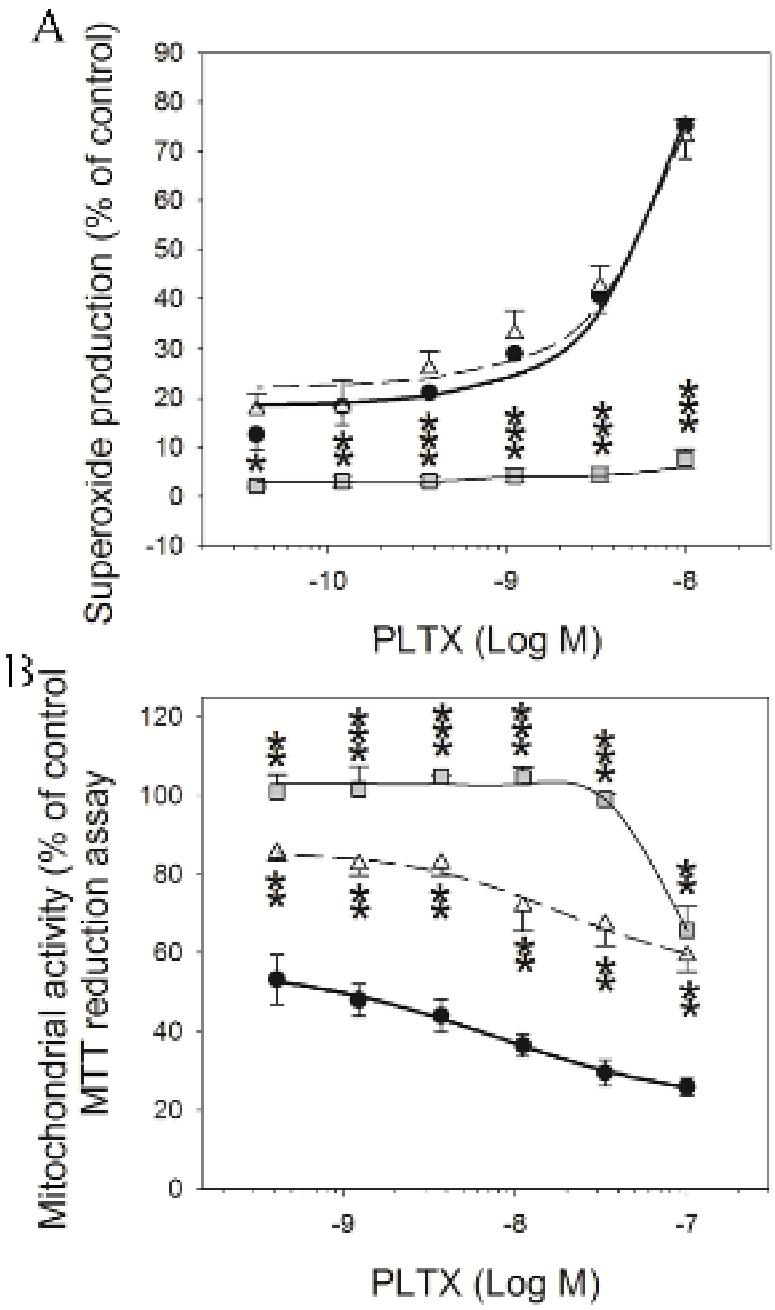

Fig. 24. *Effects of Na^+ or Ca^{2+} withdrawal on superoxide anion induced by 1 h PLTX exposure* ***(A)*** *and mitochondrial dysfunction induced by 4 h PLTX exposure* ***(B)****. Cells were exposed to PLTX in a Na^+- and Ca^{2+}-containing medium (●), in a Ca^{2+}-free medium (△) and in a Na^+-free medium (■) before performing the NBT or MTT assay. Data are reported as % of control and are the means ± SEM of 3 experiments performed in quadruplicate. Statistical differences: *, $p<0.05$; **, $p<0.01$; ***, $p<0.001$ (Student t-test).*

Consistent with the toxicity assay, reduction of cell number and morphological changes, such as disorganization of cell architecture, were observed in cells exposed to PLTX in a Na^+- and

Ca^{2+}-containing medium and in Ca^{2+}-free medium, but not in Na^{+}-free medium. As shown in figure 25, withdrawal of Na^{+} from the extracellular medium was able to prevent the morphological changes induced by 4 h exposure to $1.0x10^{-9}$ and $1.0x10^{-8}$ M PLTX, where only a moderate cell swelling was observed.

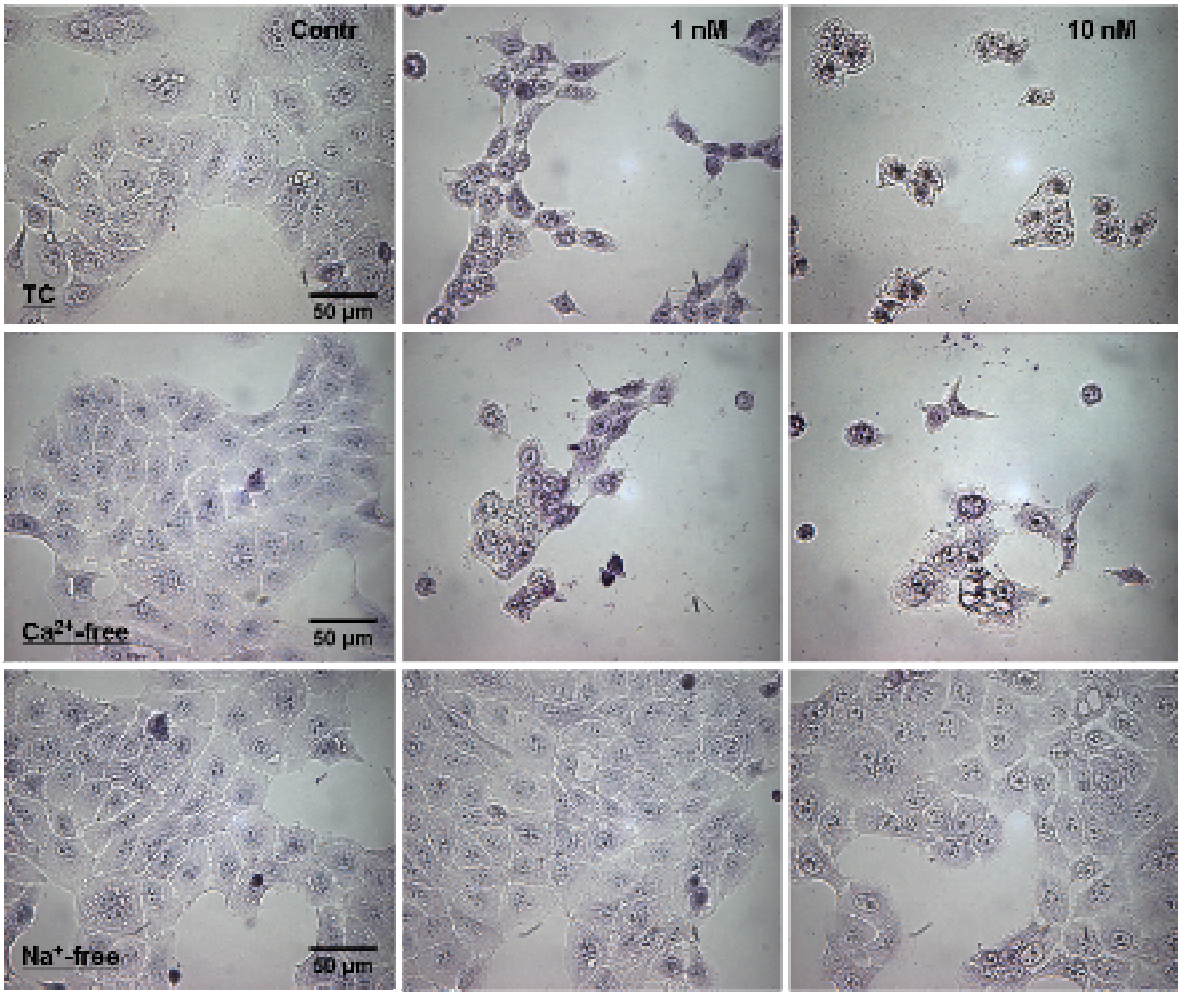

Fig. 25. *Effects of Na^{+} and Ca^{2+} withdrawal on PLTX-induced morphological changes. Cells were exposed for 4 h to $1.0x10^{-9}$ and $1.0x10^{-8}$ M PLTX in a Na^{+}- and Ca^{2+}-containing medium (TC), in a Na^{+}-free medium and in a Ca^{2+}-free medium. Cells were stained with May-Grunwald Giemsa solutions and 40x images captured with an inverted optical microscope.*

4.8 Palytoxin effects on mitochondria: role of mitochondrial permeability transition pore (MPTP)

To evaluate the effect of PLTX on mitochondria, formation of mitochondrial permeability transition pore (MPTP) was initially measured. Pore formation was monitored by comparison between JC-1 aggregates (red fluorescence, intact mitochondria) and monomers (green fluorescence, disrupted mitochondria by pore forming); the ratio between the two fluorescence is an index of pore formation.

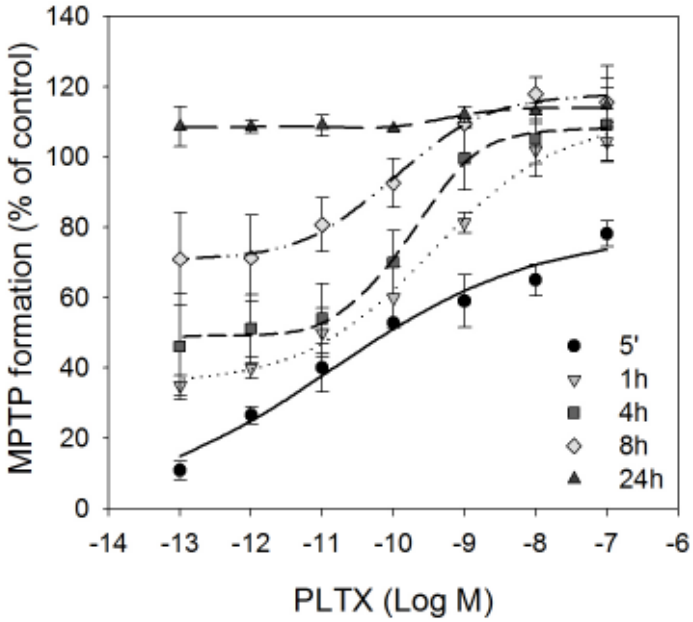

Fig. 26. *Mitochondrial permeability transition pore (MPTP) opening induced by PLTX. Cells were exposed to increasing concentrations of PLTX (10^{-13} – 10^{-7} M) for increasing time intervals up to 24 h and MPTP opening evaluated by JC-1 fluorescence. Results are presented as % of pore opening with respect to positive control (0.1 μg/mL valynomicin) and are the mean ± SEM of 5 independent experiments performed in quadruplicate.*

As reported in figure 26, exposing the cells to increasing concentrations of toxin, PLTX induced a quick opening of MPTP in a concentration-dependent manner. Indeed, yet after 5 minutes exposure, the toxin (10^{-13} – 10^{-7} M) induced a significant increase of MPTP formation with respect to the control, which reached 78±3% at the highest concentration of

toxin tested ($1.0x10^{-7}$ M). Increasing the time of exposure, MPTP formation was also time-dependent, reaching 100% formation after 24 h exposure.

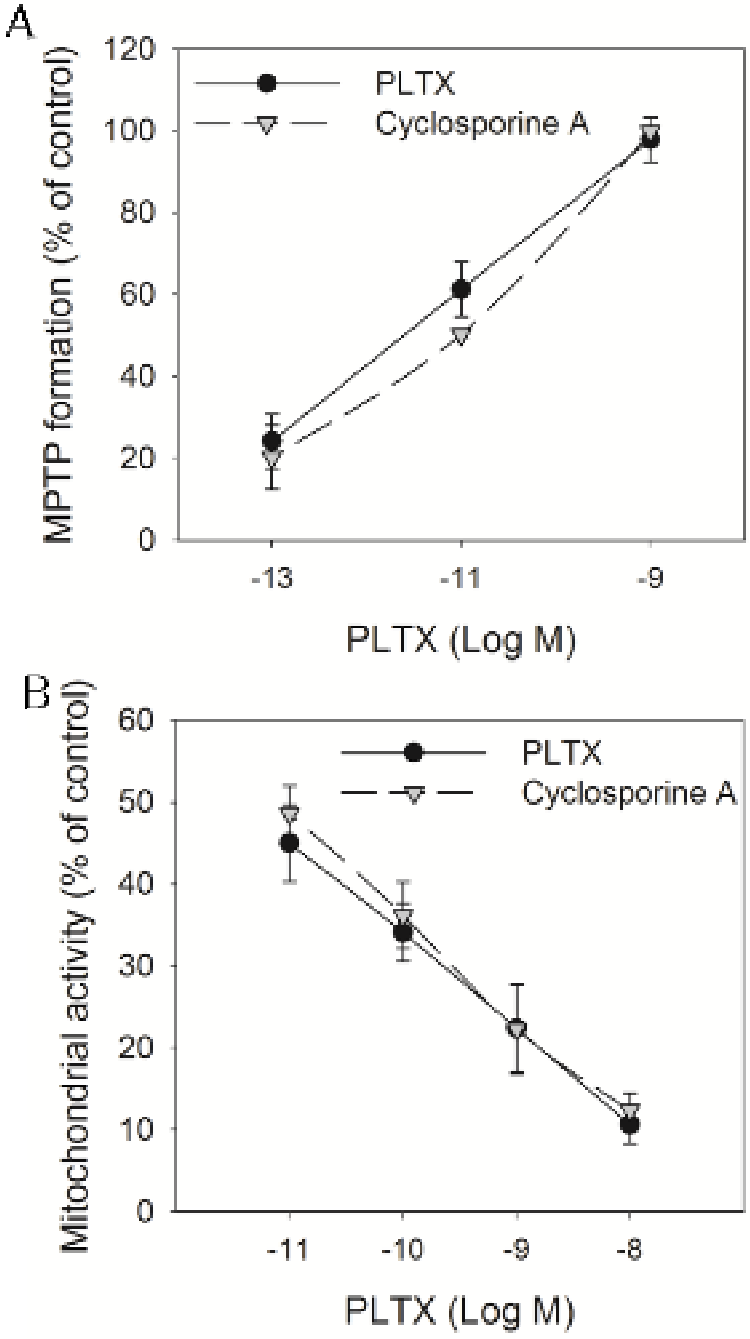

Fig. 27. *Effects of cyclosporine A on PLTX effects. Cells were pre-exposed for 1 h to $2.0x10^{-7}$ M cyclosporine A and then to the toxin;* ***(A)*** *MPTP opening was evaluated after 1 h by JC-1 fluorescence. Data are presented as % of pore opening with respect to positive control (0.1 μg/mL valynomicin).* ***(B)*** *mitochondrial dysfunction was evaluated after 4 h by MTT assay. Data are presented as % of mitochondrial activity with respect to untreated controls. Results are the means ± SEM of 4 independent experiments performed in quadruplicate.*

4.8.1 Mechanism of MPTP opening

To evaluate the mechanism of MPTP opening induced by PLTX, the toxin effect was investigated in presence of cyclosporine A, a well known inhibitor of MPTP formation by prevention of cyclophillin D binding to mitochondrial membrane. Cells were pre-exposed to $2.0x10^{-7}$ M cyclosporine A for 1 h and subsequently to the toxin. MPTP opening was then evaluated after 1 h by JC-1 fluorescence (fig. 27A) and mitochondrial dysfunction after 4 h exposure by MTT assay (fig. 27B). In presence of cyclosporine A, however, the effect of $1.0x10^{-9}$, $1.0x10^{-11}$ and $1.0x10^{-13}$ M PLTX on MPTP formation after 1 h exposure was not affected. Similarly, evaluating PLTX-induced mitochondrial dysfunction, cyclosporine A was unable to counteract the toxin effect (10^{-11} – 10^{-8} M).

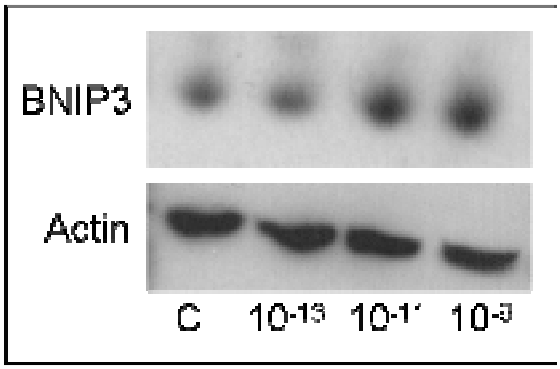

Fig. 28. *Effects of 4 h exposure to PLTX (10^{-13} – 10^{-9} M) on BNIP3 protein expression evaluated by western blot analysis. β-actin was chosen as a control protein.*

It has been reported that MPTP opening and the subsequent mitochondrial dysfunction can be also mediated by the Bcl-2/adenovirus E1B 19-kilodalton interacting protein (BNIP3). BNIP3 is an homologue protein of the BH3-proteins belonging to the anti-apoptotic Bcl-2 family. However, BNIP3 has been reported to mediate apoptotic as well as necrotic cell death through opening of MPTP (Imazu et al., 1999; Vande Velde et al., 2000; Gustafsson, 2011; Nakamura et al., 2012). Thus, the possible involvement of BNIP3 was preliminary investigated. Figure 28 shows the effects of 4 h exposure to PLTX (10^{-13} – 10^{-9} M) on BNIP3 protein expression,

evaluated by western blot analysis. With respect to the controls, an increase of BNIP3 was observed starting from 10^{-11} M PLTX, whereas protein level observed after 10^{-13} M PLTX exposure was comparable to that of the controls.

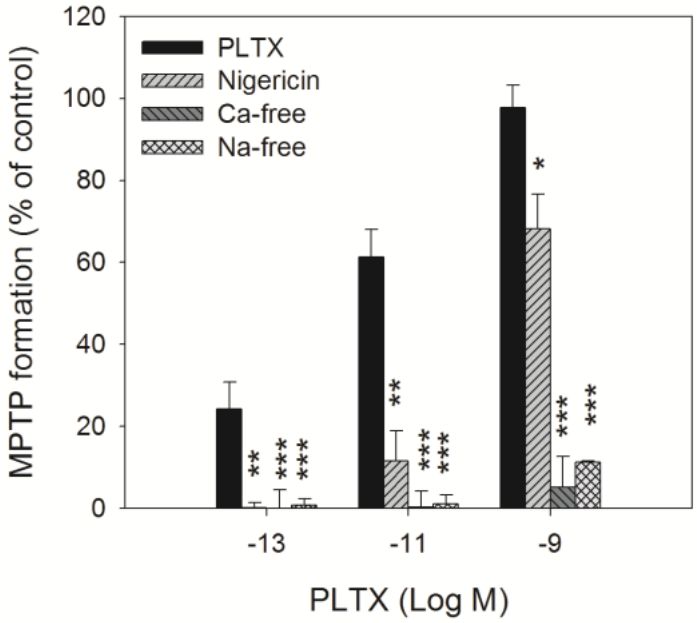

Fig. 29. *Effects of Na^+, Ca^{2+} and H^+ imbalance on MPTP opening induced by 1 h PLTX exposure. Cells were exposed to PLTX in a normal culture medium (■),in a normal culture medium containing $5.0x10^{-6}$ M nigericin (▨), in a Ca^{2+}-free medium (▩) and in a Na^+-free medium (▩) before JC-1 assay. Data are reported as % of positive control (0.1 µg/mL valynomicin) and are the means ± SEM of 4 experiments performed in quadruplicate. Statistical differences: **, $p < 0.01$; ***, $p < 0.001$ (Student t-test).*

Subsequently, the role of ionic disequilibrium induced by PLTX through Na^+/K^+-ATPase blockage on MPTP formation was investigated. Figure 29 shows PLTX-induced MPTP formation in a Ca^{2+}-free medium (D-PBS without Ca^{2+}/Mg^{2+} plus $1.0x10^{-3}$ M EGTA), in a Na^+-free medium (Locke's solution) and in a medium containing $5.0x10^{-6}$ M nigericin, an ionophore that exchanging K^+ for H^+ reduced the proton disequilibrium. Comparing to the effect of PLTX in a normal culture medium, under these conditions, MPTP formation induced by PLTX (10^{-13} - 10^{-9} M) was significantly reduced, with a marked inhibition observable both

in Ca^{2+}-free medium and in Na^{+}-free medium, where MPTP formation was almost completely abolished.

Finally, the role of two cationic transporters on PLTX-mediated effects at mitochondrial level was investigated. Indeed, MPTP opening as well as mitochondrial dysfunction were evaluated in presence of $2.0x10^{-5}$ M amiloride (inhibitor of epithelial Na^{+}-channel, ENaC) and $2.0x10^{-5}$ M 5-(N,N-Dimethyl) amiloride (DMA, inhibitor of Na^{+}/H^{+} exchanger, NHE). Cells were pre-exposed for 1 h to the inhibitors and the to the toxin (1 or 4 h). However, none of these treatments could revert PLTX-induced effects (fig. 30).

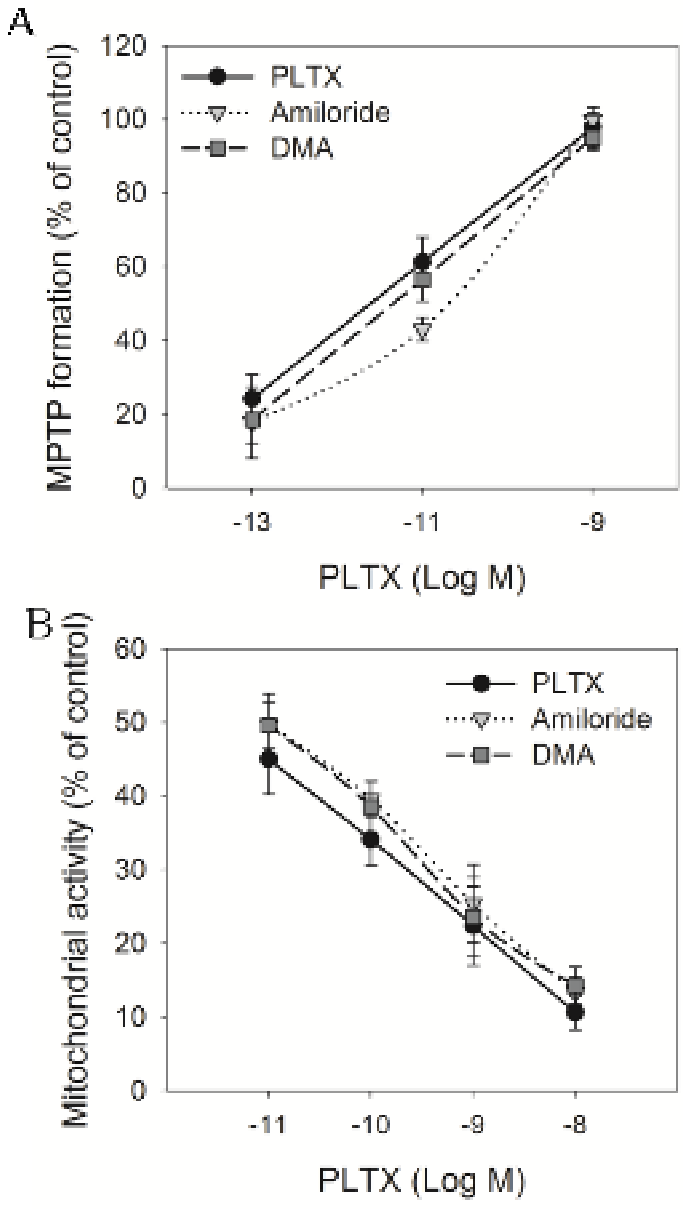

Fig. 30 (previous page). *Effects of amiloride and DMA on PLTX effects. Cells were pre-exposed for 1 h to 2.0x10^{-5} M amiloride or 2.0x10^{-5} M DMA and then to the toxin;* ***(A)*** *MPTP opening was evaluated after 1 h by JC-1 fluorescence. Data are presented as % of pore opening with respect to positive control (0.1 μg/mL valynomicin).* ***(B)*** *mitochondrial dysfunction was evaluated after 4 h by MTT assay. Data are presented as % of mitochondrial activity with respect to untreated controls. Results are the means ± SEM of 4 independent experiments performed in quadruplicate.*

4.9 Palytoxin effects on cell cycle

Since mitochondria damages may induce cell cycle arrest in order to restore mitochondrial functionalities, the two restriction points in S and G2M phases were considered. Cells were exposed for 4 or 8 h to $1.0x10^{-8}$ and $1.0x10^{-9}$ M PLTX, collected and cytofluorimetric analysis performed after staining with 10 μg/mL PI, 0.05 μg/mL FITC in presence of 40 μg/mL RNAse. As reported in table 2, with respect to the untreated control, 4 h exposure to $1.0x10^{-8}$ and $1.0x10^{-9}$ M PLTX increased the amount of cells in S phase by 19% and 18%, respectively. The delay in S phase was observable also prolonging the time of contact with the toxin up to 8 h. Similarly, cells were delayed in G2M phase after exposure to $1.0x10^{-8}$ and $1.0x10^{-9}$ M PLTX for 4 h (7% and 4%, respectively), as well as for 8 h (7% and 10%, respectively).

		% G0-G1	*p value (vs control)*	% S	*p value (vs control)*	% G2M	*p value (vs control)*
4 h	**Control**	51±2		41±1		8±1	
	$1.0x10^{-9}$ M PLTX	30±3	*< 0.001*	58±3	*< 0.01*	12±1	*< 0.01*
	$1.0x10^{-8}$ M PLTX	28±3	*< 0.001*	59±4	*< 0.01*	15±2	*< 0.01*
8 h	**Control**	59±1		34±1		7±1	
	$1.0x10^{-9}$ M PLTX	26±1	*< 0.001*	63±4	*< 0.001*	16±3	*< 0.05*
	$1.0x10^{-8}$ M PLTX	28±2	*< 0.001*	56±2	*< 0.001*	14±1	*< 0.001*

Tab. 2. *Effects of PLTX on cell cycle. Cells were exposed for 4 or 8 h to $1.0x10^{-8}$ and $1.0x10^{-9}$ M PLTX, collected and cytofluorimetric analysis performed after staining with 10 μg/mL PI, 0.05 μg/mL FITC in presence of 40 μg/mL RNAse. Results are presented as percentage of cells in G0-G1, S and G2M phases, obtained over 5 replica.*

4.10 Cell death induced by palytoxin: apoptosis or necrosis?

4.10.1 Palytoxin does not induce apoptotic cell death

Apoptosis occurrence was analyzed by caspasis activation and by apoptotic bodies formation.

As the last caspasis that are activated during the caspasis-dependent apoptotic process, caspasis 3/7 activation was initially evaluated. As showed by figure 31A, exposing the cells to PLTX (10^{-11} – 10^{-7} M) for increasing time intervals up to 24 h, no caspasis 3/7 activation was recorded after 4, 8 and 24 h exposure. The apoptotic process, however, is strictly dependent on the entity of the damage. Hence, in order to reduce PLTX cytotoxicity and to give time to the cell to recover the damage caspasis 3/7 activation was investigated after a recovery period in toxin-free medium. However, after 1 h exposure to the toxin followed by 3, 7 and 23 h of recovery time in toxin-free medium no caspasis 3/7 activation was recorded (fig. 31B).

Subsequently, it was considered the possibility of activation of caspasis 8 and 9, the two caspasis that are first activated during the extrinsic and intrinsic pathway of apoptosis, respectively. Also in this case, neither caspase 8 (fig. 32A) nor caspase 9 (fig. 32B) activations were recorded after 4, 8 and 24 h exposure to the toxin (10^{-11} – 10^{-7} M).

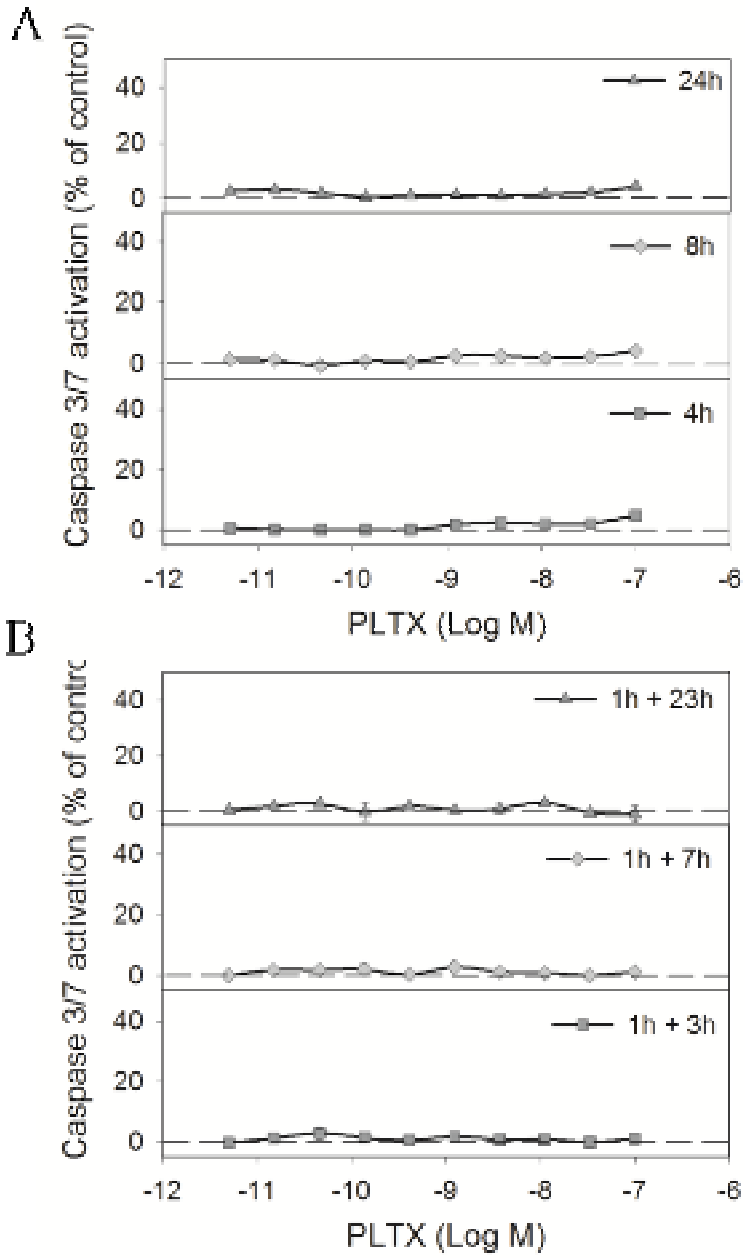

Fig. 31. *PLTX effect on caspasis 3/7 activation.* ***(A)*** *Cells were exposed to PLTX for 4, 8 and 24 h and the activation of caspasis 3/7 evaluated fluorimetrically.* ***(B)*** *Cells were exposed to PLTX for 1 h and then for increasing recovery time intervals (3, 7 and 23 h) in toxin-free medium before evaluating caspasis 3/7 activation. Data are reported as % of positive control (camptothecin 10 μM) and are the mean ± SEM of 3 experiments performed in quadruplicate.*

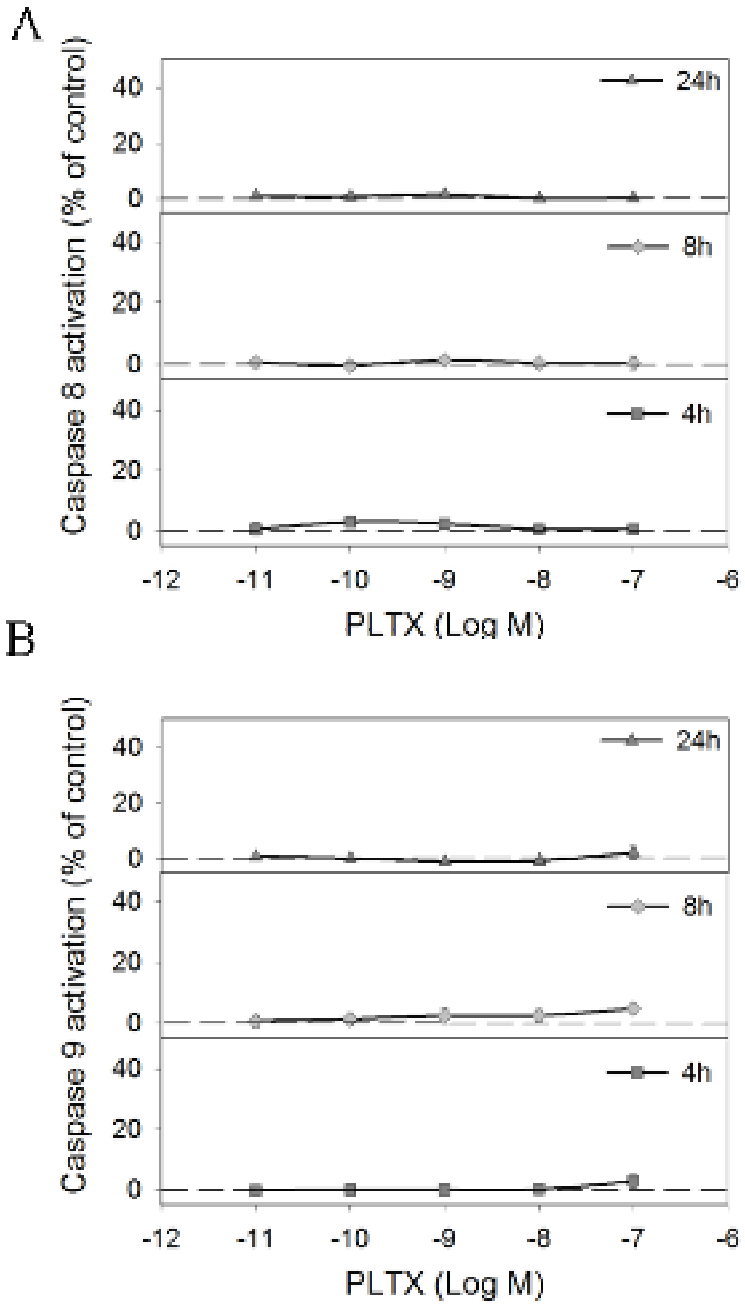

Fig. 32. *PLTX effect on caspase 8* ***(A)*** *and caspase 9* ***(B)*** *activations. Cells were exposed to PLTX for 4, 8 and 24 h and the activation of caspasis evaluated fluorimetrically. Data are reported as % of positive control (camptothecin 10 μM) and are the mean ± SEM of 3 experiments performed in quadruplicate.*

Finally, apoptosis occurrence was evaluated by measuring apoptotic bodies formation. Cells were exposed to the toxin for 4 and 8 h before nuclei staining with 1 μg/mL DAPI and immunocytotchemical analysis was then performed by fluorescence microscopy. In figure 33

the effect of 4 and 8 h exposure to $1.0x10^{-9}$ M and $1.0x10^{-8}$ M PLTX are shown. With respect to the untreated controls, formation of apoptotic bodies was almost undetectable, but nuclear morphological alterations such as fragmentations and swelling of the nuclei were observed.

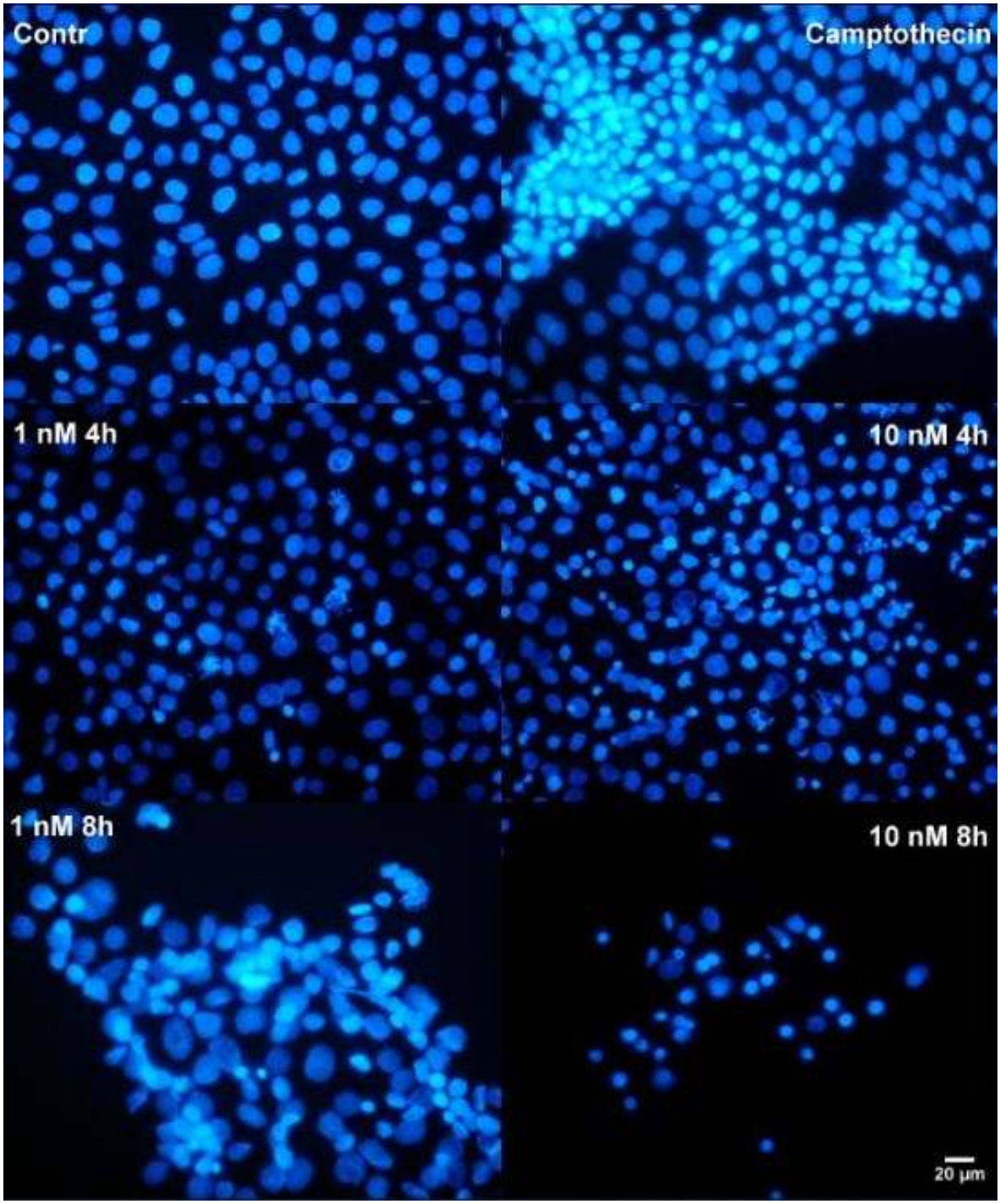

Fig. 33. *PLTX effect on apoptotic bodies formation. Cells were exposed to $1.0x10^{-9}$ M and $1.0x10^{-8}$ M PLTX for 4 and 8 h. Apoptotic bodies were evaluated by immunocytochemical analysis performed by an epifluorescence microscope after nuclei staining with DAPI. As a positive control, cells were exposed to 1.0x10-5 M camptothecin.*

4.10.2 Palytoxin induces a necrotic-like cell death

Necrosis occurrence was initially evaluated by measuring the amount of propidium iodide (PI) inside cells. PI is a membrane impermeable molecule, that can enter into the cells only after membrane disruption; hence, it is and indirect index of a necrotic-like cell death.

Cells were exposed for increasing time intervals (1 up to 24 h) to PLTX ($1.0x10^{-11}$ – $1.0x10^{-7}$ M) and the % of PI uptake with respect to the positive control (Triton-X 0.1%) was measured. As shown in figure 34, the toxin induced a concentration-dependent uptake of PI already after 1 h exposure, that was equal to 100% in cells exposed to $1.0x10^{-7}$ M PLTX. The amount of PI inside the cells increased also in a time-dependent manner, reaching 100% of uptake after 24 h exposure to all the concentrations of toxin considered.

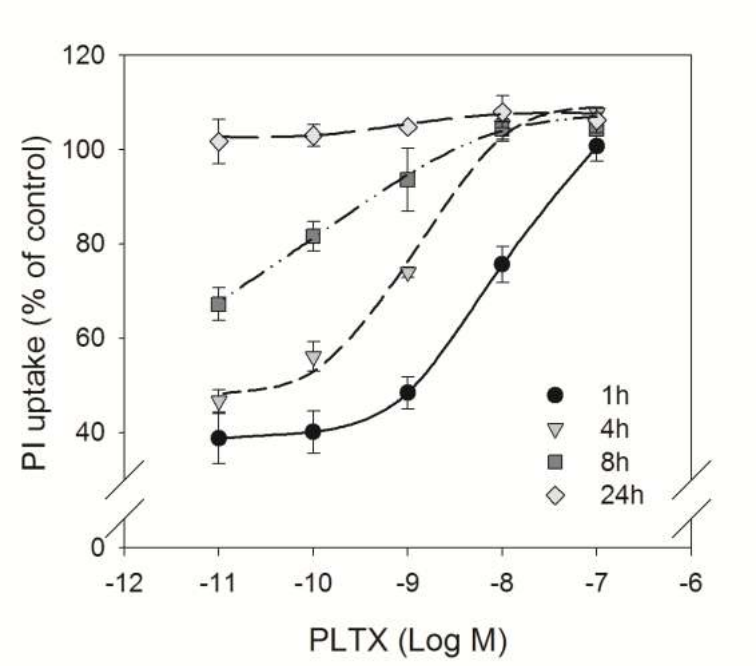

Fig. 34. *PLTX effects on necrotic cell death: PI uptake. Cells were exposed for 1 up to 24 h to PLTX ($1.0x10^{-11}$ – $1.0x10^{-7}$ M) and the amount of PI inside the cells evaluated fluorimetrically. Data are reported as % of PI uptake with respect to positive control (Triton-X 0.1%, equal to 100% lysed cells) and are the means ± SEM of 4 experiments performed in quintuplicate.*

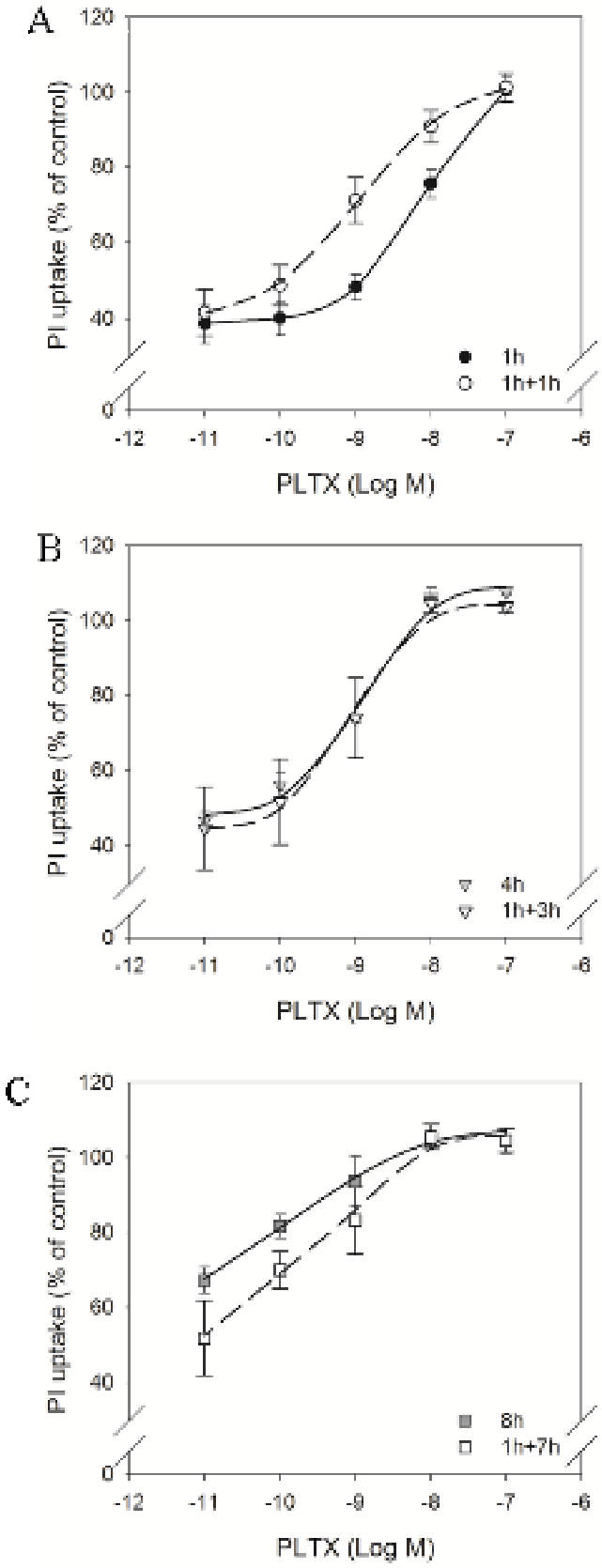

Fig. 35. *Irreversibility of PLTX-induced necrotic damage.* ***(A)*** *Cells were exposed for 1 to PLTX followed by 1 h of recovery time in toxin-free medium and the amount of PI inside the cells compared to that induced exposing the cells to the toxin for 1 h.* ***(B)*** *Cells were exposed*

for 1 to PLTX followed by 3 h of recovery time in toxin-free medium and the amount of PI inside the cells compared to that induced exposing the cells to the toxin for 4 h. ***(C)*** *Cells were exposed for 1 to PLTX followed by 7 h of recovery time in toxin-free medium and the amount of PI inside the cells compared to that induced exposing the cells to the toxin for 8 h. Data are reported as % of PI uptake with respect to positive control (Triton-X 0.1%, equal to 100% lysed cells) and are the means ± SEM of 4 experiments performed in quintuplicate.*

In order to evaluate whether the necrotic damage induced by PLTX was reversible, recovery experiments were performed exposing the cells to the toxin ($1.0x10^{-11}$ – $1.0x10^{-7}$ M) for 1 h followed by increasing recovery periods (1, 3 and 7 h) in toxin-free medium. In figure 35 the amount of PI inside the cells measured exposing the cells under the three recovery conditions are compared to those obtained after the corresponding continuative toxin exposure. Indeed, the entity of PI uptake measured after exposure of the cells to PLTX for 1 h or for 1 h followed by 1 h recovery time (fig. 35A), that obtained after 4 h exposure or after 1 h followed by 3 h recovery time (fig. 35B), as well as that obtained exposing the cells to PLTX for 8 h or for 1 h followed by 7 h recovery time (fig. 35C) did not significanly differ, indicating the irreversibility of the damage.

Occurrence of necrotic-like cell death was evaluated also by monitoring plasma membrane integrity by immunocytochemical analysis performed by confocal microscopy. In figure 36, panel A shows membrane damages and morphological changes observed exposing HaCaT cells for 4 and 8 h to $1.0x10^{-9}$ M and $1.0x10^{-8}$ M PLTX. Plasma membrane rupture was observed after 4 h exposure to $1.0x10^{-9}$ M PLTX, with subsequent leakage of cytoplasmic material after 8 h exposure. The membrane damages and the consequent loss of cellular content along with a complete destruction of cellular morphology were more evident after 8 h exposure to PLTX and were confirmed by cytofluorimetric analysis after PI and FITC staining of the cells (fig. 36B). With respect to the untreated controls, after 8 h exposure, $1.0x10^{-9}$ M and $1.0x10^{-8}$ M PLTX induced a reduction of protein content in the cells (FITC

fluorescence) and a significant alteration of cellular morphology (FITC and PI combined fluorescence).

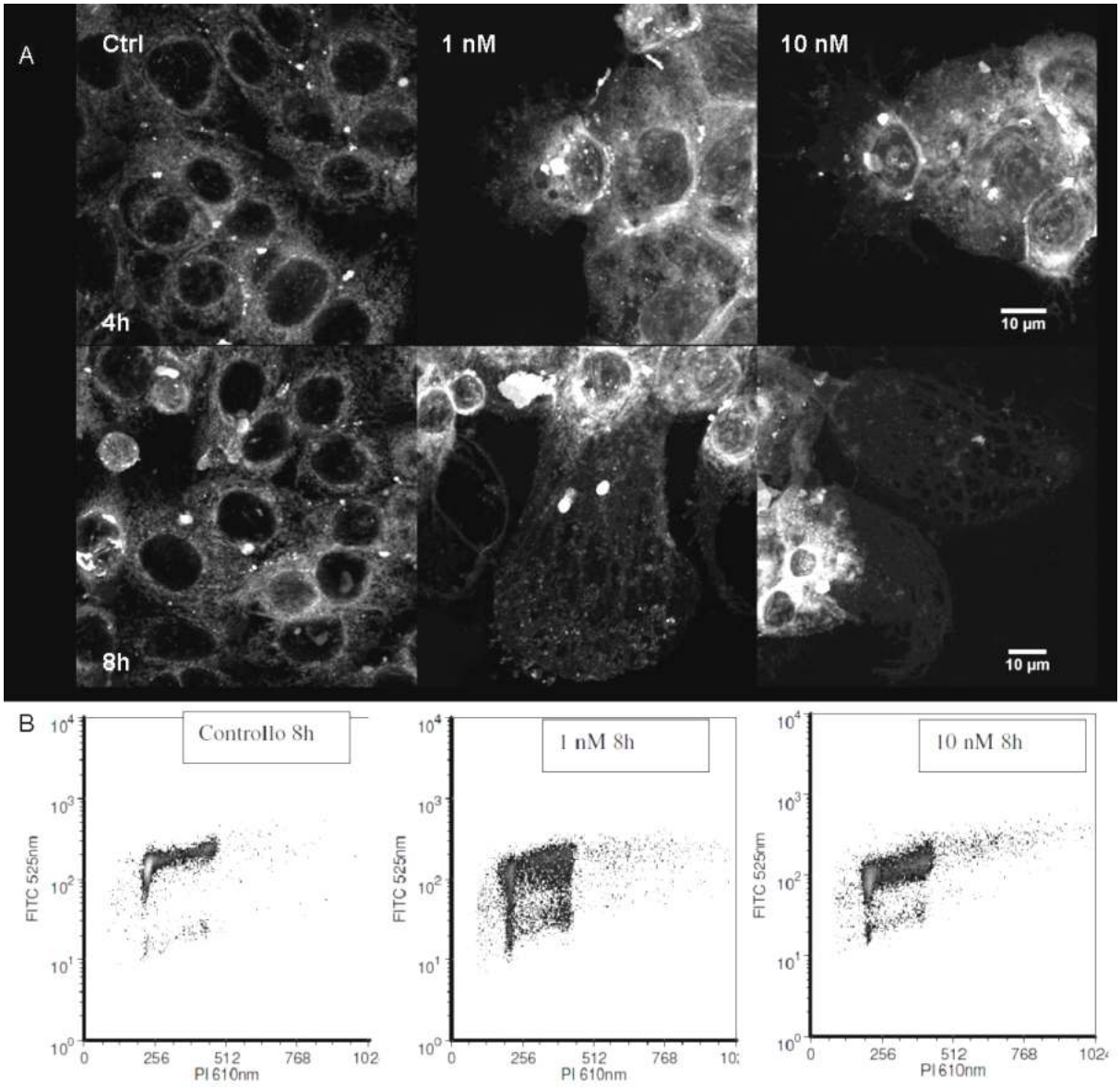

Fig. 36. *PLTX effects on cell morphology. (A) Cells were exposed to 1.0x10^{-9} M and 1.0x10^{-8} M PLTX for 4 and 8 h and after membrane staining with 10^{-4} M DiL morphological analysis performed by confocal microscopy. (B) Morphological alterations induced by 8 h exposure to 1.0x10^{-9} M and 1.0x10^{-8} M PLTX evaluated by cytofluorimetric analysis after cell staining with 10 µg/mL PI, 0.05 µg/mL FITC and 40 µg/mL RNAse.*

4.11 Effects of palytoxin on inflammatory mediators

To investigate the possibility that PLTX could induce an inflammatory response on HaCaT cells, the effect of toxin exposure on the gene expression and release of some pro-inflammatory cytokines (IL-6, IL-8, cIL-1α and TNFα) and of some inflammatory mediators involved in the metabolism of arachidonic acid (PGE_2 and LTB_4) was investigated.

4.11.1 Effects of palytoxin on pro-inflammatory cytokines

The effect of PLTX on pro-inflammatory cytokines has been investigated considering IL-8, IL-6, IL-1α and TNFα evaluating the effect on their gene expressions as well as the effect on their release by the cells.

Panel A of figure 37 shows the effect of 1, 2, 4, 12 and 24 h exposure to $1.0x10^{-11}$ M PLTX on gene expressions of these cytokines. After exposure to the toxin, total RNA was extracted, retrotranscripted to cDNA and real time PCR analysis performed using specific primers. The maximum enhancement of expression of the genes encoding for IL-8 (2.3±0.2 folds), IL-6 (5.7±1.3 folds) and TNF-α (6.3±2.2 folds) were recorded after 1 h exposure, while no changes were observed considering IL-1α. Figure 37B shows the effects of 1 h exposure to the toxin on the same genes followed by recovery times of 1, 3, 11 and 23 h in toxin-free medium. Also under these conditions, the highest over expression of genes encoding for IL-8 and IL-6 occurred after short exposure times, resulting, respectively, in 2.7±0.4 and 8.7±2.1 folds increase after 1h followed by 1h recovery time. Considering TNF-α upregulation of the corresponding gene occurred within the intermediate exposure conditions, such as 1h followed by 3h (4.5±0.9 folds) and 11h (4.6±1.2 folds) of recovery time. Finally, similarly to the continuative exposure, also under recovery conditions no difference were recorded for IL-1α.

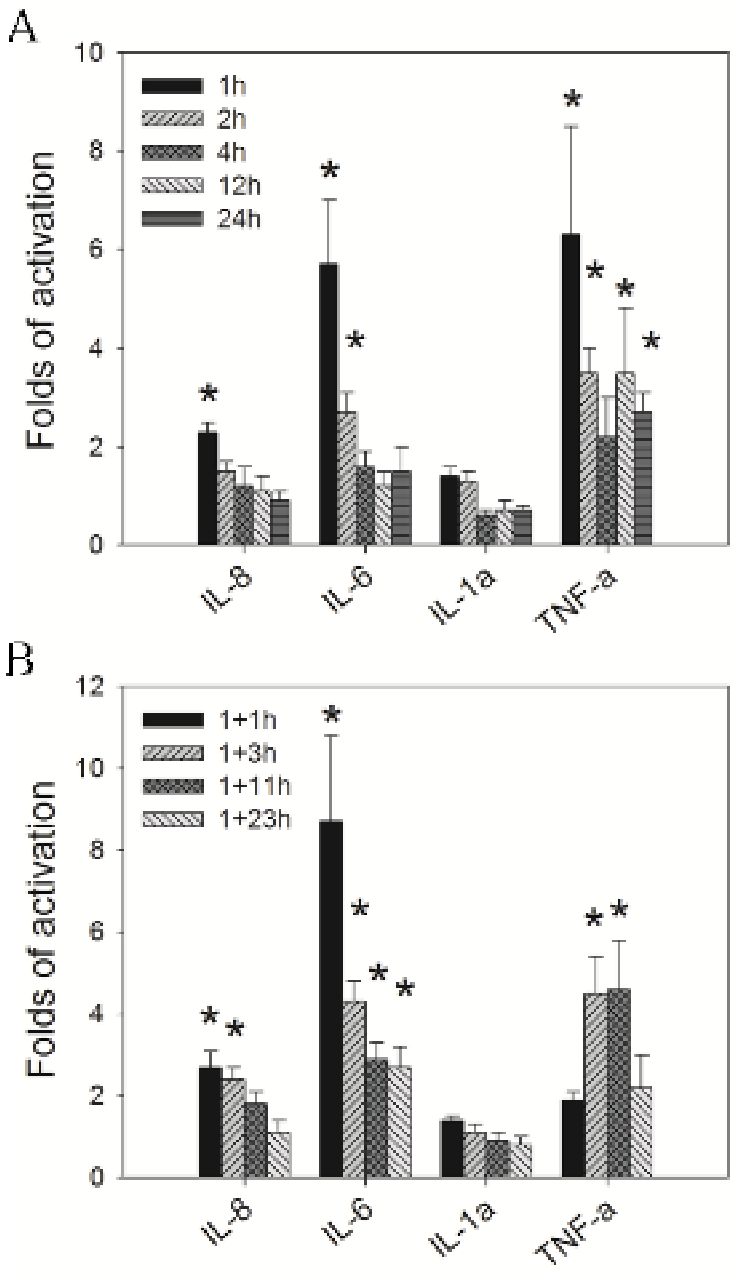

Fig. 37. *Effects of PLTX on IL-8, IL-6, IL-1α and TNF-α gene expressions.* ***(A)*** *Effects of continuous exposure to PLTX on cytokines gene expressions. Cells were exposed for increasing time intervals (1 up to 24h) to 1.0x10^{-11} M PLTX and gene expressions evaluated by real time PCR* ***(B)*** *Effect of recovery conditions on cytokines gene expressions. Cells were exposed for 1 h to 1.0x10^{-11} M PLTX followed by recovery time intervals of 1 up to 23 h in toxin-free medium an gene expressions evaluated by real time PCR. Statistical differences: *, $p < 0.05$ (Student t-test).*

However, evaluating the release of these cytokines by ELISA tests, it was found that these early gene over-expressions were not accompanied by a release of the corresponding cytokine by the cells. Indeed, exposing the cells to $1.0x10^{-11}$ M PLTX for the same time intervals considered for the gene expression analysis, cytokines release occurred only after longer exposure times (24 h and 1h + 23 h of recovery time), at least considering IL-8 and IL-6 (fig. 38). In particular, 24 h exposure induced a release of 465±120 ng/mL IL-8 ($p < 0.05$), that represents an increase of more than 3 folds with respect to untreated controls (150±40 ng/mL). Moreover, the highest release of IL-8 (694±49 ng/mL, $p < 0.01$) was recorded after 1 h toxin exposure followed by 23 h of recovery time, with an increase of 4.6 folds.

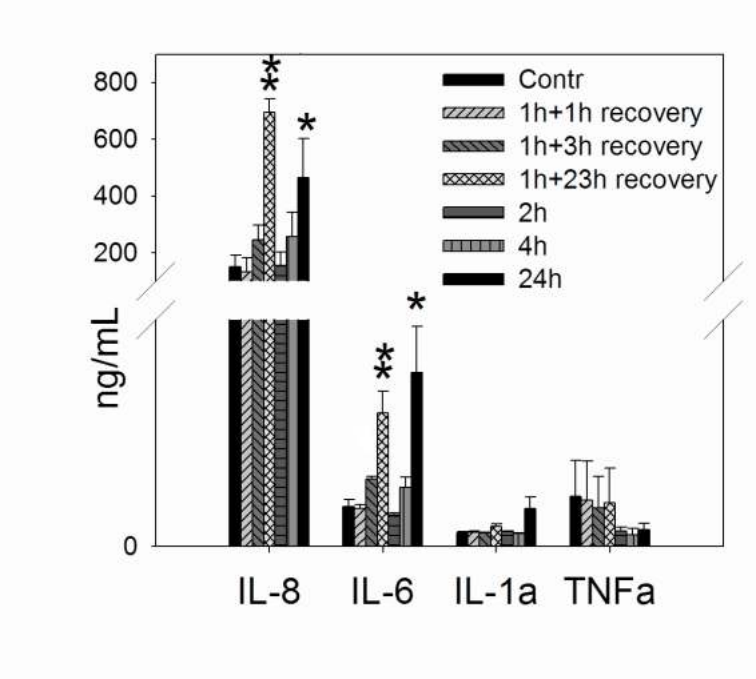

Fig. 38. *Effects of PLTX on cytokines (IL-8, IL-6, IL-1α and TNFα) release. Cells were exposed to $1.0x10^{-11}$ M PLTX for different time intervals: continuative exposure (2 up to 24 h) as well as recovery conditions (1 h exposure followed by increasing recovery times in toxin-free medium). Cell culture medium was then collected and assayed by ELISA test. Data are presented as ng/mL of cytokine released by the cells and are the mean ± SEM of three independent experiments performed in duplicate.*

The same situation occurred considering IL-6. Indeed, 24 h exposure to the toxin, induced a release of 31±8 ng/mL IL-6 ($p < 0.05$), with an increase of over 4 folds with respect to the

untreated controls (7±1 ng/mL). Also under the corresponding recovery condition (1 h of PLTX exposure followed by 23 h of recovery time) IL-6 release was enhanced to 24±3 ng/mL ($p < 0.01$), with an increase of more than 3 folds.

On the contrary, no effects on the release of IL-1α and TNFα were observed at all the exposure condition tested (fig. 38).

4.11.2 Effects of palytoxin on PGE_2 and LTB_4

The effect of PLTX at the inflammatory level was then evaluated considering PGE_2 and LTB_4, products of arachidonic acid metabolism in response to inflammatory stimuli. The same culture medium used to evaluated the release of pro-inflammatory cytokines were used to measure the amount of PGE_2 and LTB_4 released by the cells. Indeed, considering PGE_2, it was found that $1.0x10^{-11}$ M PLTX induced a significant release with respect to the untreated control starting after 2 h exposure. The release was time-dependent, at least up to 24 h exposure. On the contrary, no effect were observed after recovery periods of 1 up to 23 h in toxin-free medium indicating that PGE_2 release is a direct effect of the toxin and that does not require a recover of the damage (fig. 39).

By contrast, evaluating LTB_4, the release of this mediator was not detectable indicating that it is not involved in PLTX-induced skin inflammation (data not shown).

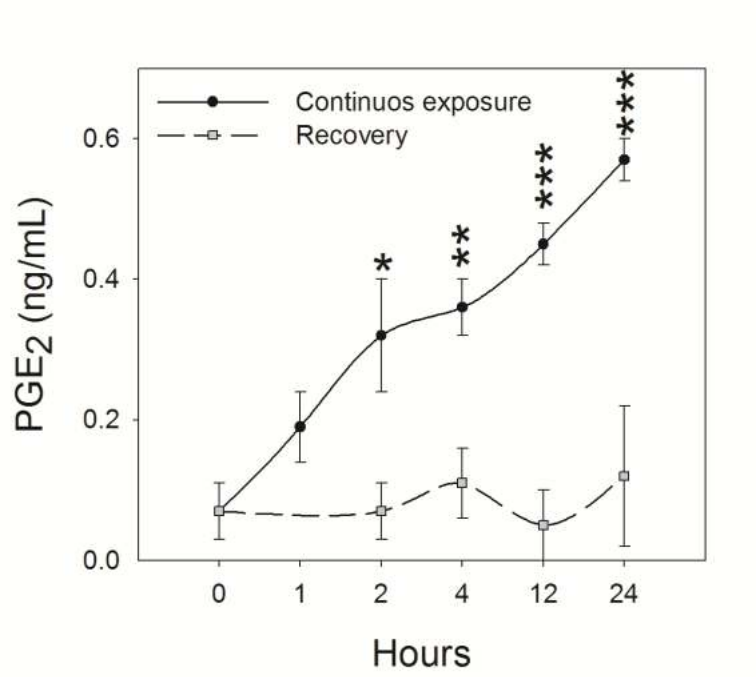

Fig. 39. *Effects of PLTX on PGE_2 release. Cells were exposed to $1.0x10^{-11}$ M PLTX for different time intervals: continuative exposure (2 up to 24 h; ●) as well as recovery conditions (1 h exposure followed by increasing recovery times in toxin-free medium; □). Cell culture medium was then collected and assayed by ELISA test. Data are presented as ng/mL of PGE_2 released by the cells and are the mean ± SEM of three independent experiments performed in duplicate.*

5. Discussion

Despite the increasing cases of dermatitis ascribed to PLTX skin contact (Deeds and Schwartz, 2010; Durando et al., 2007; Gallitelli, personal communication; Hoffmann et al., 2008; Nordt et al., 2009; Tichadou et al., 2010), little is known about its cutaneous toxicity and the mechanisms involved in its toxic activity. Actually, the only study that investigated the ability of PLTX to induce skin irritation was carried out by Fujiki et al. in 1986. In this paper, PLTX was defined as a non-PMA tumour promoter and a skin irritant on the basis of its ability to cause ears erythema in mice after 24 h of treatment with an ED_{50} of 0.02 μg/ear (dose of PLTX causing reddening in 50 % of the treated mice).

With the aim to deeper investigate the effects of PLTX on epidermal cells, this *in vitro* study was carried out using HaCaT keratinocytes. HaCaT cell line is considered a predictive model for evaluating skin toxicity and an ideal model for first-round screening of dermotoxic agents (Gibbs, 2009) due to its morphological and functional properties that are similar to those of normal keratinocytes (Boukamp et al, 1988).

To obtain a characterization of the mechanism of PLTX-induced irritation as nearly complete as possible, the study has taken into account four important aspects:

- PLTX-induced cytotoxic effects: PLTX toxic properties on HaCaT cells have been evaluated and characterized identifying the sequence of intracellular events that leads to cell death.
- PLTX-induced oxidative stress: since a possible intracellular pathway involved in PLTX-mediated cytotoxicity could be the ability of the toxin to induce oxidative stress, the ROS species involved and the mechanisms of their production has been investigated.
- PLTX-induced cell death: the type of cell death (necrosis *vs* apoptosis) induced by the toxin has been investigated along with the underlying mechanisms.

- PLTX-induced pro-inflammatory effects: the ability of PLTX to induce the synthesis and/or the release of pro-inflammatory mediators such as cytokines and arachidonic acid metabolism products has been finally evaluated as a mechanism by which PLTX can induce dermatological lesions.

5.1 Characterization of palytoxin cytotoxicity

Cytotoxicity of PLTX in HaCaT cells was investigated by three methods that evaluate different end points: the MTT reduction assay, that measures the dehydrogenases activity in mitochondria, the SRB assay, that indicates cell density through to the amount of adherent cells and, finally, the LDH release, a cytoplasmic enzyme that indicates plasma membrane rupture.

Firstly, we investigated the relationship between PLTX concentrations and its cytotoxic effects. The MTT assay showed that PLTX decreased the mitochondrial activity in HaCaT cells with an EC_{50} value of $6.1\pm1.3x10^{-11}$ M after 4 h exposure. Basing on this result it appears that HaCaT cells are slightly more sensitive to PLTX than Neuro-2a cells (Ledreux et al., 2009) and the neuroblastoma cell line NG108-15 (Cañete and Diogène, 2008), previously tested by the MTT assay. The concentration-dependency of the cytotoxic effect of PLTX was confirmed by SRB assay (EC_{50} of $4.7\pm0.9x10^{-10}$ M) and by evaluating the release of LDH (EC_{50} of $1.8\pm0.1x10^{-8}$ M) after 4 h contact. Concentration- and time-dependent release of LDH induced by PLTX has been also demonstrated on other cell lines such as the human neuroblastoma BE(2)-M17 cell line (Valverde et al., 2008a), the human adenocarcinoma Caco-2 cells (Valverde et al., 2008b) and the breast cancer MCF7 cell line (Bellocci et al, 2008).

The different EC_{50} values found in our experiments with the three assays within the same time of exposure, reflect the degree of the damage induced by PLTX, on the basis of the evaluated

end points. Indeed, within 4 h exposure, rupture of the plasma membrane, with a consequent leakage of LDH, was found at PLTX concentrations in the nanomolar range, whereas reduction of cell mass was observed at 50 times lower concentrations. However, the most sensitive target appeared to be the mitochondria, which activity was affected by picomolar concentrations of PLTX. On the whole, these results suggest that mitochondrial dysfunction is one of the earliest event among the chain of cellular alterations that takes place after PLTX exposure.

Regarding the time-dependency of PLTX effect on HaCaT cells, time course analysis by SRB assay demonstrated that a time of contact as short as 1 h and a concentration as low as 1.0×10^{-10} M are sufficient to induce the death of 20% of total cells. Under continuous exposure to the toxin, 50% of cell death occurred within 5.1 h (T½). On the other hand, more than 40% of cell death was found in cells exposed for 1 h to an even lower PLTX concentration (1.0×10^{-11} M), followed by a recovery time of 24 h in a toxin-free medium. Under these conditions, the T½ value decreased from 5.1 to 1.3 h. These results suggest that even after a short time of contact and at very low concentrations, PLTX can cause an irreversible damage in human keratinocytes.

This high level of cytotoxicity as well as the quick onset of these effects could be explained by a rapid interaction of the toxin with its molecular target. Hence, experiments were carried out to characterize PLTX binding on HaCaT cells in culture. By immunocytochemical analysis it was possible to detect, for the first time, the binding of PLTX to intact cells and the immuno co-localization analysis suggested that PLTX binding sites are expressed on cell plasma membrane. These results are in accordance with the notion that the primary PLTX molecular target is the Na^+/K^+-ATPase that is located on the plasma membrane (Habermann and Chhatwall, 1982). It has been previously demonstrated that the glycoside ouabain, a well known blocker of Na^+/K^+-ATPase, is able to inhibit some biological activities of PLTX

(Habermann and Chhatwall, 1982; Schilling et al., 2006; Vale-Gonzalez et al., 2007; Pelin et al., 2012) and we also found that PLTX cytotoxic effects on HaCaT cells, such as mitochondrial dysfunction, loss of cell mass and LDH release, were reverted by ouabain. We thus took advantage from the ability of ouabain to compete for the Na^+/K^+-ATPase in order to characterize PLTX binding to intact HaCaT cells by saturation experiments. The binding of PLTX was found to be saturable and reversible with a binding constant (Kd) of $3x10^{-10}$ M. Association experiments, carried out exposing the cells to a PLTX concentration equal to the Kd value for increasing time intervals, demonstrated that the binding was rapid, reaching the equilibrium after 10 minutes of exposure. On the whole, these results are in good agreement with the quick onset of PLTX effects and with the high potency of the toxin in determining cytotoxicity, the mitochondrial dysfunction being the earliest and most sensitive target involved in cellular damage.

5.2 The mitochondrial-mediated oxidative stress is only partially involved in palytoxin cytotoxicity

Mitochondrial membrane depolarization and the consequent reduction of mitochondrial activity that seem to be the earliest events induced by PLTX on HaCaT cells, are strictly related to increased production of ROS. In general, when oxidative stress overcomes skin antioxidant capacity, the subsequent modification of cellular redox state leads to degenerative processes (Wu et al., 2010).

Hence, the possible involvement of oxidative stress production in PLTX toxic effects has been evaluated. Firstly, we investigated the reactive oxygen species produced after exposure to PLTX, measuring the changes of O_2^-, $ONOO^-$ and NO levels. We found that PLTX caused a concentration-related increase of O_2^- production, in accordance with data reporting the ability of the toxin to induce superoxide anion formation in human neutrophils (Gabrielson et

al., 1992; Kano et al., 1987) and in human intestinal cells (Pelin et al., 2012), as well as to alter DJ-1 oxidative stress response protein (Sala et al., 2009). By contrast, neither NO nor ONOO- production seems to be induced by the toxin.

Subsequently, to investigate the possible mechanism of superoxide anion production, gene and protein expressions of enzymes involved in ROS generation (NOX-2, the three NOS isoforms iNOS, eNOS and nNOS, XOD and COX 1 and 2) have been evaluated. Real time PCR indicated no changes in COX-1 and COX-2 mRNA expressions after PLTX exposure from 1 up to 24h. On the contrary, XOD, NOX-2 and NOSs mRNA levels were significantly altered. In particular, the first two showed an early gene over-expression after short exposure times (1-4 h) that returned to the baseline in the subsequent times (up to 24 h). Evaluating the role of iNOS, the analysis of mRNA levels displayed an early overexpression detectable after 1 h exposure, and a delayed induction of eNOS and nNOS isoforms mRNAs after longer exposure time (12 h). Hence, the observed gene overexpressions have been tentatively associated to an increase of the corresponding protein levels. Indeed, western blot analysis confirmed an early increase (1 – 4 h) of NOX-2 and iNOS protein expression, whereas XO protein expression could not be tested, since antibodies against human XO are not, to our knowledge, commercially available.

On the basis of PCR and western blot analysis, we investigated the functional role of these enzymes in PLTX-induced superoxide production and cytotoxicity using selective inhibitors. In particular, XOD and COX did not appear to be involved since the respective inhibitors allopurinol and indomethacin were ineffective in reducing PLTX-induced O_2^-.production. The ability of DPI, a nonspecific inhibitor of both NOX and NOS, to inhibit O_2^- production and slightly counteract mitochondrial damage, suggested a possible role of these two enzymes, in line with PCR and western blot analysis. However, the selective inhibitor of NOX apocynin, was ineffective in both experimental conditions, whereas NMMA, inhibitor of NOS,

significantly reduced only O_2^- produced by high (10^{-8} M) but no by low (10^{-9} and 10^{-10} M) PLTX concentrations. Furthermore, the simultaneous presence of NMMA and apocynin did not reproduce DPI effect on both superoxide production and mitochondrial activity and, paradoxically, the co-administration was even ineffective. Hence, a prominent role of these enzymes in causing PLTX-induced oxidative stress seems unlikely, also considering the modest effect of DPI on reversing PLTX-induced mitochondrial dysfunction.

Beside NOX and NOS, DPI has been reported to inhibit superoxide production induced by the activity of the mitochondrial flavoenzyme NADH-ubiquinone oxidoreductase (complex I) (Li and Trush, 1998). In the present model, rotenone, an inhibitor of mitochondrial complex I, did not affect PLTX-mediated superoxide production but slightly reduced mitochondrial dysfunction. The ability of PLTX to induce O_2^- production could thus be ascribed to a generic activation of flavoenzymes, with a particular role of NOS in inducing superoxide anion and of complex I in mediating mitochondrial dysfunction. However, considering that rotenone was unable to reduce O_2^- production and that the ability of both rotenone and DPI to inhibit PLTX-induced mitochondrial damage was moderate, it is reasonable to believe that these pathways are only partially involved in PLTX-induced cytotoxicity.

An alternative, putative intracellular pathway that can lead to superoxide production is the sustained intracellular ionic disequilibrium that follows PLTX binding to the Na^+/K^+-ATPase. Indeed, O_2^- production induced by the toxin was completely abolished in presence of ouabain. It is widely accepted that the binding of PLTX to the Na^+/K^+-ATPase causes the conversion of the pump into a cationic pore, resulting in an intracellular accumulation of Na^+, and consequent increase of intracellular Ca^{2+} levels. On turn, Ca^{2+} overload can trigger Ca^{2+}-dependent intracellular events culminating in cell distress and death (Schilling et al., 2006; Sheridan et al., 2005; Ares et al., 2005). However, intracellular Na^+ increase has been demonstrated to be directly responsible for PLTX-mediated cell toxicity (Dubois and Cohen,

1977; Muramatsu et al., 1984; Sheridan et al., 2005). On HaCaT cells we found that Na^+ removal from cell medium almost completely abolished PLTX-induced O_2^- production, impairment of mitochondrial activity and appearance of morphological changes, notwithstanding the presence of extracellular Ca^{2+} ions. These findings suggest that intracellular Na^+ accumulation is the first and crucial step in mediating PLTX-induced early cell damage. Regarding the role played by Ca^{2+} in mediating PLTX citotoxicity in HaCaT cells, withdrawal of this ion did not prevent or lessen PLTX-induced superoxide production or changes in cell morphology, suggesting a predominant, even exclusive, role of Na^+ ions in mediating the occurrence of these effects.

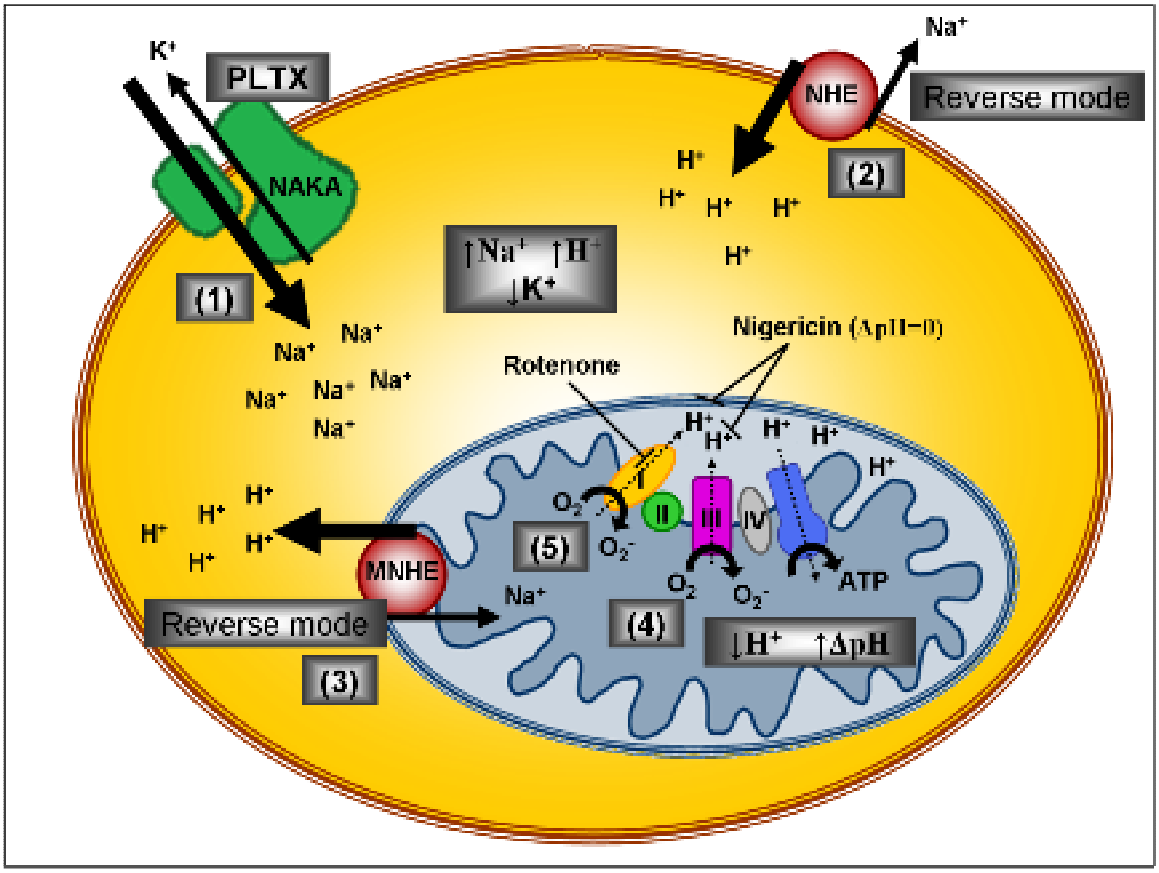

Fig. 40. *Proposed mechanism for PLTX induced superoxide anion production. PLTX binding to Na^+/K^+-ATPase (NAKA) induces intracellular overload of Na^+ (1) followed by intracellular increase of H^+ by reverse functioning of Na^+/H^+ exchanger (NHE, 2). This ionic imbalance may reverse the mitochondrial Na^+/H^+ exchanger activity (MNHE, 3), with consequent increase of ΔpH across H^+-impermeable mitochondrial inner membrane and overproduction of superoxide anion by reverse electron transports through complex III (4) and complex I (5). Superoxide production is prevented by the ionophore nigericin that dissipate ΔpH and by rotenone that inhibits complex I activity.*

Thus, excluding the classical Ca^{2+}-dependent pathway, a mitochondrial-mediated, Na^+-dependent route was taken in consideration as a possible way to induce oxidative stress.

The overload of Na^+ induced by the toxin has been reported to interfere with the functioning of the Na^+/H^+ exchanger (NHE), resulting in an intracellular proton accumulation (Rossini and Bigiani, 2011). In a such compromised ionic balance situation, with elevated intracellular concentrations of H^+ and Na^+ and loss of K^+, it is presumable that the pH gradient (ΔpH) through the H^+-impermeable mitochondrial inner membrane increases. This situation can be worsened by the reverse functioning of the mitochondrial Na^+/H^+ exchanger (MNHE) that under physiological conditions exchanges cytosolic H^+ for mitochondrial Na^+. In presence of high cytosolic concentrations of Na^+, the reverse functioning of MNHE may reduce H^+ concentrations in mitochondrial matrix (Garciarena et al., 2008), where proton flux is strictly controlled to maintain the correct ΔpH across the mitochondrial inner membrane. The increase of ΔpH can cause an increase of mitochondrial superoxide production by reversing electron transport within the electron chain to the NADH-ubiquinone oxidoreductase (complex I), as well as to the complex III, (Lambert and Brand, 2004; Brand et al., 2004). A cartoon depicting the proposed series of events is reported in figure 40. In presence of nigericin, an ionophore that exchanges K^+ for H^+ causing dissipation of ΔpH, PLTX-dependent superoxide production was significantly reduced. This last result suggests that in this model O_2^- production depends primarily on the increased ΔpH across the inner membrane induced by PLTX. However, since in presence of rotenone superoxide production induced by PLTX was not inhibited, it is possible that superoxide formation is catalysed by complex III, whose activity depends on ΔpH as well (Moroney et al., 1984). Interestingly, when nigericin and rotenone were simultaneous administered, a synergistic effect was evidenced in reducing both ROS production and mitochondrial dysfunction, posing a link between PLTX-induced cytotoxicity and oxidative stress. Superoxide production, however, does not seem to be the main pathway leading to cellular sufferance and appears to be the consequence of the

interference with different enzymes, more likely flavoenzymes, the *primum movens* being the ionic imbalance.

5.3 Palytoxin-mediated mitochondrial damage induces necrotic cell death through MPTP opening.

On the whole, the results discussed so far suggest that the mitochondrial dysfunction driven by the ionic imbalance due to the increase of intracellular Na^+ levels is the key event involved in the mechanisms by which PLTX exerts its cytotoxic effects in human skin keratinocytes. One of the main causes of mitochondrial membrane depolarization, with consequent reduction of mitochondrial activity, could be induction of oxidative stress (Wu et al., 2010). However, in HaCaT cells a prominent involvement of oxidative stress in PLTX-induced cytotoxicity seems to be unlikely. Indeed, oxidative stress seems to be more a reaction to a complex stress condition than the cause of cytotoxicity. Hence, further experiments were carried out in order to identify the intracellular pathways that lead to PLTX-induced mitochondrial damage. The results could be useful for the identification of strategies aimed to blocking the series of events involved in cell death and, to some extent, also the irritative symptoms.

In this scenario, mitochondrial damage can be caused by mitochondrial permeability transition pore (MPTP) opening in the inner mitochondrial membrane. Pore opening results in mitochondrial dysfunction and depolarization with uncoupled oxidative phosphorylation and ATP hydrolysis, ultimately leading to cell death (Javadov et al., 2009). Indeed, MPTP opening induced by PLTX was found to be concentration- and time-dependent, and, more interestingly, occurred after an exposure time as short as 5 minutes. The rapidity of this event, together with the binding data suggesting a very quick interaction of the toxin with the cells, indicate that MPTP opening could be the earliest event responsible for PLTX-induced mitochondrial dysfunction and is supported by previous data showing the ability of the toxin

to induce mitochondrial depolarization in intestinal and neuroblastoma cell lines (Valverde et al., 2008a, 2008b).

Hence, the mechanism of MPTP opening has been investigated. Up to now, three molecules are believed to be involved in MPTP assembly: adenine nucleotide translocase (ANT) in the inner membrane, cyclophillin-D (CyP-D) in the matrix and the voltage-dependent anion channel (VDAC) in the outer membrane (Leung and Halestrap, 2008; Javadov et al., 2009). We thus investigated the involvement of CyP-D in mediating PLTX cytotoxic effects using cyclosporine A, a well known inhibitor of MPTP formation by prevention of cyclophillin D binding to the mitochondrial inner membrane (Norman et al., 2010). Under these conditions, however, PLTX-induced MPTP opening as well as mitochondrial dysfunction were not prevented. It has been reported that MPTP opening and the subsequent mitochondrial dysfunction can be also mediated by the Bcl-2/adenovirus E1B 19-kilodalton interacting protein (BNIP3) (Vande Velde et al., 2000). BNIP3 is primarily located in the mitochondria, where it is integrated into the mitochondrial membrane. It is well documented that overexpression of BNIP3 leads to loss of mitochondrial membrane potential and cell death via MPTP opening (Imazu et al., 1999; Vande Velde et al., 2000; Gustafsson, 2011; Nakamura et al., 2012). In the present model, a partial involvement of BNIP3 in PLTX-induced MPTP opening seems to be likely. Western blot analysis, in fact, demonstrated a slight increase in BNIP3 protein expression after PLTX exposure with respect to the untreated control. However, BNIP3 is believed to be primarily involved in mitochondria turnover via autophagy, targeting the damaged mitochondria that need to be removed (Gustafsson, 2011; Nakamura et al., 2012). Moreover, its mechanism of action is still a matter of debate; hence, another possible mechanism of MPTP opening has been investigated. MPTP opening is a Ca^{2+}-dependent event, but is known to be regulated also by mitochondrial H^{+} concentrations (Bernardi et al., 1992). Accordingly, we found that PLTX-induced MPTP opening was totally abolished in Ca^{2+}-free medium and partially reduced in presence of nigericin, that can inhibit

H^+ imbalance. Quite interestingly, however, MPTP opening was inhibited also in Na^+-free medium, and to the same extend as in Ca^{2+}-free medium. These results suggest once more that in the HaCaT cell model Na^+ imbalance is the critical step in PLTX-mediated cytotoxicity. In skin keratinocytes, ion fluxes are strictly controlled. Among all, NHE regulates protonic balance (Sarangarajan et al., 2001; Behne et al., 2002) and epithelial Na^+-channel (ENaC) (Brouard et al., 1999; Guitard et al., 2004) are the most important Na^+ regulators in the skin. However, a feasible role for these cationic transporters seems to be excluded since their blockade did not result in a reduction of PLTX effects. From these data it has been possible to conclude that MPTP opening and, therefore, mitochondrial dysfunction, could be considered as passive cellular reaction to the sustained ionic imbalance induced by the toxin, rather than a biochemical controlled response. It seems likely, indeed, that within a very short exposure time the huge overload of Na^+ and the subsequent supply of water may induce mitochondria swelling up to mitochondrial membrane disruption. However, further experiments are required to demonstrate this hypothesis.

It is well known that one of the major consequences of mitochondrial dysfunction and MPTP opening (collapse of the mitochondrial inner transmembrane potential, uncoupling of the respiratory chain, hyperproduction of superoxide anions) could be the induction of cell death via an apoptotic process (Javadov and Karmazyn, 2007). On the other hand, MPTP opening seems to induce mainly necrotic cell death (Leung and Halestrap, 2008). In conclusion, however, the outcome of apoptosis or necrosis as well as cell survival can be determined by the intensity of the insult (Ziegler and Groscurth, 2004). The observed delay in S and G2M phases induced by PLTX can be interpreted, for instance, only as the blockade of the cell cycle in order to restore mitochondrial functionalities. These observations are in line with a previous study carried out on the intestinal Caco-2 cell line concluding that the effects of PLTX were very unspecific, inducing both a primary necrosis and a secondary apoptosis (Valverde et al., 2008b). In the present model, however, apoptosis seems to be not induced by

PLTX. With this aim caspasis 3/7 (the last caspasis activated during the apoptotic process), caspasis 8 (the first activated within the extrinsic pathway) and caspasis 9 (the first activated during the intrinsic pathaway) (Ashkenazi and Herbst, 2008) have been evaluated. None of these caspasis was found to be induced by the toxin, neither under recovery conditions that reduced the entity of the insult and may give more time to the cell to recover from the damage. Similarly, no apoptotic bodies formation was recorded. On the contrary, morphological changes showing a necrotic-like fragmentation of nuclei were observed. By contrast, the observed concentration- and time-dependent uptake of PI, reaching 100% of uptake already after only 1 h exposure, clearly demonstrates necrosis occurrence. Indeed, it is widely known that PI is a membrane-impermeable molecule that can enter into the cells only after membrane rupture, a feature of necrotic-like cell death. On the other hand, some indications of necrosis appearance were already given by the concentration-dependent release of LDH, indicating plasma membrane rupture and, therefore, a direct marker of necrotic cell death. Furthermore, confocal images have definitely revealed the typical morphology alterations of necrosis after PLTX exposure. Up to now several data reported PLTX-induced morphological changes, such as rounding of cell shape, detachment from support or cell swelling (Sheridan et al., 2005; Valverde et al., 2008a; 2008b; Louzao et al., 2011), but no information about the nature of cell death were given. In contrast, from the present data it has been possible to assess dramatic cellular alterations such as membrane interruption, leakage of the cytoplasmic content with a subsequent complete destruction of cellular architecture. On the whole, these data, that are in accordance with a recent paper demonstrating necrotic occurrence in PC-12 cell line after PLTX exposure (Sagara et al., 2011), clearly demonstrated that independently on the concentration or the time of exposure, on HaCaT cells PLTX induces necrosis rather than apoptosis.

5.4 Playtoxin-dependent skin inflammation is induced by release of pro-inflammatory cytokines and prostaglandins.

Considering the clinical available data and the toxin chemical nature, it is conceivable that PLTX induces an irritative-based topical inflammation rather than an allergic response. Recently it has been suggested a case definition of "palytoxin dermatitis", characterized by a maculo-papular and/or erythematous dermatitis, sometimes accompanied by systemic symptoms (Tubaro et al., 2011). However, symptomatic treatments of "palytoxin dermatitis" are not standardized and involved anti-inflammatory corticosteroids, non steroidal anti-inflammatory drugs (NSAID), usually associated to intravenous infusion fluids. Moreover, in view of the frequent related respiratory symptoms especially during *Ostreopsis* exposure, these treatments are associated to a therapy involving the use of nebulised β_2-agonists, inhaled and systemic corticosteroids together with oxygen therapy (Tubaro et al., 2011).

Understanding the nature of skin inflammation could be extremely useful for the correct pharmacological treatment of the symptoms. As described above, Fujiki et al. (1986) defined the skin irritant properties of PLTX. Irritant contact dermatitis (ICD) is a non-immunological, local inflammatory skin reaction localised in epidermis in response to irritant chemical exposure (Welss et al., 2004), which initiation and modulation consist mainly in generation of cytokines.

Thus, to characterize PLTX skin irritation four of the most important pro-inflammatory cytokines have taken in consideration: the skin inflmammation promoter IL-1α, the inflammation acute phase mediator IL-6, the chemoattractant IL-8 and TNF-α, involved in the development of skin inflammation. The present results show an early upregulation of IL-6, IL-8 and TNF-α genes observable yet after 1 h PLTX exposure. However, these early gene over-expressions were not accompanied by a release of the corresponding cytokine from the cells that, at least considering IL-6 and IL-8 occurs after longer exposure time (i.e. 24 h). On

the contrary, no effects on TNF-α and IL-1α release were recorded, discarding their involvement at least in the initial phase of skin inflammation. These data, anyway, corroborate the use of anti-inflammatory corticosteroids to reduce gene transcription encoding for pro-inflammatory cytokines such as IL-6 and IL-8. Moreover, the evidence of the chemoattractant IL-8 increase could suggest an involvement of other cellular types such as neutrophils, macrophage and dendritic cells, therefore, sustaining the inflammatory response. This observation implicates the necessity of further studies performed on these cellular model in order to deeper investigate this aspect.

Another important pathway driving cutaneous inflammation is based on the arachidonic acid (AA) metabolism products, such as prostaglandins (PGs) and leukotrienes (LTs) (Bickers and Athar, 2006). In this contest, high level of PGE_2 (Welss et al., 2004) and LTB_4 (Ruzicka et al., 1986) has been found to be released after irritation. Moreover, LTB_4 is one of the most potent chemoattractant agents for polymorphonuclear cells (Black et al. 1985). Hence, the attention has been focused on these mediators. The toxin induces a time-dependent release of PGE_2 from the cells, starting after 2 h exposure. On the contrary, in the present model LTB_4 was not detectable. This results justify the use of NSAID, especially in the early phases of inflammation. This observation is also supported by the fact that under recovery conditions PGE_2 release was comparable to the untreated controls, suggesting that this mediator is probably involved in the induction of the inflammatory reaction and not in the maintenance of the response.

On the whole, these results suggest that an integrated therapy based on the use of corticosteroids and NSAID could be useful to reduce the inflammatory symptoms that have been observed at the skin level after contact with PLTX. However, a more complete study based on different cells (i.e dendritic cells, Langherans cells, or neutrophils) known to be

involved in the initiation and modulation of skin inflammation is required. Further experiments are in progress to fulfil this aspect.

6. Conclusions

Clinical cases of poisonings after cutaneous exposure to PLTX during *Ostreopsis* blooms and after handling toxic zoanthids are well known and probably underestimated in number. Despite the increasing cases of dermatitis ascribed to PLTX skin contact, little is known about its cutaneous toxicity and the related mechanism. Hence, this *in vitro* study was carried out on HaCaT skin keratinocytes with the aim to characterize PLTX skin toxicity. The main results can be summarize as follows. The remarkable cytotoxic effect of PLTX on HaCaT cells can be explained by the high affinity of binding observed in the order of 10^{-10} M only after 10 minutes exposure. In line with this result, PLTX exerts its cytotoxicity in the pico – nanomolar range after short time exposure and mitochondria turned out to be the most sensitive intracellular target of the toxin. Indeed, mitochondria seems to be the main actor of PLTX activity through a very quick opening of MPTP induced after only 5 minutes by the ionic imbalance, driven mainly by the massive intracellular overload of Na^+. This effect is explained by the peculiar mechanism of action of the toxin: the binding to the Na^+/K^+-ATPase and its subsequent transformation in a unspecific cationic channel. The compromised ionic balance and the reversed ionic fluxes through mitochondria induce oxidative stress with huge production of superoxide anion by the cells in response to the insult. In this scenario, the sustained MPTP opening together with the oxidative damages induce by superoxide anion and the elevated, abnormal Na^+ and Ca^{2+} levels induce cell swelling, plasma membrane ruptures and, ultimately, a necrotic-like cell death (fig. 41).

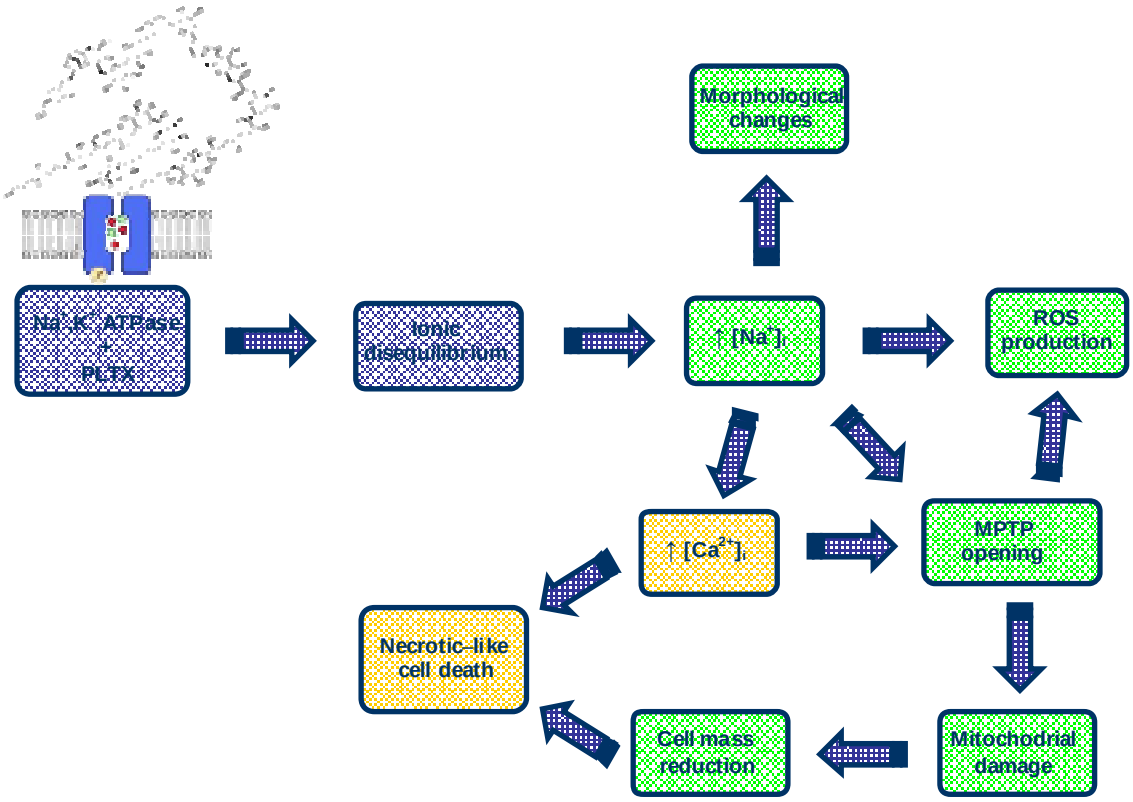

Fig. 41. *Sequence of intracellular events leading to PLTX-induced cell death. The ionic imbalance induced by the interaction of the toxin with the Na+/K+-ATPase increase the intracellular level of Na+ and, therefore, of Ca2+ with a consequent sustained opening of MPTP and impairment of mitochondrial activities. As a consequence, mitochondrial-mediated ROS production increases. Ultimately, MPTP opening together with ionic imbalance and oxidative stress induce necrotic-like cell death occurrence.*

The present results suggest a harmful potential of the toxin after cutaneous exposure. It is important to underline that PLTX has not always been quantified in water samples concurrently with the clinical reports ascribing dermotoxicity to the toxin exposure. However, an indirect evaluation of entity of the cutaneous exposure to PLTX or PLTX-like compounds can be extrapolated from *Ostreopsis* cells density recorded in the Mediterranean sea concomitantly to the dermatitis cases. Indeed, natural plankton samples, as well as cultured *O. ovata* cells collected along Genoa coasts during 2005 and 2006 toxic outbreaks, revealed the presence of a putative PLTX (PLTX) and ova-a at concentrations of 0.55 and 3.85×10^{-12}

g/cell, respectively (Ciminiello et al., 2006; 2008). Moreover, Guerrini and co-workers (2010) quantified at the end of the stationary phase of cultured *O. ovata* collected along Tyrrhenian coasts in August 2006, 1.90×10^{-12} g/cell of PLTX and 3.27×10^{-11} g/cell of ova-a, corresponding to 8.69×10^{-6} g/L and 1.92×10^{-4} g/L culture medium, respectively. Even if a prevalence of ova-a was found, the concentration of released PLTXs in the water (6.13×10^{-6} g/L of PLTX and 6.12×10^{-5} g/L of ova-a) was one-two orders of magnitude higher than the lowest EC_{50} value we found after 4 h exposure (6.1×10^{-11} M obtained by the MTT assay, equal to 1.63×10^{-7} g/L), making feasible a correlation between the observed effects *in vitro* and the dermatological problems observed during *O. ovata* blooms.

Finally, to fill another important gap in literature, the effects of PLTX on some pro-inflammatory mediators have been evaluated. The early release of PGE_2 together with a delayed release of IL-6 and IL-8, probably involved in the development of the inflammation, let us to suggest a therapy that combines NSAID at the very initial phase and anti-inflammatory corticosteroids.

On the whole, these results give new and almost complete insights regarding PLTX intracellular pathway leading to cell death and put a rationale for the treatment by the sanitary authorities of the so called “palytoxin dermatitis”.

7. References

Alcala, A.C., Alcala, L.C., Garth, J.S., Yasumura, D., Yasumoto, T., 1988. Human fatality due to ingestion of the crab *Demania reynaudii* that contained a palytoxin-like toxin. Toxicon 26 (1), 105-107.

Aligizaki, K., Katikou, P., Milandri, A., Diogène, J., 2011. Occurrence of palytoxin.group toxins in seafood and future strategie sto complement the present state of the art. Toxicon 57 (3), 390-399.

Amir, I., Harris, J.B., Zar, M.A., 1997. The effect of palytoxin on neuromuscular junctions in the anococcygeus muscle of the rat. J. Neurocytol. 26 (6): 367-76.

Ansel, J., Perry, P., Brown, J., Damm, D., Phan, T., Hart, C., Luger, T., Hefeneider, S., 1990. Cytokine modulation of keratinocyte cytokines. J. Invest. Dermatol. 94 (6): 101S-107S.

Ares, I.R., Louzao, M.C., Vieytes, M.R., Yasumoto, T., Botana, L.M., 2005. Actin cytoskeleton of rabbit intestinal cells is a target for potent marine phycotoxins. J. Exp. Biol. 208, 4345-4354.

Armstrong, R:W:, Beau, J.M., Cheon, S.H., Christ, W.J., Fujioka, H., Ham, W.H., Hawkins, L.D. et al., 1989. Total synthesis of a full protected palytoxin carboxylic acid. J. Am. Chem. Soc. 111: 7525.

Artigas, P., Gadsby, D.C., 2004. Large diameter of palytoxin-induced Na/K pump channels and modulation of palytoxin interaction by Na/K pump ligands. J. Gen. Physiol. 123 (4): 357-376.

Ashkenazi, A., Herbst, R.S., 2008. To kill a tumor cell: the potential of proapoptotic receptor agonists. J. Clin. Invest. 118 (6): 1979-1990.

Attaway, D.H., Ciereszko, L.S., 1974. Isolation and partial charcaterization of Caribbean palytoxin. Proceedings of Second International Coral Reef Symposium I, Great Barrier Reef Community, Brisbane.

Battocchi, C., Totti, C., Vila, M., Masó, M., Capellacci, S., Accoroni, S., Reñe, A., Scardi, M., Penna, A., 2010. Monitoring toxic microalgae Ostreopsis (dinoflagellate) species in coastal waters of the Mediterranean Sea using molecular PCR-based assay combined with light microscopy. Mar. Poll. Bull. 60, 1074-1084.

Behne, M.J., Meyer, J.W., Hanson, K.M., Barry, N.P., Murata, S., Crumrine, D., Clegg, R.W., Gratton, E., Holleran, W.M., Elias, P.M., Mauro, T.M., 2002. NHE1 regulates the stratum corneum permeability barrier homeostasis. Microenvironment acidification assessed with fluorescence lifetime imaging. J. Biol. Chem. 277 (49): 47399-47406.

Bellocci, M., Ronzitti, G., Milandri, A., Melchiorre, N., Grillo, C., Poletti, R., Yasumoto, T., Rossini, G.P., 2008. A cytolytic assay for the measurement of palytoxin based on a cultured monolayer cell line. Anal. Biochem. 374 (1), 48-55.

Beress, L., Zwick, J., Kolkenbrock, J., Kaul, P.N., Wassermann, O., 1983. A method for the isolation of the Caribbean palytoxin (C-PTX) from the coelenterate (zoanthid) Palythoa caribaeorum. Toxicon 21, 285-290.

Bernardi, P., Vassanelli, S., Veronese, P., Colonna, R., Szabo´, I., Zoratti, M., 1992. Modulation of the mitochondrial permeability transition pore. Effect of protonsand divalent cations. J. Biol. Chem. 267: 2934–2939.

Bickers, D.R., Athar, M., 2006. Oxidative stress in the pathogenesis of skin disease. J. Invest. Dermatol. 126 (12): 2565-2575.

Black, A.K., Barr, R.M., Wong, E., Brain, S., Greaves, M.W., Dickinson, R., Shroot, B., Hensby, C.N., 1985. Lipoxygenase products of arachidonic acid in human inflamed skin. Br. J. clin. Pharmac. 20: 185-190.

Boukamp, P., Petrussevska, R.T., Breitkreutz, D., Hornung, J., Markham, A., Fusenig, N.E., 1988. Normal keratinization in a spontaneously immortalized aneuploid human keratinocyte cell line. J. Cell. Biol. 106, 761-771.

Brand, M.D., Affourtit, C., Esteves, T.C., Green, K., Lambert, A.J., Miwa, S., Pakay, J.L., Parker, N., 2004. Mitochondrial superoxide: production, biological effects, and activation of uncoupling proteins. Free Radic. Biol. Med. 37 (6): 7557-67.

Brescianini, C., Grillo, C., Melchiorre, N., Bertolotto, R., Ferrari, A., Vivaldi, B., Icardi, G., Gramaccioni, L., Funari, E., Scardala, S., 2006. Ostreopsis ovata algal blooms affecting human health in Genova, Italy, 2005 and 2006. Euro Surveill. 11.

Briganti, S., Picardo, M., 2003. Antioxidant activity, lipid peroxidation and skin diseases. What's new. J. Eur. Acad. Dermatol. Venereol. 17 (6): 663-669.

Brouard, M., Casado, M., Djelidi, S., Barrandon, Y., Farman, N., 1999. Epithelial sodium channel in human epidermal keratinocytes: expression of its subunits and relation to sodium transport and differentiation. J. Cell. Sci. 112 (19): 3343-3352.

Cañete, E., Diogène, J., 2008. Comparative study of the use of neuroblastoma cells (Neuro-2a) and neuroblastomaxglioma hybrid cells (NG108-15) for the toxic effect quantification of marine toxins. Toxicon 52 (4), 541-550.

Chung, H.Y., Baek, B.S., Song, S.H., Kim, M.S., Huh, J.I., Shim, K.H., Kim, K.W., Lee; K.H. 1997. Xanthine dehydrogenase/xanthine oxidase and oxidative stress. Age 20: 127-140.

Ciminiello, P., Dell'Aversano, C., Fattorusso, E., Forino, M., Magno, G.S., Tartaglione, L., Grillo, C., Melchiorre, N., 2006. The Genoa 2005 outbreak. Determination of putative palytoxin in Mediterranean Ostreopsis ovata by a new liquid chromatography tandem mass spectrometry method. Anal. Chem. 78, 6153-6159.

Ciminiello, P., Dell'Aversano, C., Fattorusso, E., Forino, M., Tartaglione, L., Grillo, C., Melchiorre, N., 2008. Putative palytoxin and its new analogue, ovatoxin-A in Ostreopsis ovata collected along the Ligurian coasts during the 2006 toxic outbreak. J. Am. Soc. Mass. Spectrom. 19, 111-120.

Ciminiello, P., Dell'Aversano, C., Dello Iacovo, E., Fattorusso, E., Forino, M., Grauso, L. Tartaglione, L., Florio, C., Lorenzon, P., De Bortoli, M., Tubaro, A., Poli, M., Bignami, G., 2009. Stereostructure and biological activity of 42-hydroxy-palytoxin: a new palytoxin analogue from Hawaiian Palythoa subspecies. Chem. Res. Toxicol. 22, 1851-1859.

Ciminiello, P., Dell'Aversano, C., Dello Iacovo, E., Fattorusso, E., Forino, M., Grauso, L., Tartaglione, L., Guerrini, F., Pezzolesi, L., Pistocchi, R., Vanucci, S., 2012. Isolation and structure elucidation of ovatoxin-a, the major toxin produced by *Ostreopsis ovata*. J. Am. Chem. Soc. 134: 1869-1875.

Coca, R., Soler F., and Fernandez-Belda, F. 2008. Characterization of the palytoxin effect on Ca^{2+}-ATPase from sarcoplasmic reticulum (SERCA). Arch. Biochem. Biophys. 478 (1): 36-42.

Deeds, J.D., Schwartz, M., 2010. Human risk associated with palytoxin exposure. Toxicon 56, 150-162.

Di Turi, L., Lo Caputo, S., Marzano, M.C., Pastorelli, A.M., Pompei, M., Rositani, L., Ungaro, N., 2003. Ostropsidiaceae (Dynophyceae) presence along the coastal area of Bari. Biol. Mar. Mediterr. 10, 675-678.

Dodd, F., Limoges, M., Boudreau, R.T.M., Rowden, G., Murphy, P.R., Too, C.K.L., 2000. L-Arginine inhibits apoptosis via a NO-dependent mechanism in Nb2 Lymphoma cells. J. Cell. Biochem. 77: 624–634.

Dubois, J.M., Cohen, J.B., 1977. Effect of palytoxin on membrane and potential and current of frog myelinated fibers. J. Pharmacol. Exp. Ther. 201 (1), 148-145.

Durando, P., Ansaldi, F., Oreste, P., Moscatelli, P., Marensi, L., Grillo, C., Gasparini, R., Icardi, G., 2007. Ostreopsis ovata and human health: epidemiological and clinical features of respiratory syndrome outbreaks from a two year syndromic surveillance, 2005-2006, in northwest Italy. Euro Surveill. 12 (23).

Elias, P.M., 1983. Epidermal lipids, barrier function, and desquamation. J. Invest. Dermatol. 80 (Suppl): 44s-49s.

Feliciani, C., Gupta, A.K., Saucier, D.N., 1996. Keratinocytes and cytokine/growth factors. Crit. Rev. Oral. Biol. Med. 7 (4): 300-318.

Fink, K., Duval, A., Martel, A., Soucy-Faulkner, A., Grandvaux, N., 2008. Dual role of NOX2 in respiratory syncytial virus- and sendai virus-induced activation of NF-kappaB in airway epithelial cells. J. Immunol. 180: 6911-6922.

Frolova, G.M., Kuznetsova, T.A., Mikhailov,, V.V., Eliakov G.B., 2000. An enzyme linked immunosorbent assay for detecting palytoxin-producing bacteria. Russian J. Bioorg. Chem. 26: 285-289.

Fujiki, H., Suganuma, M., Nakayasu, M., Hakii, H., Horiuchi, T., Takayama, S., Sugimura, T., 1986. Palytoxin is a non-12-O-tetradecanoylphorbol-13-acetate type tumor promoter in two-stage mouse skin carcinogenesis. Carcinogenesis 7 (5), 707-710.

Gabrielson, E.W., Kuppusamy, P., Povey, A.C., Zweier, J. L., Harris, C.C., 1992. Measurement of neutrophil activation and epidermal cell toxicity by palytoxin and 12-O-tetradecanoylphorbol-13-acetate. Carcinogenesis 13 (9), 1671-1674.

Gallitelli, M., Ungaro, N., Addante, L.M., Procacci, V., Gentiloni, N., Sabbà, C., 2005. Respiratory illness as a reaction to tropical algal blooms occurring in a temperate climate. JAMA 293, 2599-2600.

Garciarena, C.D., Caldiz, C.I., Correa, M.V., Schinella, G.R., Mosca, S.M., Chiappe de Cingolani, G.E., Cingolani, H.E., Ennis, I.L., 2008. Na^+/H^+ exchanger-1 inhibitors decrease myocardial superoxide production via direct mitochondrial action. J. Appl. Physiol. 105: 1706–1713.

Gibellini, D., De Crignis, E., Ponti, C., Cimatti, L., Borderi, M., Tschon, M., Giardino, R., Re, M.C., 2008. HIV-1 triggers apoptosis in primary osteoblasts and HOBIT cells through TNFalpha activation. J. Med. Virol. 80: 1507-1514.

Gibbs, S., 2009. In vitro irritation models and immune reactions. Skin. Pharmacol. Physiol. 22 (2): 103-113.

Gleibs, S., Mebs, D., Werding, B., 1995. Studies on the origin and distribution of palytoxin in a Caribbean coral reef. Toxicon 33, 1531-1537.

Gleibs, S., Mebs, D., 1999. Distribution and sequestration of palytoxin in coral reef animals. Toxicon 37, 1521-1527.

Guennoun, S., Horisberger, J.D., 2000. Structure of the 5th transmembrane segment of the Na,K-ATPase alpha subunit: a cysteine-scanning mutagenesis study. FEBS Lett. 482 (1-2): 144-148.

Guennoun, S., Horisberger, J.D., 2002. Cysteine-scanning mutagenesis study of the sixth transmembrane segment of the Na,K-ATPase alpha subunit. FEBS Lett. 513 (2-3): 277-281.

Guerrini, F., Pezzolesi, L., Feller, A., Riccardi, M., Ciminiello, P., Dell'Aversano, C., Tartaglione, L., Dello Iacovo, E., Fattorusso, E., Forino, M., Pistocchi, R., 2010. Comparative growth and toxin profile of cultured *Ostreopsis ovata* from the Tyrrhenian and Adriatic Seas. Toxicon 55 (2-3), 211-220.

Guitard, M., Leyvraz, C., Hummler, E., 2004. A nonconventional look at ionic fluxes in the skin: lessons from genetically modified mice. News Physiol. Sci. 19: 75-79.

Gustafsson, A.B., 2011. Bnip3 as a dual regulator of mitochondrial turnover and cell death in the myocardium. Pediatr. Cardiol. 32: 267–274.

Habermann, E., Chhatwal, G.S., 1982. Ouabain inhibits the increase due to palytoxin of cation permeability of erythrocytes. Naunyn. Schmiedebergs. Arch. Pharmacol. 319 (2), 101-107.

Habermann, E., 1989. Review article. Palytoxin acts through Na+/K+ATPase. Toxicon 27, 1175-1187.

Hansen, G., Turquet, J., Quod, J.P., Ten-Hage, L., Lugomela, C., Kyewalyanga, M., Hurbungs, M., Wawiye, P., Ogongo, B., Tunje, S., Rakotoarinjanahary, H., 2001. Potentially harmful algae of the West Indian Ocean: a guide based on a preliminary survey. In: IOC Manuals and Guides, 41. Intergovernmental Oceanographic Commission of UNESCO, Paris, 105 pp.

Harmel, N., Apell, H.J., 2006. Palytoxin-induced effects on partial reaction of the Na,K-ATPase. J. Gen. Physiol. 128 (1): 103-118.

Hashimoto, Y., Fusetani, N., Kimuta, S., 1969. Aluterin: a toxin of filefish *Alutera scripta*, probably originating from a zoantharian. Bull. Jap. Soc. Scient. Fish. 35: 1086-1093.

Hilgemann, D.W., 2003. From a pump to a pore: how palytoxin opens the gates. PNAS 100 (2): 386-388.

Hoffmann, K., Hermanns-Clausen, M., Buhl, C., Buchler, M.W., Schemmer, P., Mebs, D., Kauferstein, S., 2008. A case of palytoxin poisoning due to contact with zoanthid corals through skin injury. Toxicon 51, 1535-1537.

Hancock, J.T., Desikan, R., Neill, S.J., 2001. Role of reactive oxygen species in cell signalling pathways. Biochem. Soc. Trans. 29 (2): 345-350.

Houliston, R.A., Keogh, R.J., Sugden, D., Dudhia, J., Carter, T.D., Wheeler-Jones, C.P., 2002. Protease-activated receptors upregulate cyclooxygenase-2 expression in human endothelial cells. Thromb. Haemost. 88: 321-328.

Imazu, T., Shimizu, S., Tagami, S., Matsushima, M., Nakamura, Y., Miki, T., Okuyama, A., Tsujimoto, Y., 1999. Bcl-2/E1B 19kDa-interacting protein 3-like protein (Bnip3L) interacts with Bcl-2/Bcl-xL and induces apoptosis by altering mitochondrial membrane permeability. Oncogene 18: 4523–4529.

Inuzuka, T., Uemura, D., Arimoto, H., 2008. The conformation features of palytoxin in aqueous solution. Tetrahedron 64: 7718-7723.

Ito, K., Urakawa, N., Koike, H., 1982. Cardiovascular toxicity of palytoxin in anesthetized dogs. Arch. Int. Pharmacodyn. Ther. 258 (1): 146-154.

Ito, E., Yasumoto, T., 2009. Toxicological studies on palytoxin and ostreocin-D administered to mice by three different routes. Toxicon 54 (3), 244-251.

Javadov, s., Karmazyn, M., Escobales, N., 2009. Mitochondrial permeability transition pore opening as a promising therapeutic target in cardiac diseases. J. Pharmacol. Exp. Ther. 330 (3): 670-678.

Javadov, S., Karmazyn, M., 2007. Mitochondrial permeability transition pore opening as an endpoint to initiate cell death and as a putative target for cardioprotection. Cell. Physiol. Biochem. 20: 1–22.

Kano, S., Iizuka, T., Ishimura, Y., Fujiki, H., Sugimura, T., 1987. Stimulation of superoxide anion formation by the non-TPA type tumor promoters palytoxin and thapsigargin in porcine and human neutrophils. Biochem. Biophys. Res. Commun. 143 (2), 672-677.

Katikou, P., 2008. Palytoxin and analogues: ecobiology and origin, chemistry, metabolism, and chemical analysis. In: Botana, L.M. (Ed.), Seafood and Freshwater Toxins. Pharmacology, Physiology and Detection. CRC Press, Boca Raton, pp. 631-663.

Kerbrat, A.S., Amzil, Z., Pawlowiez, R., Golubic, S., Sibat, M., Darius, H.T., Chinain, M., Laurent, D., 2011. First evidence of palytoxin and 42-hydroxy-palytoxin in the marine cyanobacterium *Trichodesmium*. Mar. Drugs 9: 543-560.

Kermarec, F., Dor, F., Armengaud, A., Charlet, F., Kantin, R., Sauzade, D., de Haro, L., 2008. Health risks related to Ostreopsis ovata in recreational waters. Env. Risques Santé 7, 357-363.

Kishi, Y., 1989. Natural product synthesis: palytoxin. Pure. Appl. Chem. 61: 313.

Kockskamper, J., Ahmmed, G.U., Zima, A.V., Sheehan, K.A., Glitsch, H.G., Blatter, L.A., 2004. Palytoxin disrupts cardiac excitation.contraction coupling through interactions with P-type ion pumps. Am. J. Physiol. Cell. Physiol. 287: 527-538.

Lambert, A.J., Brand, M.D., 2004. Superoxide production by NADH:ubiquinone oxidoreductase (complex I) depends on the pH gradient across the mitochondrial inner membrane. Biochem. J. 382 (2): 511-517.

Lee, W.J., Wu, C.S., Lin, H., Lee, I.T., Wu, C.M., Tseng, J.J., Chou, M.M., Sheu, W.H., 2009. Visfatin-induced expression of inflammatory mediators in human endothelial cells through the NF-kappaB pathway. Int. J. Obes. (Lond). 33: 465-472.

Ledreux, A., Krys, S., Bernard, C., 2009. Suitability of the Neuro-2a cell line for the detection of palytoxin and analogues (neurotoxic phycotoxins). Toxicon 53 (2), 300-308.

Leung, A.W., Halestrap, A.P., 2008. Recent progress in elucidating the molecular mechanism of the mitochondrial permeability transition pore. Biochim. Biophys. Acta. 1777 (7-8): 946-952.

Li, Y., Trush, M.A., 1998. Diphenyleneiodonium, an NAD(P)H oxidase inhibitor, also potently inhibits mitochondrial reactive oxygen species production. Biochem. Biophys. Res. Commun. 253: 295–299.

Louzao, M.C., Ares, I.R., Cagide, E., Espiña, B., Vilariño, N., Alfonso, A., Vieytes, M.R., Botana, L.M., 2011. Palytoxins and cytoskeleton: An overview. Toxicon 57 (3): 460-469.

Mahnir, V.M., Kozlovskaya, E.P., Kalinovsky, A.I., 1992. Sea anemone *Radianthus macrodactylus*-a new source of palytoxin. Toxicon 30 (11): 1449-1456.

Mangialajo, L., Bertolotto, R., Cattaneo-Vietti, R., Chiantore, M., Grillo, C., Lemee, R., Melchiorre, N., Moretto, P., Povero, P., Ruggirei, N., 2008. The toxic benthic dinoflagellate *Ostreopsis ovata*: quantification of proliferation along the coastline of Genoa, Italy. Mar. Poll. Bull. 56, 1209–1214.

Monteiro-Riviere, N.A., 2010. Toxicology of the skin, Target Organ Toxicology Series, Vol. 29, Informa Healthcare, New York London.

Monteiro-Riviere, N.A., Bristol, D.G., Manning, T.O., Rogers, R.A., Riviere, J.E., 1990. Interspecies and interregional analysis of the comparative histologic thickness and laser Doppler blood flow measurements at five cutaneous sites in nine species. J. Invest. Dermatol. 95 (5): 582-586.

Monti, M., Minocci,M., Beran, A., Ivesa, L., 2007. First record of *Ostreopsis cfr. ovata* on macroalgae in the Northern Adriatic Sea. Mar. Poll. Bull. 54: 598–601.

Moore, R.E., Bartolini, G., 1981. Structure of palytoxin. J. Am. Chem. Soc. 103, 2491-2494.

Moore, R.E., Helfrich, P., Patterson, G.M.L., 1982. The deadly seaweed of Hana. Oceanus 25, 54-63.

Moore, R.E., Scheuer, P.J., 1971. Palytoxin: A new marine toxin from a coelenterate. Science 172, 495-498.

Moroney, P.M., Scholes, T.A., Hinkle, P.C., 1984. Effect of membrane potential and pH gradient on electron transfer in cytochrome oxidase. Biochemistry 23: 4991–4997.

Muramatsu, I., Uemura, D., Fujiwara, M., Narahashi, T., 1984. Characteristics of palytoxin-induced depolarization in squid axons. J. Pharmacol. Exp. Ther. 231 (3), 488-494.

Nakamura, Y., Kitamura, N., Shinogi, D., Yoshida, M., Goda, O., Murai, R., Kamino, H., Arakawa, H., 2012. BNIP3 and NIX mediate MIEAP-induced accumulation of lysosomal proteins within mitochondria. PLoS One 7 (1): e30767.

Nakanishi, A., Yoshizumi, M., Morita, K., Murakumo, Y., Houchi, H., Oka, M., 1991. Palytoxin: a potent stimulator of catecholamine release from cultured bovine adrenal chromaffin cells. Neurosci. Lett. 121 (1-2): 163-165.

Noguchi, T., Hwang, D.F., Arakawa, O., Daigo, K., Sato, S., Ozaki, H., Kawai, N., 1987. Palytoxin as the causative agent in the parrotfish poisoning. In: Gopalakrishnakone P. and C.K. Tan, Editors, Progress in Venom and Toxin Research, National University of Singapore, Singapore, pp. 325–335.

Nordt, S.P., Wu, J., Zahller, S., Clark, R.F., Cantrell, F.L., 2009. Palytoxin poisoning after dermal contact with zoanthid coral. J. Emer. Med. 2009), doi:10.1016/j.jemermed.2009.05.004.

Norman, K.G., Canter, J.A., Shi, M., Milne, G.L., Morrow, J.D., Sligh, J.E., 2010. Cyclosporine A suppresses keratinocyte cell death through MPTP inhibition in a model for skin cancer in organ transplant recipients. Mitochondrion 10 (2): 94-101.

Oku, N., Sata, N.U., Matsunaga, S., Uchida, H., Fusetani, N., 2004. Identification of palytoxin as a principle which causes morphological changes in rat 3Y1 cells in the zoanthid *Palythoa* aff. *margaritae*. Toxicon 43, 21-25.

Onuma, Y., Satake, M., Ukena, T., Roux, J., Chanteau, S., Rasolofonirina, N., Ratsimaloto, M., Naoki, H., Yasumoto, T., 1999. Identification of putative palytoxin as the cause of clupeotoxism. Toxicon. 37 (1), 55-65.

Pelin, M., Sosa, S., Della Loggia, R., Poli, M., Tubaro, A., Dercorti, G., Florio, C., 2012. The cytotoxic effect of palytoxin on Caco-2 cells hinders their use for in vitro absorption studies. Food Chem Toxicol.50 (2): 206-211.

Pierzchalska, M., Soja, J., Woś, M., Szabó, Z., Nizankowska-Mogielnicka, E., Sanak, M., Szczeklik, A., 2007. Deficiency of cyclooxygenases transcripts in cultured primary bronchial epithelial cells of aspirin-sensitive asthmatics. J. Physiol. Pharmacol. 58: 207-218.

Qiu, L.Y., Swarts, H.G., Tonk, E.C., Willems, P.H., Koenderink, J.B., De Pont, J.J., 2006. Conversion of the low affinity Ouabain-binding site of non-gastric H,K ATPase into a high affinity binding site by substitution of only five amino acids. J. Biol. Chem. 281 (19): 13533-13539.

Reilly, D.M., Parslew, R., Sharpe, G.R., Powell, S., Green, M.R., 2000. Inflammatory mediators in normal, sensitive and diseased skin types. Acta. Derm. Venereol. 80 (3): 171-174.

Rhodes, L., 2011. World-wide occurrence of the toxic dinoflagellate genus Ostreopsis Schmidt. Toxicon 57 (3): 400-407.

Rodrigues, A.M., Almeida, A.C., Infantosi, A.F., Teixeira, H.Z., Duarte, M.A., 2008. Model and simulation of Na^+/K^+ pump phosphorylation in the presence of palytoxin. Comput. Biol. Chem. 32 (1): 5-16.

Rossini, G.P., Bigiani, A., 2011. Palytoxin action on the Na(+),K(+)-ATPase and the disruption of ion equilibria in biological systems. Toxicon 57 (3): 429-439.

Ruzicka, T., Simmet, T., Peskar, B.A., Ring, J., 1986. Skin levels of arachidonic acid derived in¯ammatory mediators and histamine in atopic dermatitis and psoriasis. J. Invest. Dermatol. 86: 105-108.

Sagara, T., Nishibori, N., Itoh, M., Morita, K., Her, S., 2011. Palytoxin causes nonoxidative necrotic damage to PC12 cells in culture. J. Appl. Toxicol. doi: 10.1002/jat.1728.

Sala, G.L., Bellocci, M., Rossini, G.P., 2009. The cytotoxic pathway triggered by palytoxin involves a change in the cellular pool of stress response proteins. Chem. Res. Toxicol. 22 (12): 2009-2016.

Sansoni, G., Borghini, B., Camici, G., Casotti, M., Righini, P., Rustighi, C., 2003. Fioriture algali di *Ostreopsis ovata* (Gonyaulacales: Dinophyceae): un problema emergente. Biol. Amb. 17: 17-23.

Sarangarajan, R., Shumaker, H., Soleimani, M., Le Poole, C., Boissy, R.E., 2001. Molecular and functional characterization of sodium--hydrogen exchanger in skin as well as cultured keratinocytes and melanocytes. Biochim. Biophys. Acta. 1511 (1): 181-192.

Satoh, E., Nakazato, Y., 1991. Mode of action of palytoxin on the release of acetylcholine from rat cerebrocortical synaptosomes. J. Neurochem. 57: 1276-1280.

Scheiner-Bobis, G., Hubschle, T., Diener, M., 2002. Action of palytoxin on apical H^+/K^+ ATPase in rat colon. Eur. J. Biochem. 269 (16): 3905-3911.

Schilling, W.P., Snyder, D., Sinkins, W.G., Estacion, M., 2006. Palytoxin-induced cell death cascade in bovine aortic endothelial cells. Am. J. Physiol. Cell. Physiol. 291 (4): C657-667.

Sheridan, R.E., Desphande, S.S., Adler, M., 2005. Cytotoxic actions of palytoxin on aortic smooth muscle cells in culture. J. Appl. Toxicol. 25 (5): 365-373.

Seemann, P., Gernert, C., Schmitt, S., Mebs, D., Hentschel, U., 2009. Detection of hemolytic bacteria from *Palythoa caribaeorum* (Cnidaria, Zoantharia) using a novel palytoxin-screening assay. Antonie van Leeuwenhoek 96: 405–411.

Sosa S., Del Favero G., De Bortoli M., Vita F., Soranzo M.R., Beltramo D., Ardizzone M., Tubaro A., 2009. Palytoxin toxicity after acute oral administration in mice. Toxicol. Lett. 191 (2-3): 253-259.

Suh, E.M., Kishi, Y., 1994. Synthesis of palytoxin from palytoxin carboxylic acid. J. Am. Chem. Soc. 116 (24): 11205–11206.

Szabó, C., 2003. Multiple pathways of peroxynitrite cytotoxicity. Toxicol Lett. 140-141: 105-12.

Taniyama, S., Mahmud, Y., Terada, M., Takatani, T., Arakawa, O., Noguki, T., 2002. Occurrence of a food poisoning incident by PLTX from a serranid *Epinephelus* sp. In Japan. J. Nat. Toxins 11: 277-282.

Tatsumi, M., Takahashi, M., Ohizumi, Y., 1984. Mechanism of palytoxin-induced [3H]norepinephrine release from a rat pheochromocytoma cell line. Mol. Pharmacol. 25 (3): 379-383.

Tichadou, L., Glaizal, M., Armengaud, A., Grossel, H., Lemée, R., Kantin, R., Lasalle, J.L., Drouet, G., Rambaud, L., Malfait, P., de Haro, L., 2010. Health impact of unicellular algae of the *Ostreopsis* genus blooms in the Mediterranean Sea: experience of the French Mediterranean coast surveillance network from 2006 to 2009. Clin Toxicol (Phila). 48 (8): 839-844.

Tognetto, L., Bellato, S., Moro, I., Andreoli, C., 1995. Occurrence of *Ostreopsis ovata* (Dinophyceae) in the Tyrrhenian Sea during summer 1994. Bot. Mar. 38: 291-295.

Törmä, H., Geijer, S., Gester, T., Alpholm, K., Berne, B., Lindberg, M., 2006. Variations in the mRNA expression of inflammatory mediators, markers of differentiation and lipid-

metabolizing enzymes caused by sodium lauryl sulphate in cultured human keratinocytes. Toxicol. In Vitro. 20: 472-479

Totti, C., Cucchiari, E., Romagnoli, T., Penna, A., 2007. Bloom of *Ostreopsis ovata* on the Conero riviera (NW Adriatic Sea). Harmful Algae News 33: 12–13.

Tubaro, A., Durando, P., Del Favero, G., Ansaldi, F., Icardi, G., Deeds, J.R., Sosa, S., 2011. Case definitions for human poisonings postulated to palytoxins exposure. Toxicon 57 (3): 478-495.

Turner, C.P., Toye, A.M., Jones, O.T., 1998. Keratinocyte superoxide generation. Free Radic. Biol. Med. 24 (3): 401-407.

Uemura, D., Ueda, D., Hirata, Y., Naoki, H., Iwashita, T., 1981. Further studies on palytoxin. II. Structure of palytoxin. Tetrahedron Lett. 22: 2781-2784.

Uemura, D., Hirata, Y., Iwashita, T., Naoki, H., 1985. Studies on Palytoxins. Tetrahedron 41, 1007–1017.

Vale, C., Alfonso, A., Suñol, C:, Vieytes, M.R., Botana, L.M., 2006. Modulation of calcium entry and glutamate release in cultured cerebellar granule cells by Palytoxin. J. Neurosci. Res. 83: 1393-1406.

Vale-Gonzalez, C., Pazos, M.J., Alfonso, A., Vieytes, M.R., Botana, L.M., 2007. Study of the neuronal effects of ouabain and palytoxin and their binding to Na,K-ATPases using an optical biosensor. Toxicon 50 (4), 541-552.

Valverde, I., Lago, J., Reboreda, A., Vieites, J.M., Cabado, A.G., 2008a. Characteristics of palytoxin-induced cytotoxicity in neuroblastoma cells. Toxicol. In Vitro 22 (6), 1432-1439.

Valverde, I., Lago, J., Vieites, J.M., Cabado, A.G., 2008b. In vitro approaches to evaluate palytoxin-induced toxicity and cell death in intestinal cells. J. Appl. Toxicol. 28 (3), 294-302.

Vande Velde, C., Cizeau, J., Dubik, D., Alimonti, J., Brown, T., Israels, S., Hakem, R., Greenberg, A.H., 2000. BNIP3 and genetic control of necrosis-like cell death through the mitochondrial permeability transition pore. Mol. Cell Biol. 20 (15): 5454-5468.

Vila, M., Garcés, E., Masó, M., 2001. Potentially toxic epiphytic dinoflagellate assemblages on macxroalgae in the NW Mediterranean. Aquat. Microbiol. Ecol. 26, 51-60.

Wattenberg, E.V., 2007. Palytoxin: exploiting a novel skin tumor promoter to explore signal transduction and carcinogenesis. Am. J. Physiol. Cell. Physiol. 292 (1): C24-32.

Welss, T., Basketter, D.A., Schröder, K.R., 2004. In vitro skin irritation: facts and future. State of the art review of mechanisms and models. Toxicol. In Vitro 18 (3): 231-243.

Wolf, K., Schulz, C., Riegger, G.A., Pfeifer, M., 2002. Tumour necrosis factor-alpha induced CD70 and interleukin-7R mRNA expression in BEAS-2B cells. Eur. Respir. J. 20: 369-375.

Wu, C.H., 2009. Palytoxin: membrane mechanism of action. Toxicon 54, 1183-1189.

Wu, Y.T., Wu, S.B., Lee, W.Y., Wei, Y.H., 2010. Mitochondrial respiratory dysfunction-elicited oxidative stress and posttranslational protein modification in mitochondrial diseases. Ann. NY Acad. Sci. 1201, 147-156.

Ziegler, U., Groscurth, P., 2004. Morphological features of cell death. News Physiol. Sci. 19: 124-128.

Zingone, A., Siano, R., D'Alelio, D., Sarno, D., 2006. Potentially toxic and harmful microalgae from coastal waters of the Campania region (Tyrrhenian Sea, Mediterranean Sea). Harmful Algae 5, 321–337.